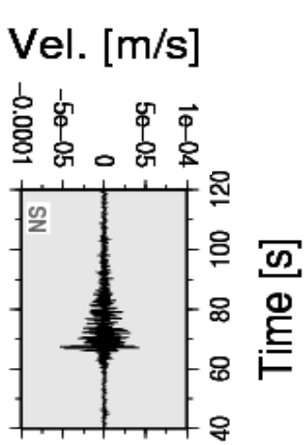

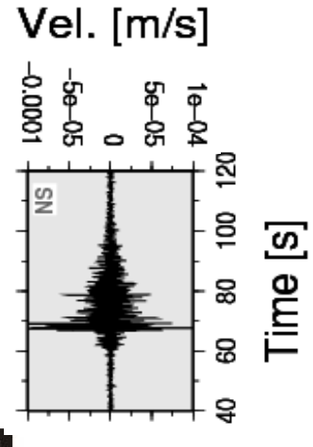

Frequenza di risonanza degli edifici

Interazione suolo struttura

Faglia

Effettidella geologia locale

Propagazione

Spettro della sorgente

MZS - Engineering Seismology

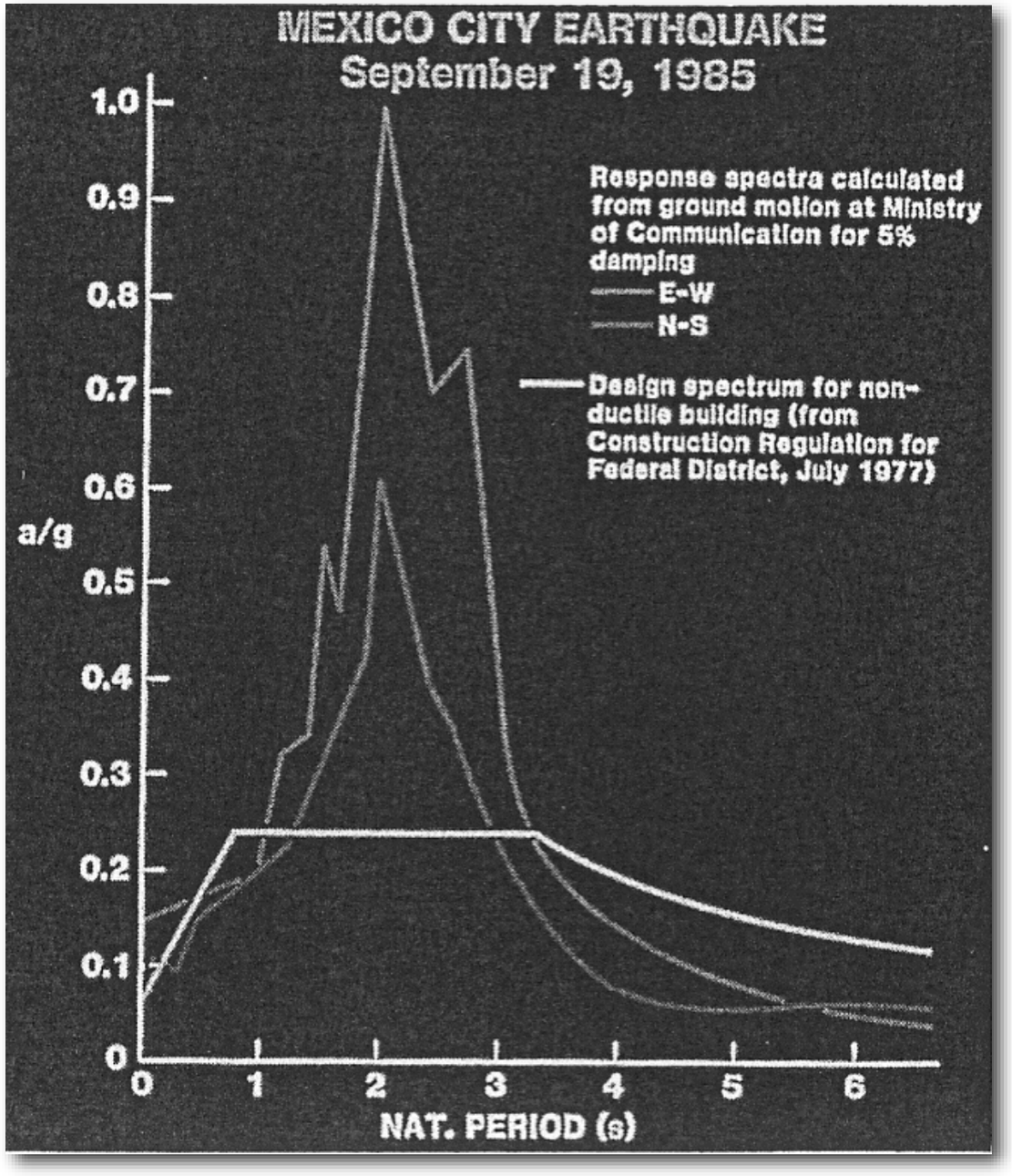

Michoacan 1985 event: way to DF...

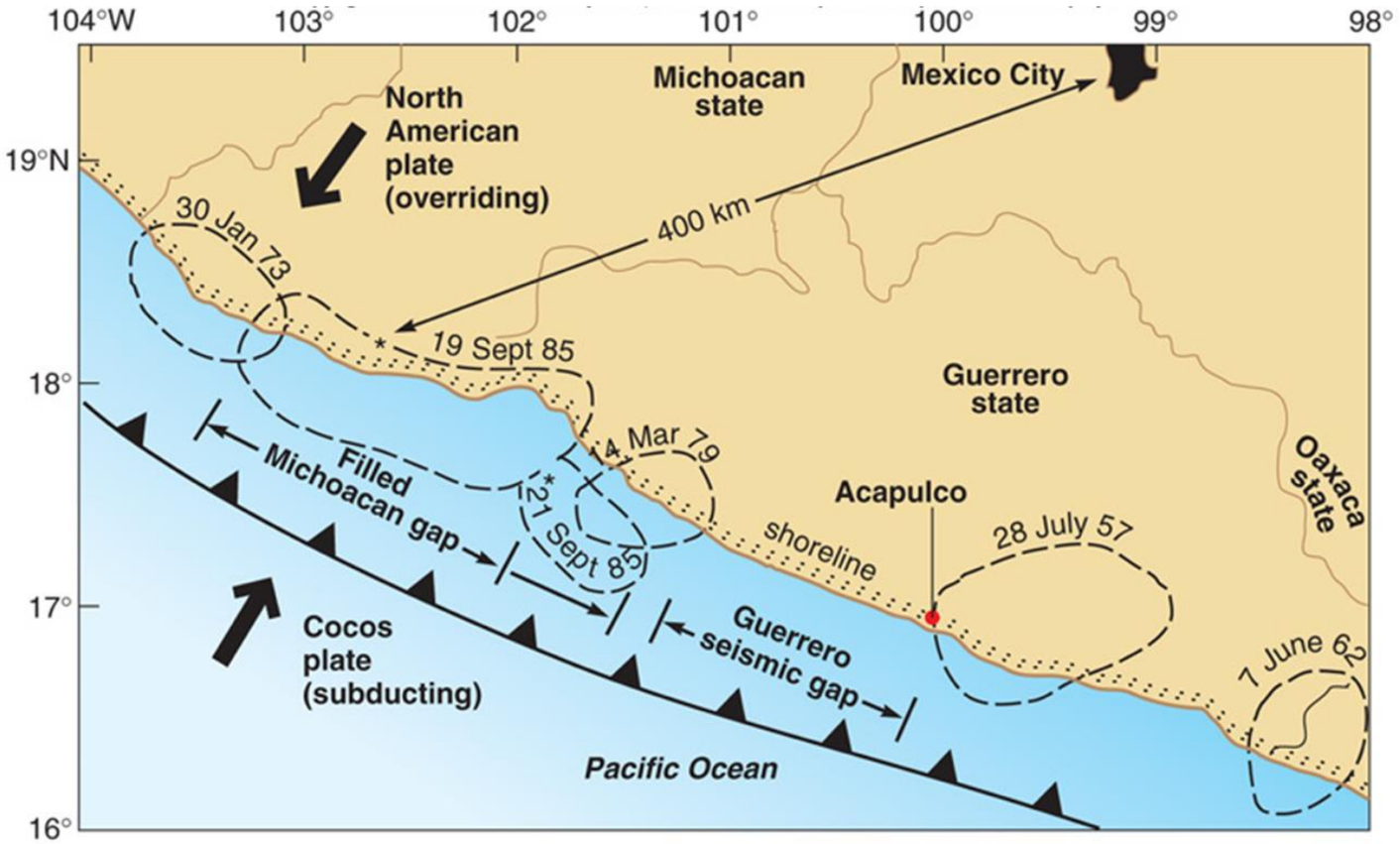

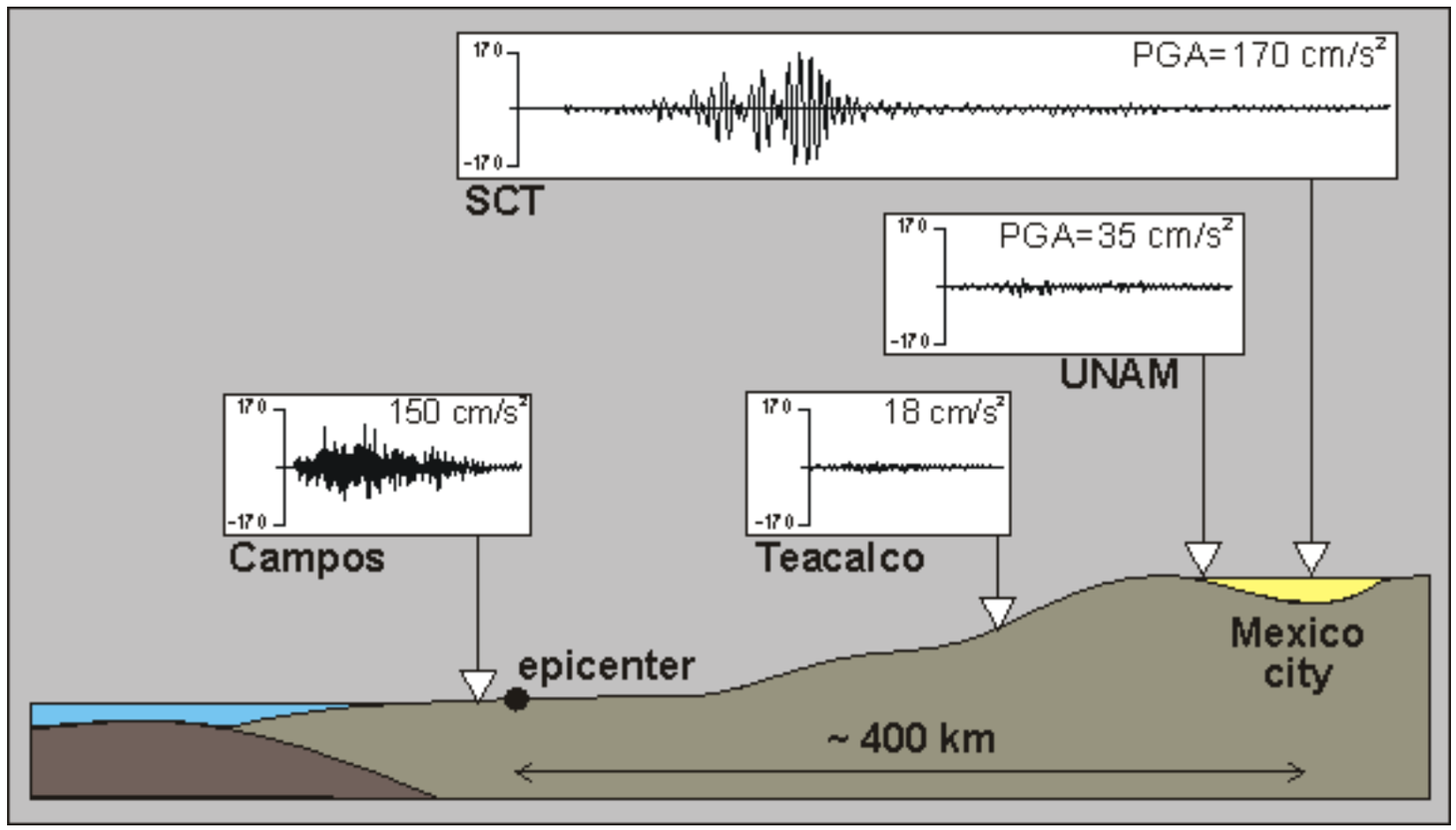

Tenochtitlan and Mexico City (DF)

La ciudad de Tenochtitlan y su entorno en el siglo XVI Pintura de Miguel Covarrubias, Museo Nacional de Antropología, México DF

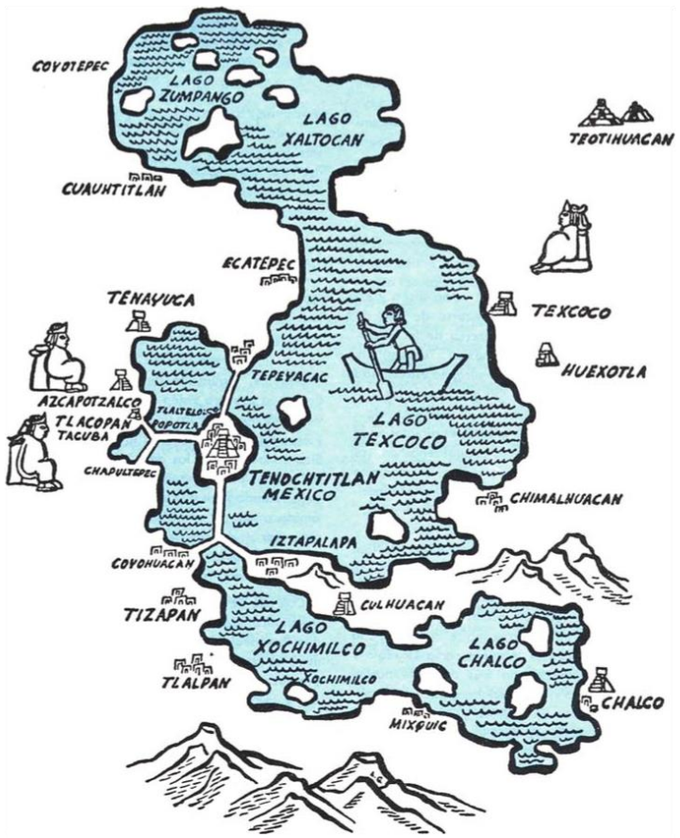

The actual boundaries of the World Heritage Property follows the boundaries of the Historical Monuments Zones, according to the limits of the city in the 19th century (perimeter A), and a buffer zone (perimeter B)

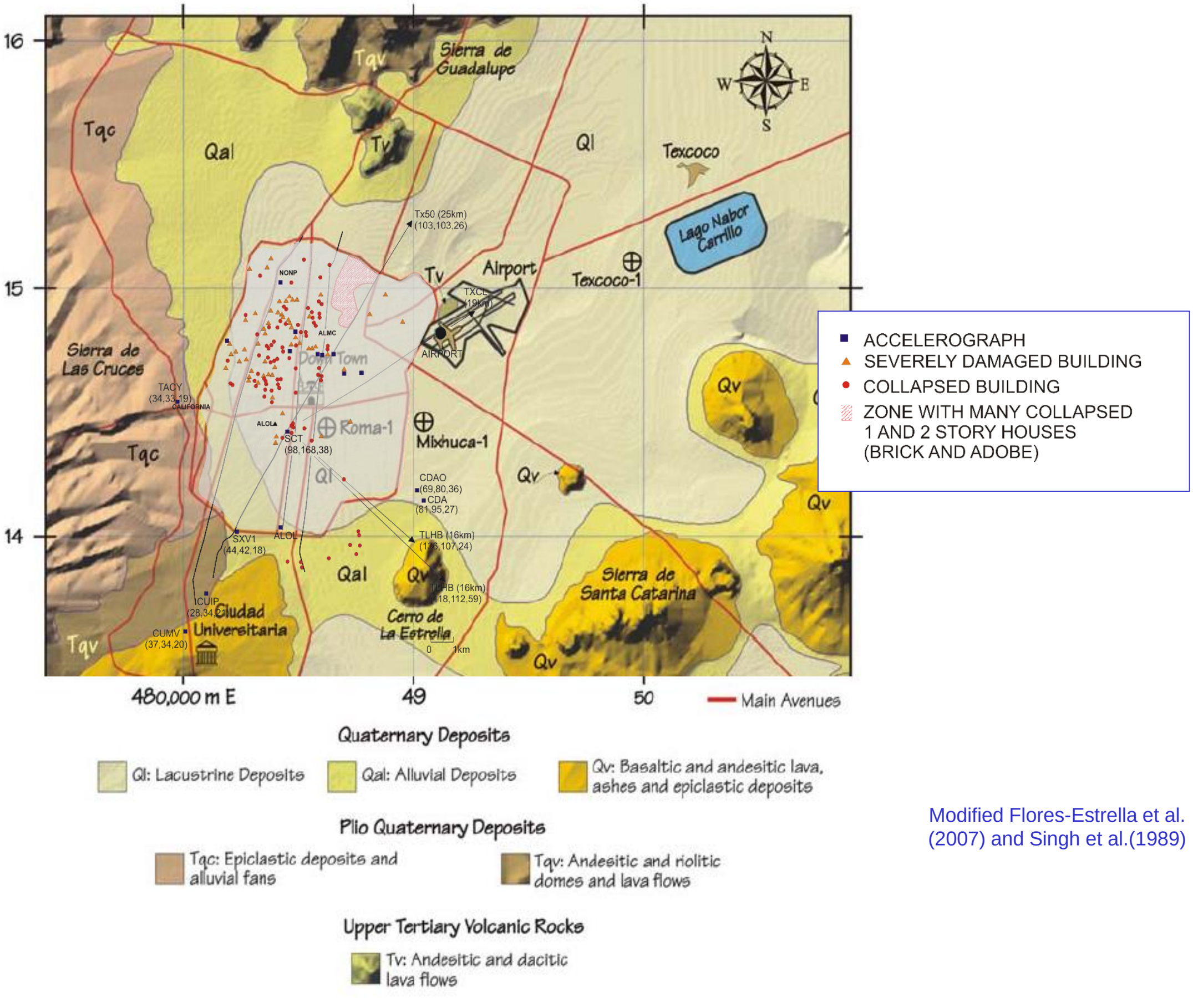

Modified Flores-Estrella et al. (2007) and Singh et al.(1989)

Michoacan 1985 event: GM in DF

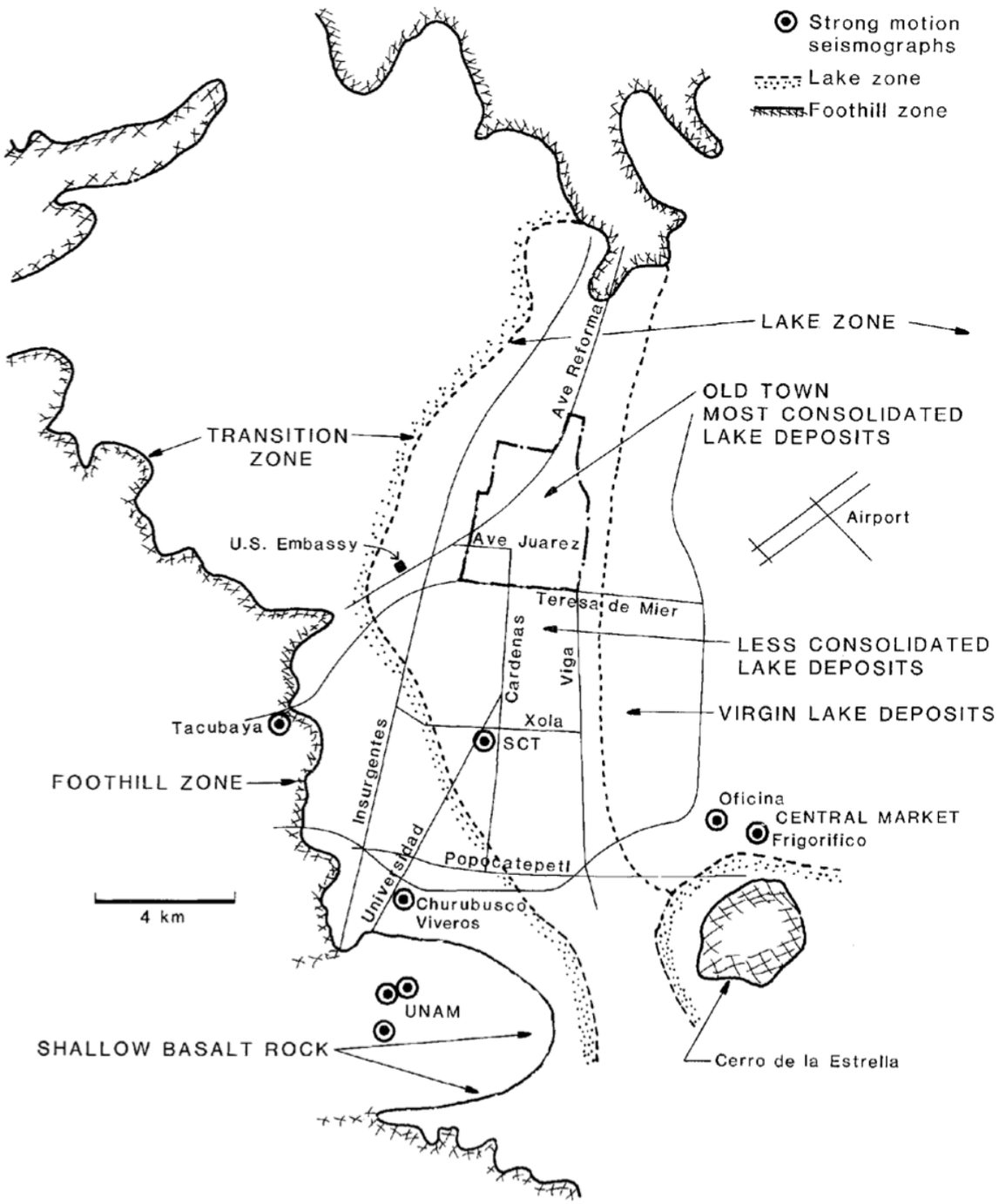

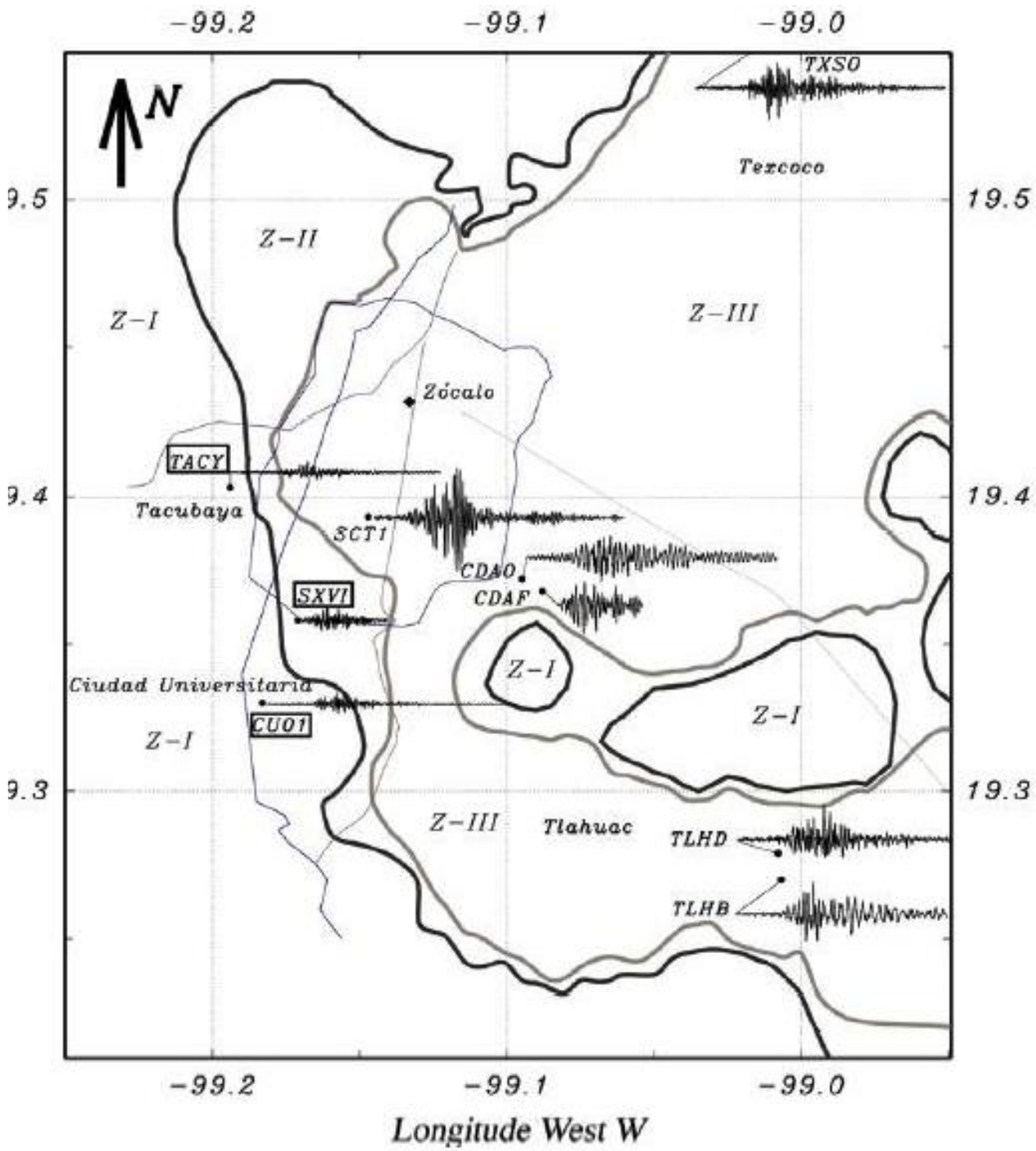

Michoacan 1985 event: damage in DF

Wreckage of a twenty-one-story building in Conjunto Pino Suarez Complex

Totally destroyed office building in the foreground, while the 44-floor Torre Latinoamericana office building, in the background on the right, stands

Effetti di sito: Valle di Gubbio

L’ampiezza delo scuotimento AUMENTA!
all’aumentare della distanza dalla sorgente!

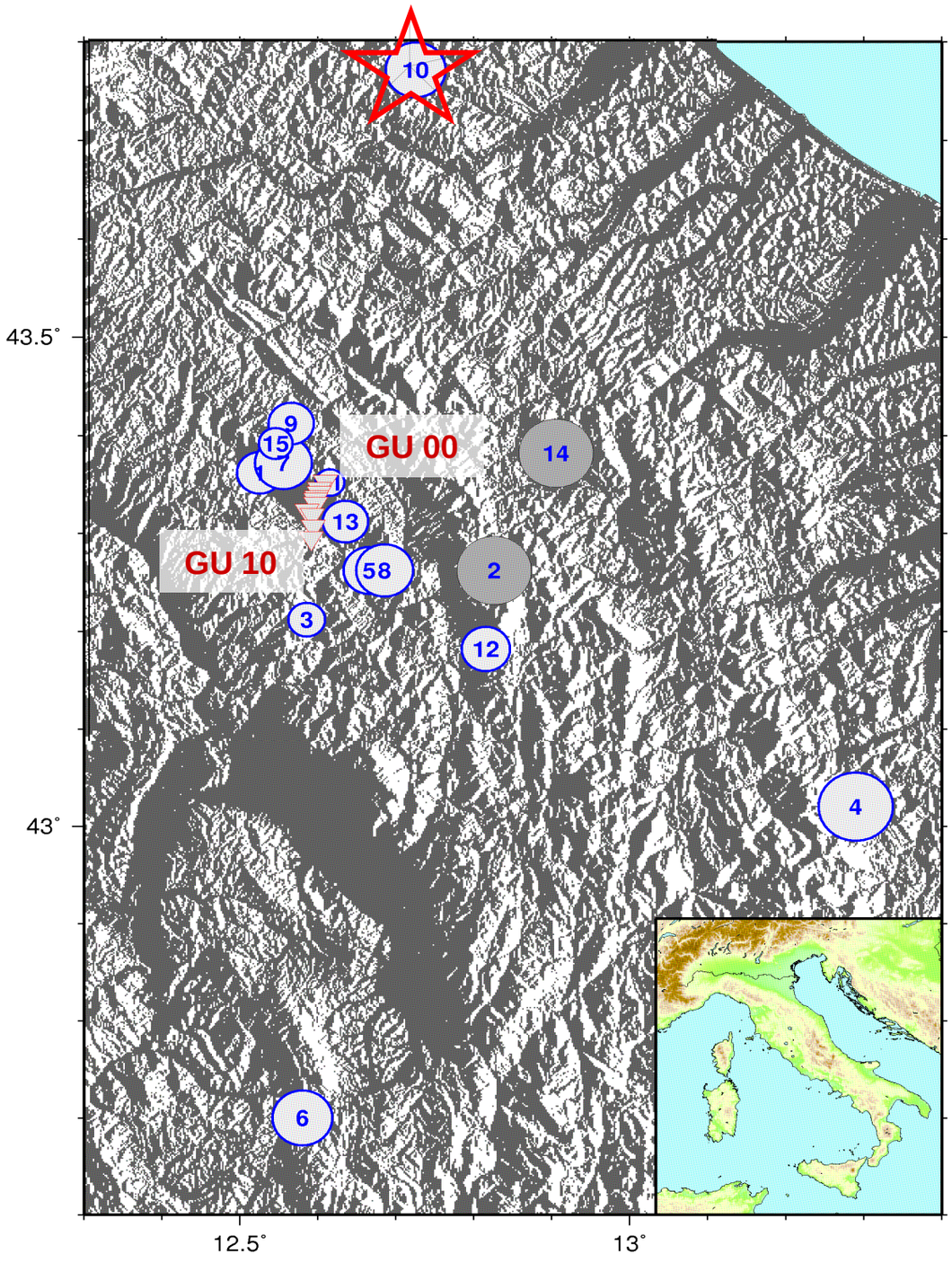

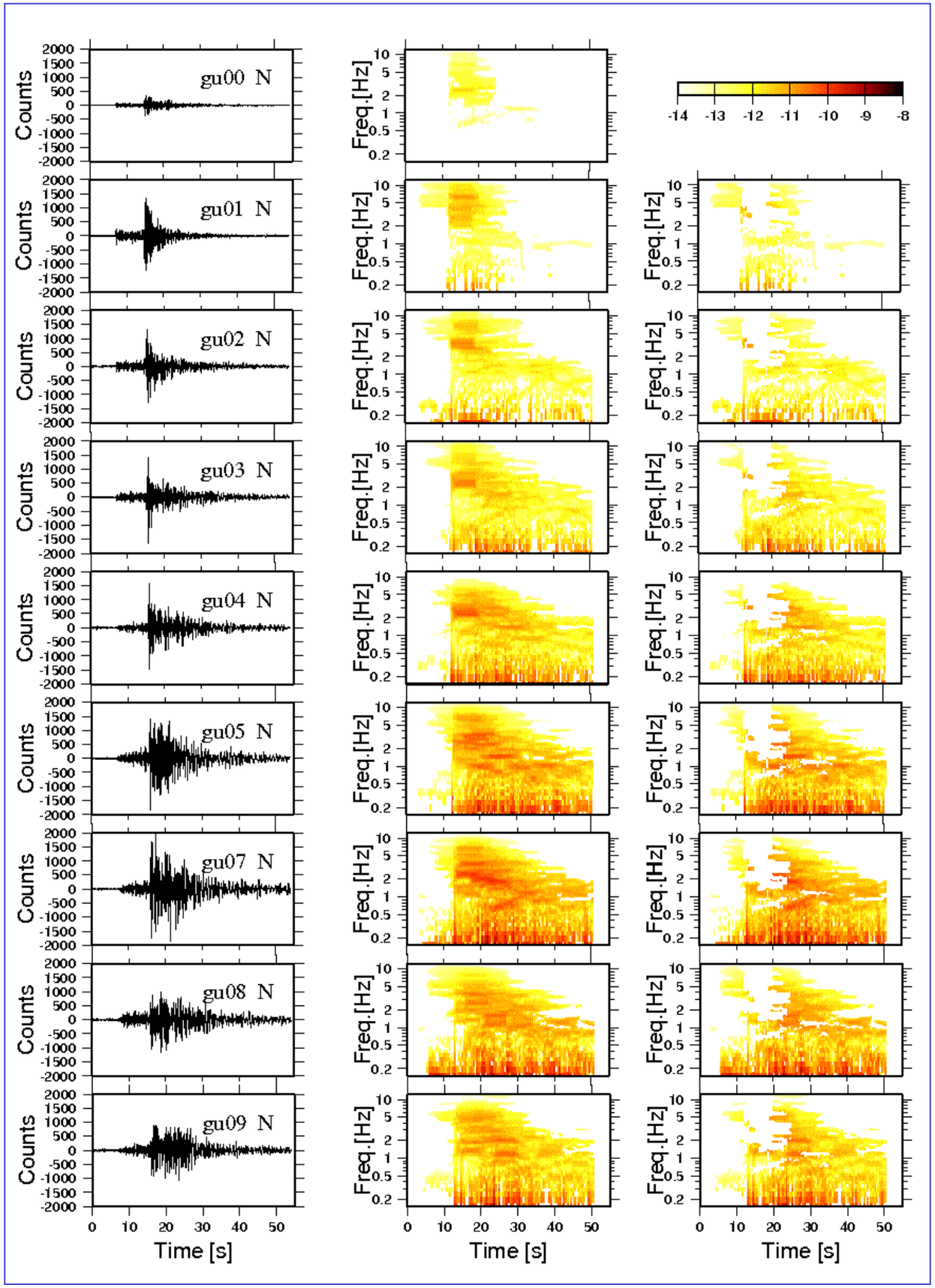

UNIVERSITÀ DEGLI STUDI DI TRIESTE

La banda di frequenza amplificata dipende dalla struttura del sottosuolo

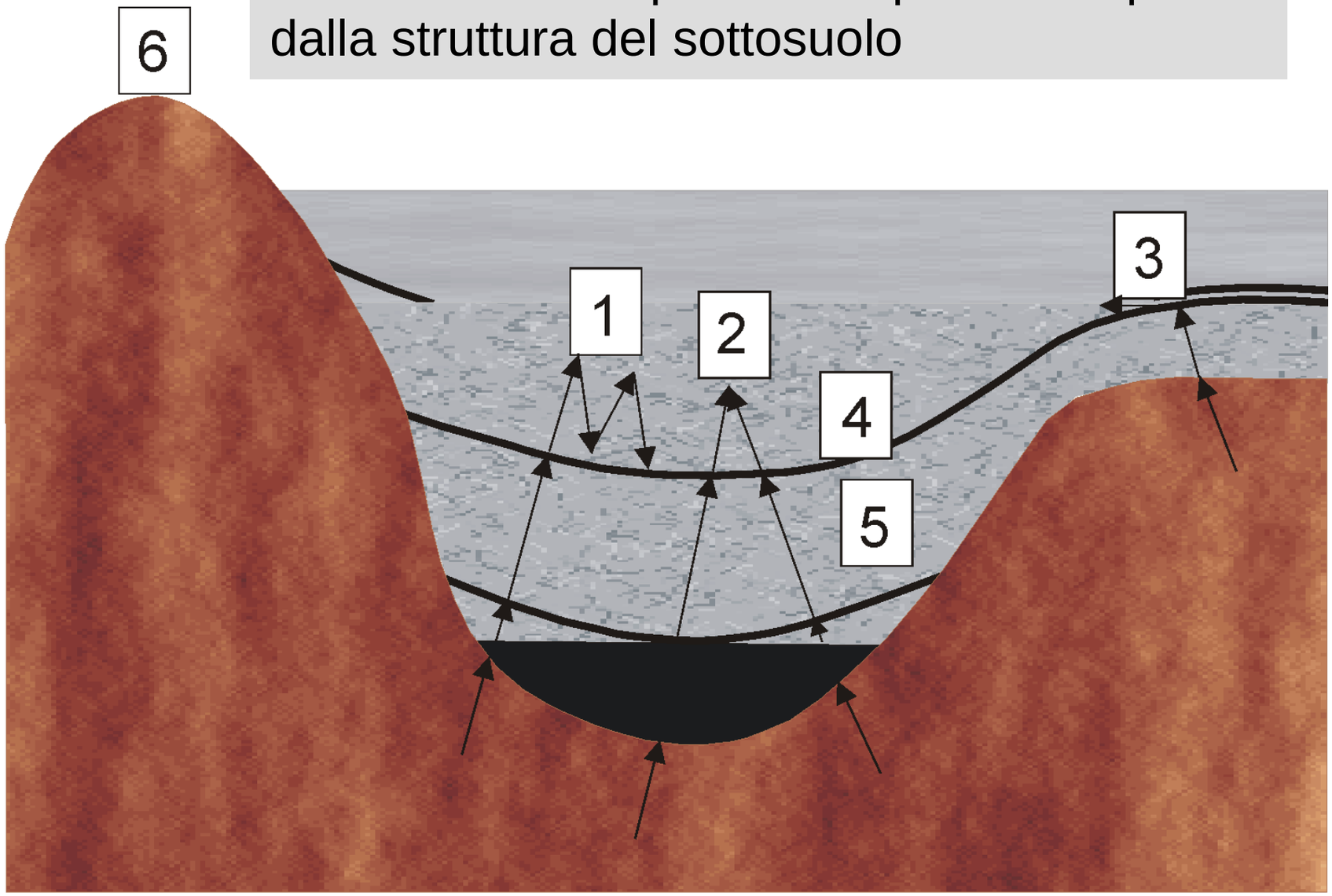

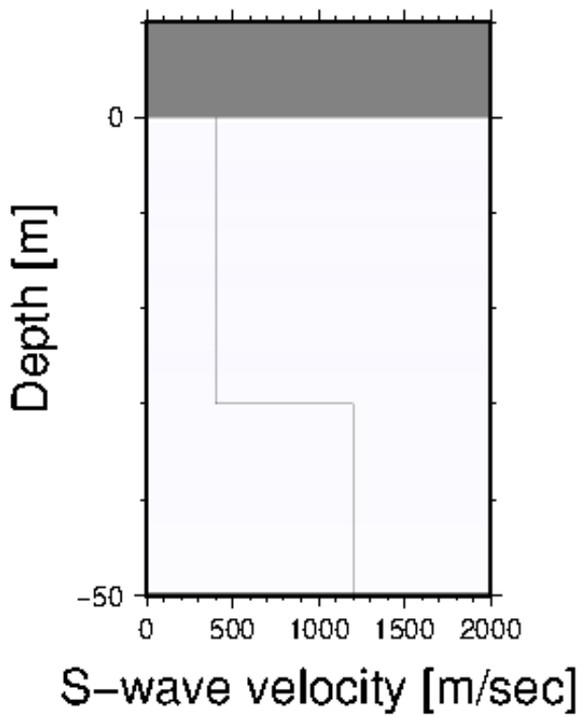

1 - Resonance due to impedance contrasts, 2 - Focusing due to subsurface topography, 3 - Body waves converted to surface waves, 4 - Water content, 5 - Randomness of the medium and 6 - Surface topography

Modified after Safak (2001)

Response spectra

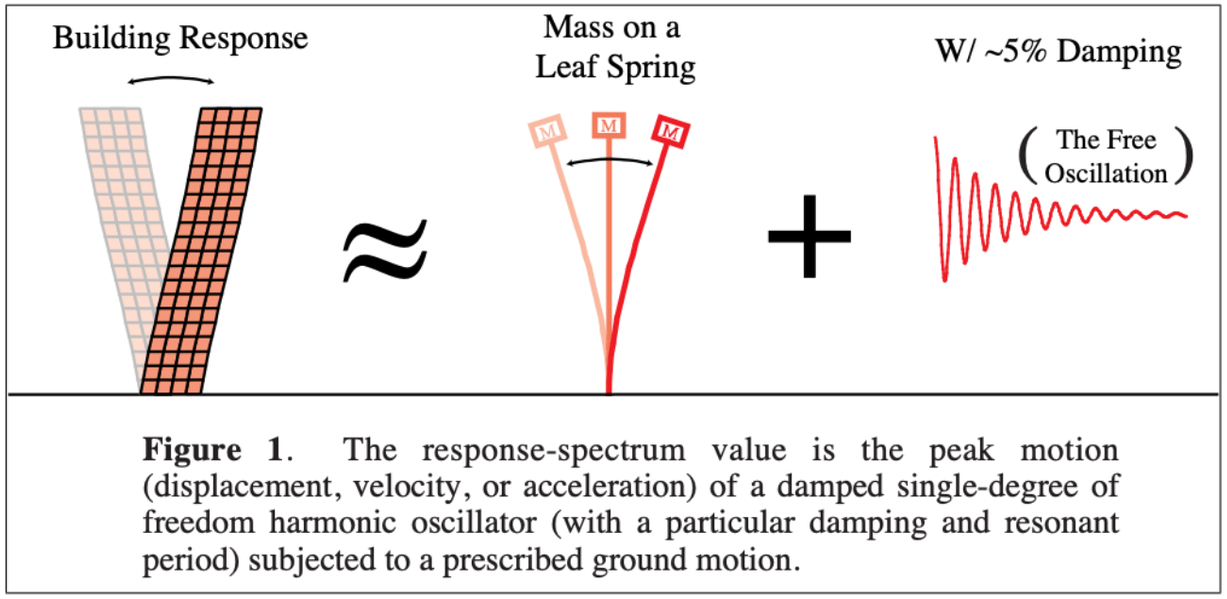

Figure 1. The response-spectrum value is the peak motion (displacement, velocity, or acceleration) of a damped single-degree of freedom harmonic oscillator (with a particular damping and resonant period) subjected to a prescribed ground motion.

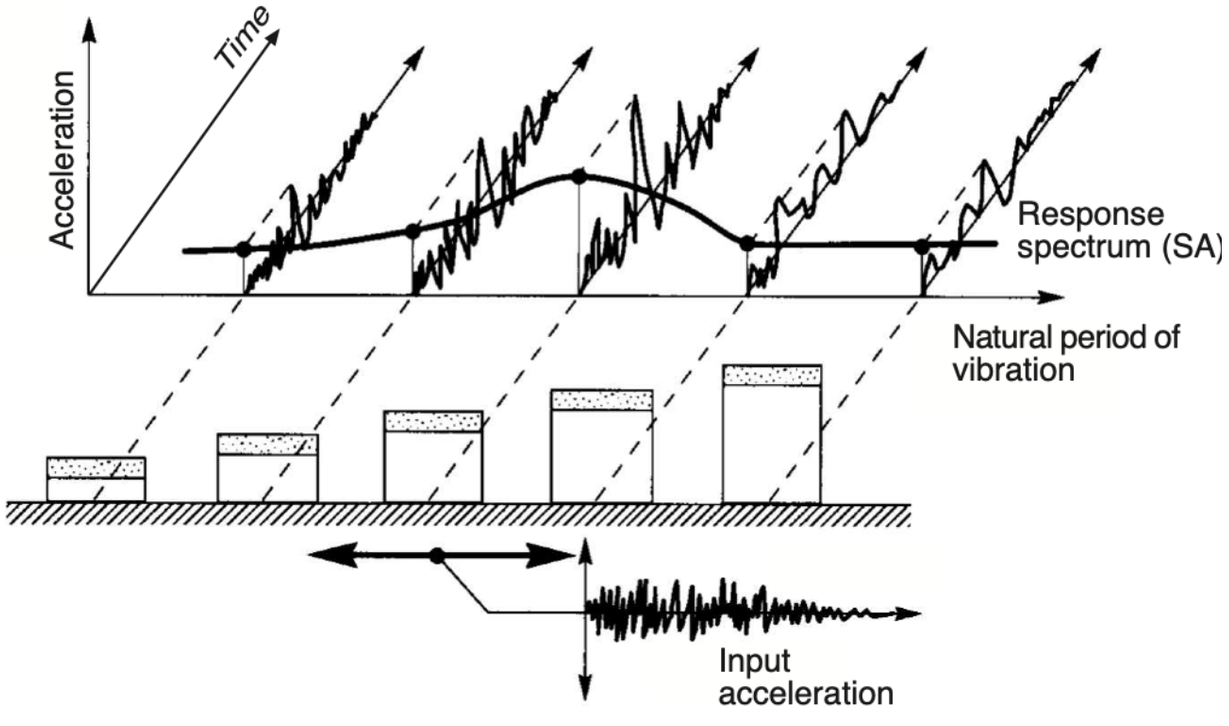

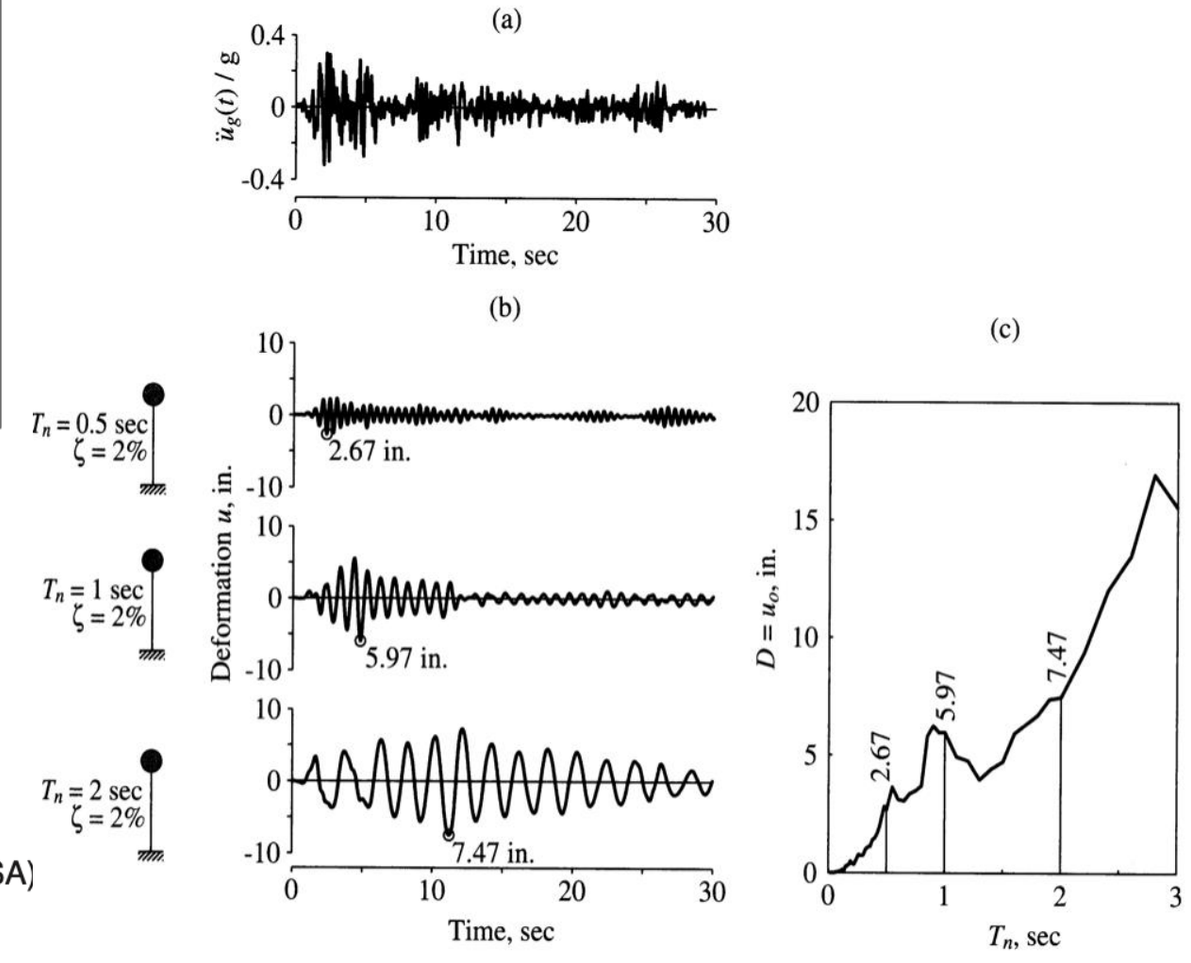

Figure 6.6.1 (a) Ground acceleration; (b) deformation response of three SDF systems with $\zeta = 2\%$ and $T_n = 0.5$, 1, and 2 sec; (c) deformation response spectrum for $\zeta = 2\%$.

Relative displacement

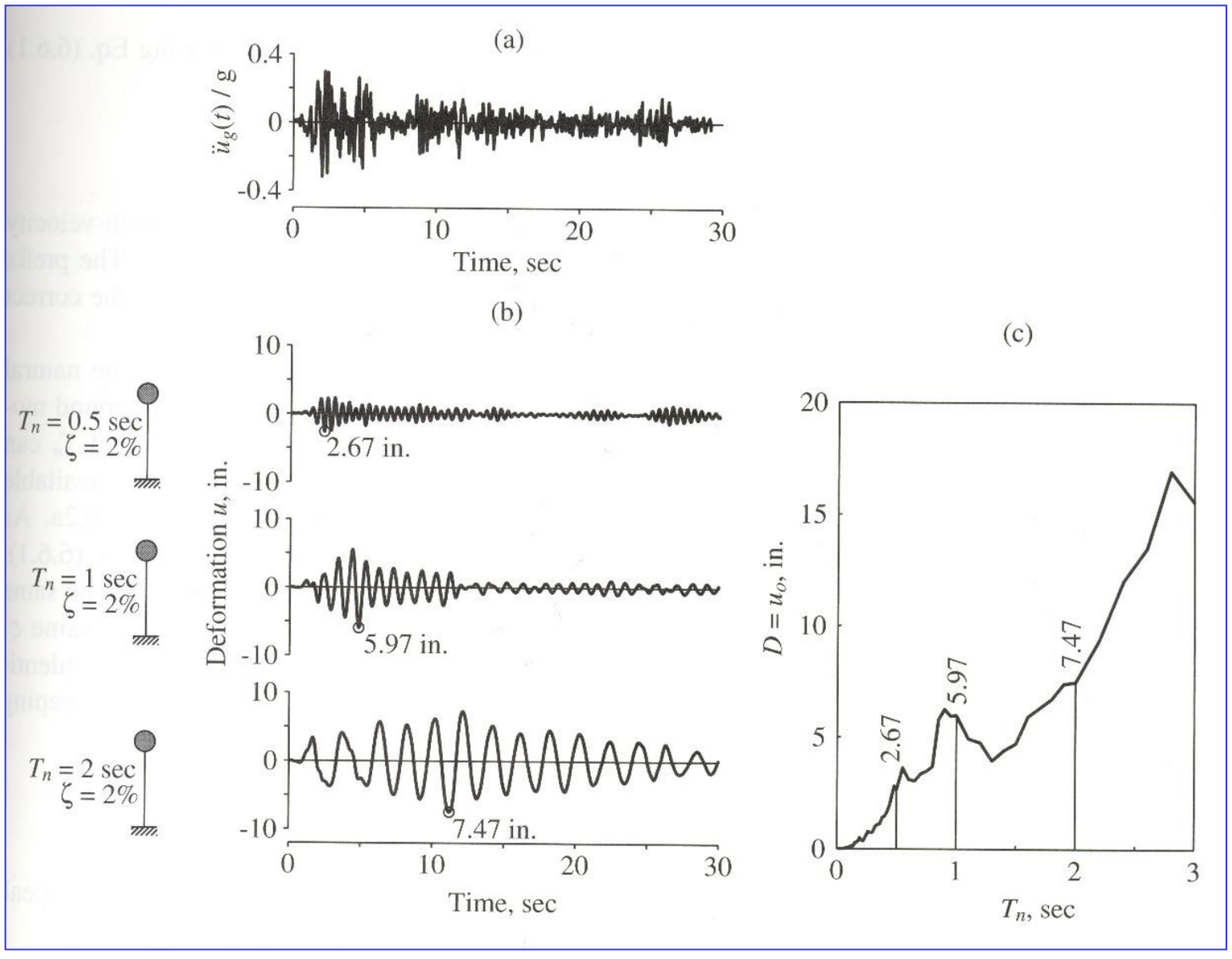

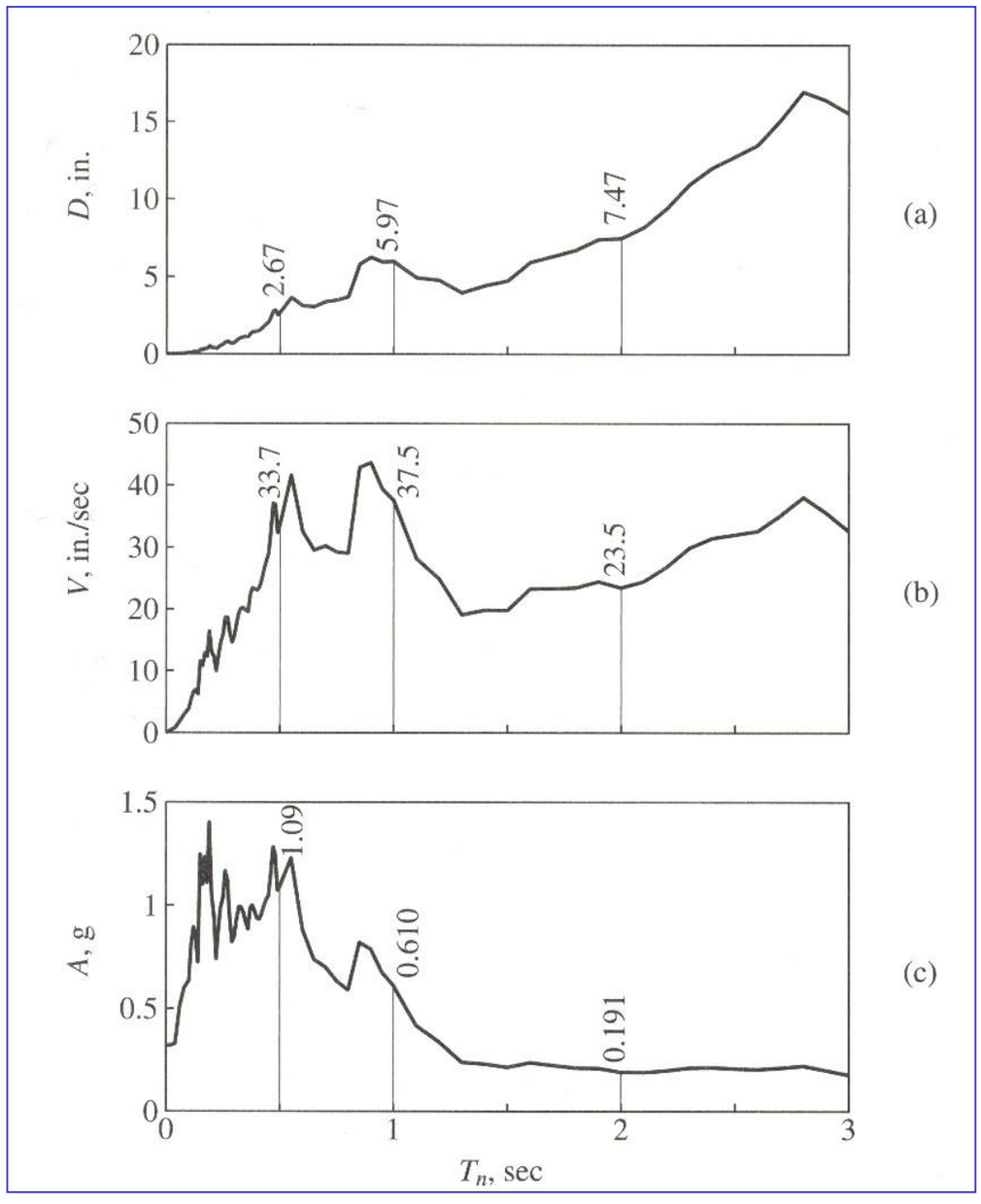

Pseudo Velocity and Pseudo accelerations

Since PSV and PSA are obtained by SD simply multiplying for a factor □

The 3 spectra can be diplayed on the same plot

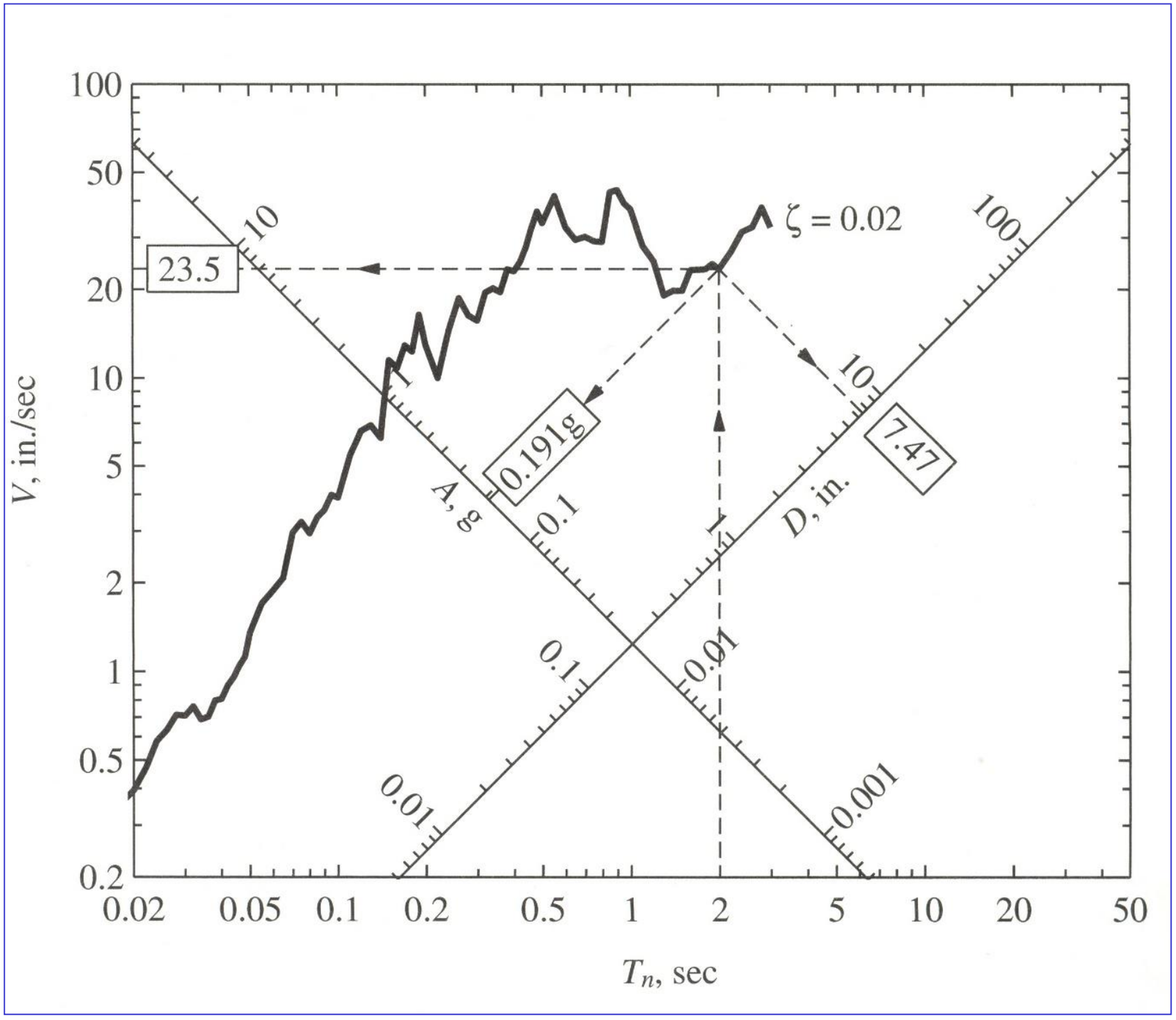

Response spectra

Critically damped system ($\xi = 1$).

2. Overdamped system ($\xi > 1$).

3. Underdamped system ($\xi < 1$)

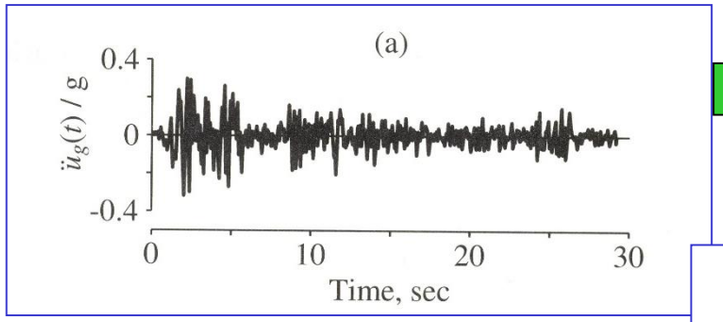

La risposta dell'oscillatore dipende dalla sua frequenza e dallo smorzamento!

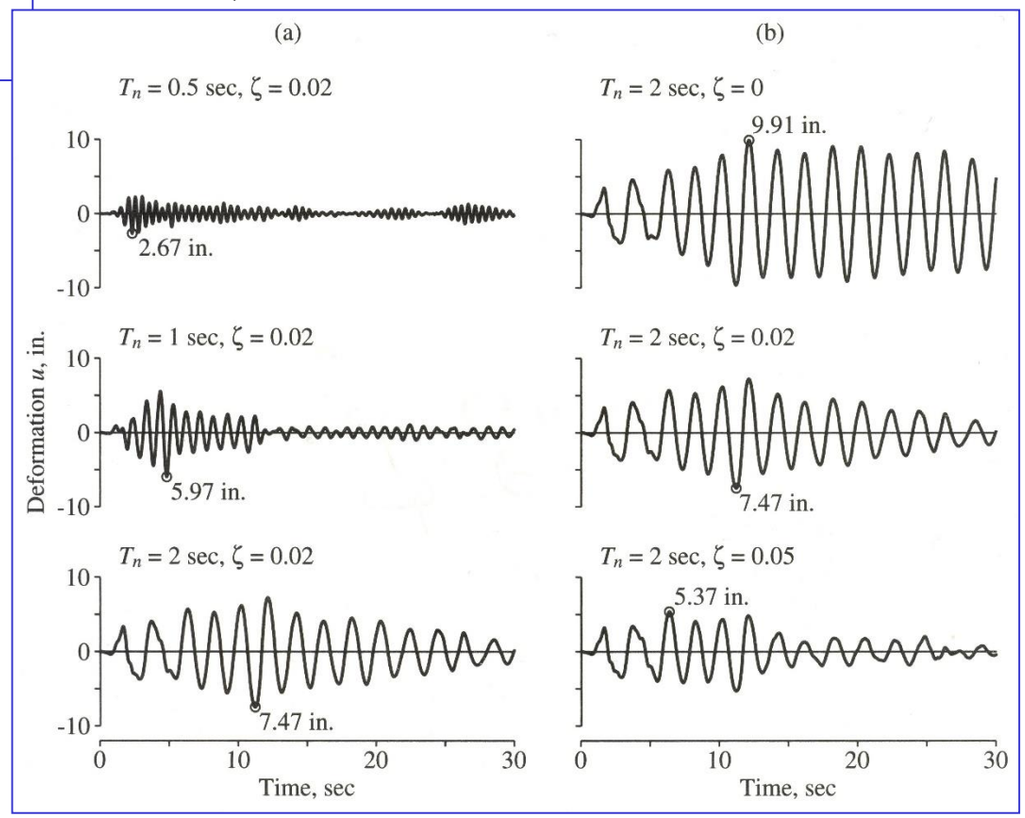

SHA dualism: P & D

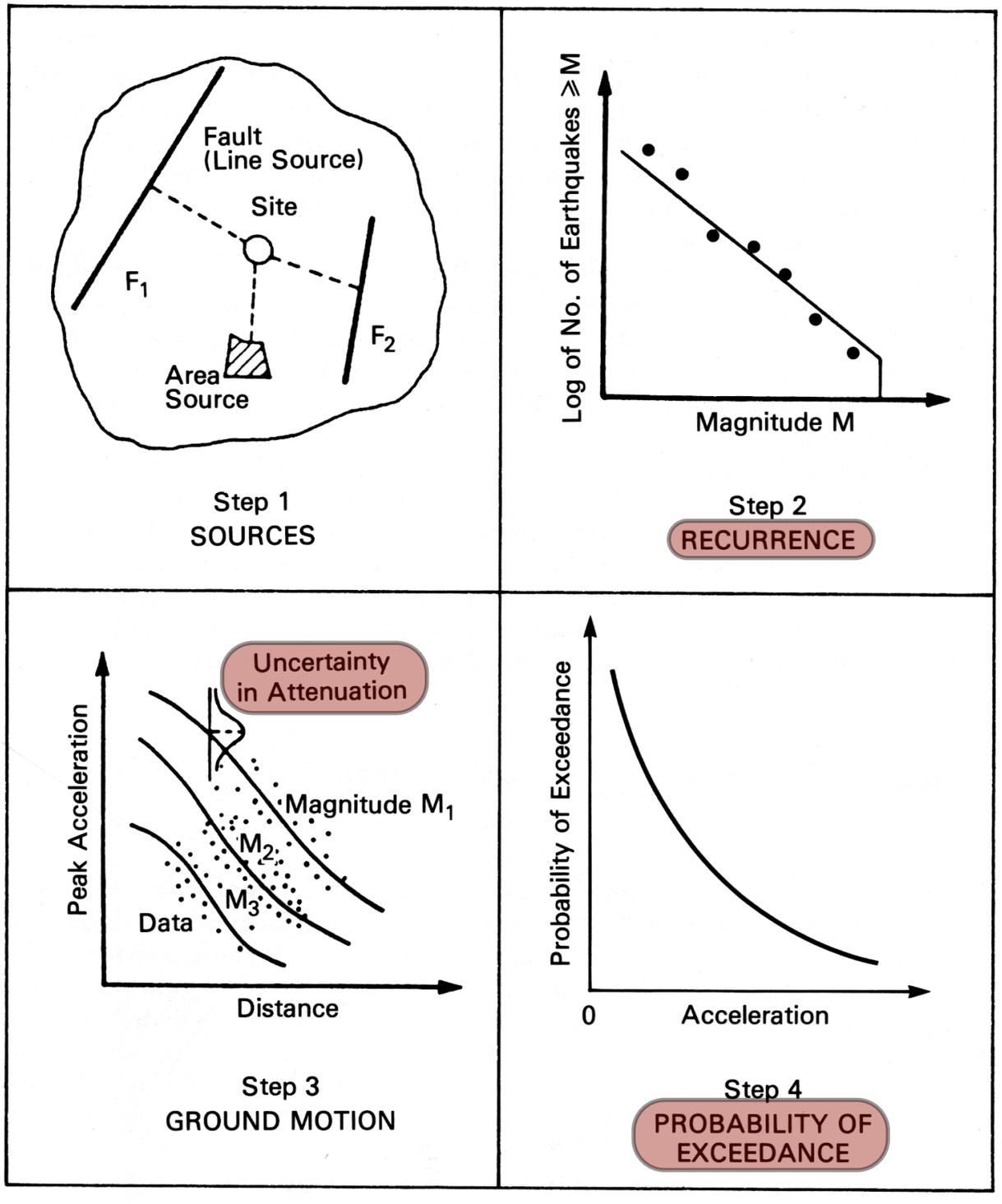

FIGURE 10.2 Basic steps of probabilistic seismic hazard analysis (after TERA Corporation 1978).

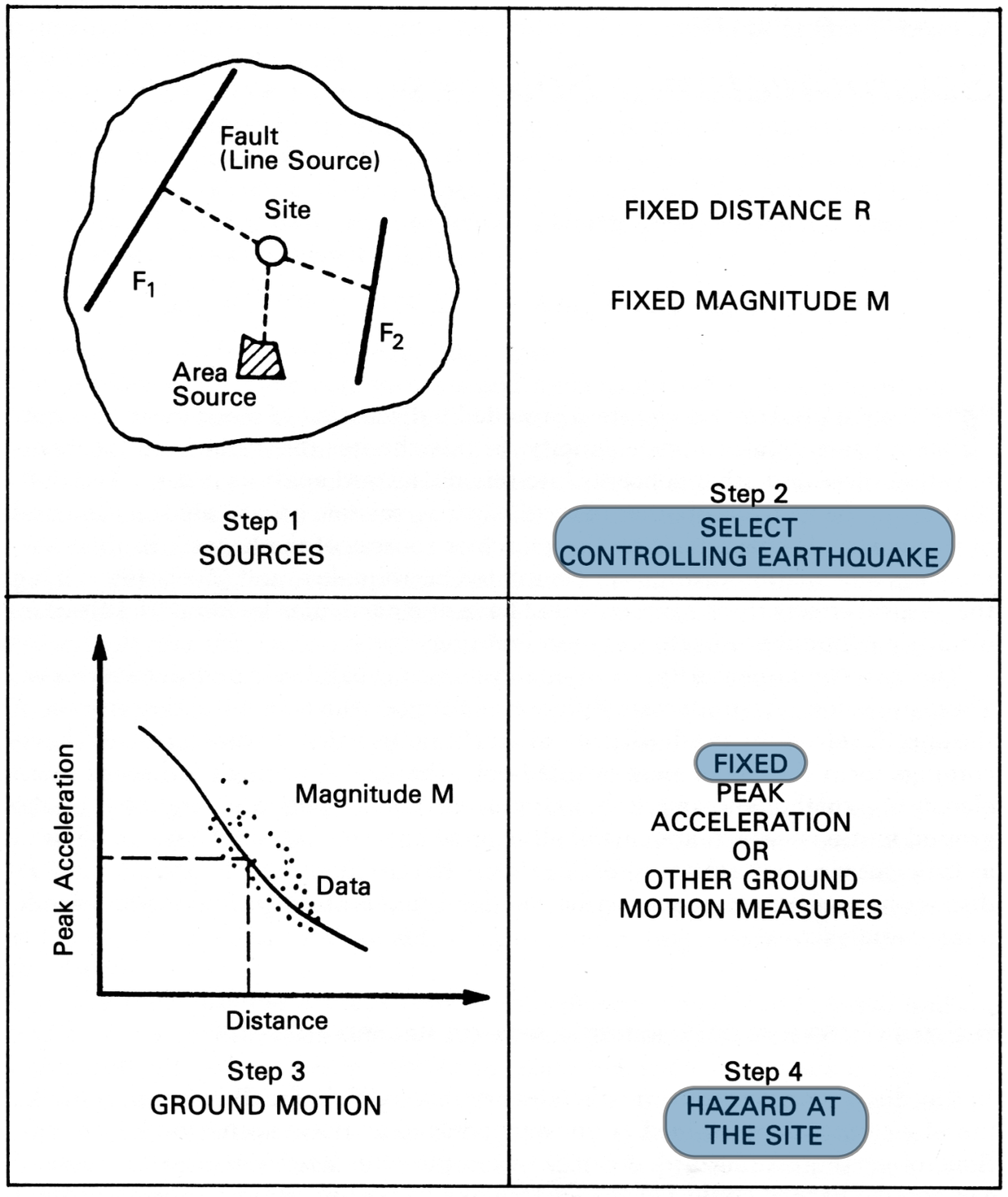

FIGURE 4.1 Basic steps of deterministic seismic hazard analysis (after TERA Corporation 1978).

"Earthquake Hazard Analysis", Reiter, 1990

Seismic Zonation and Catalogs

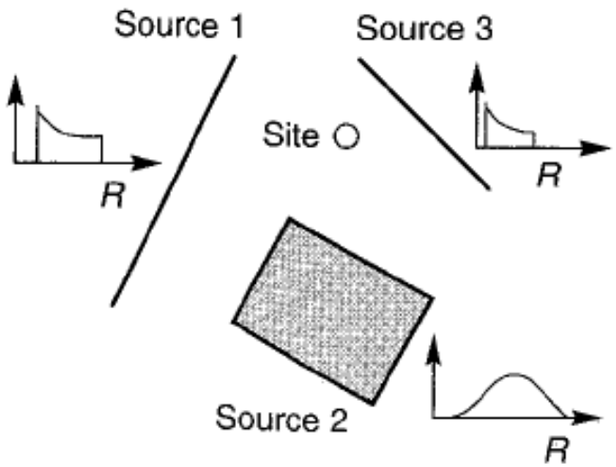

STEP 1

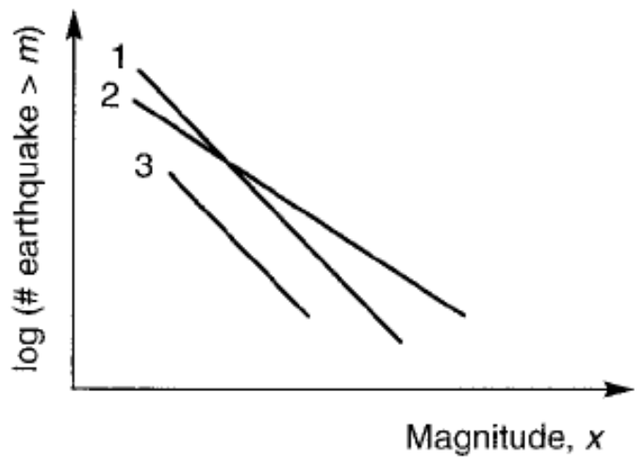

STEP 2

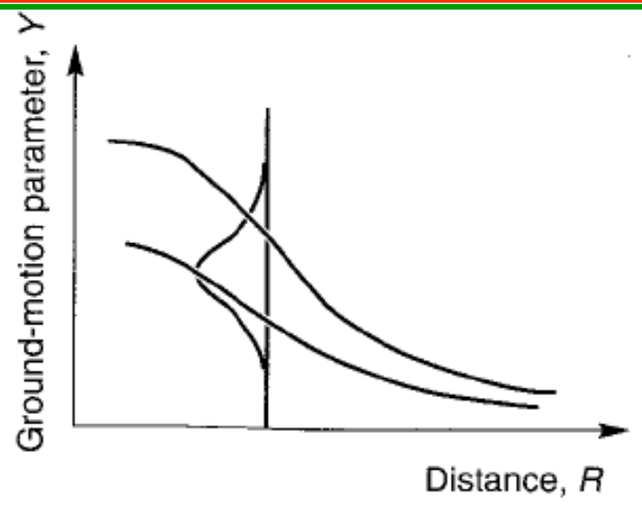

STEP 3

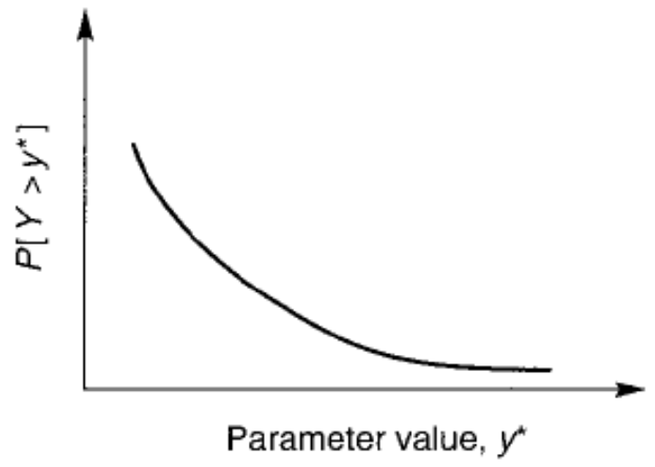

STEP 4

GMPEs and Probability of exceedance

Credit to Kramer's book

Issues regarding magnitude

The **advantages** of magnitude scales are

They can be determined directly from the seismogram, without the need for sophisticated processing.

The units of order 1 are intuitively attractive.

	to 2.9	Minor	Generally not felt but recorded	1000/day
3	to 3.9	Minor	Often felt, but rarely cause damage.	49000/year
4	to 4.9	Light	Noticeable shaking, damage unlikely.	6200/year
5	to 5.9	Moderate	Can cause damage to poor quality buildings	800/year
6	to 6.9	Strong	Destructive in areas up to *ca.*160 km.	120/year
7	to 7.9	Major	Serious damage over larger areas.	18/year
8	to 8.9	Great	Serious damage over areas of 100's km.	1/year
9	to 9.9	Great	Serious damage over areas of 1000' s km.	1/20 years

Earthquake distribution

AS noted, the numbers of earthquakes of a given size decreases by about an order of magnitude per magnitude unit increase.

Quantified by the ***Gutenberg-Richter*** relation:

$$\log N = a_1 - bM$$

where *N* is the number of earthquakes with a magnitude greater than *M* occurring in a given time (cumulative) or

$$\log n = a_2 - bM$$

n is (*dN/dM*), and a_1, a_2 and *b* are constants for a given

Right: Frequency-magnitude for all earthquakes M>5 between 1968-97.

The value of *b* is generally about 1, even for individual seismic areas.

(*Stein & Wysession, 2003*

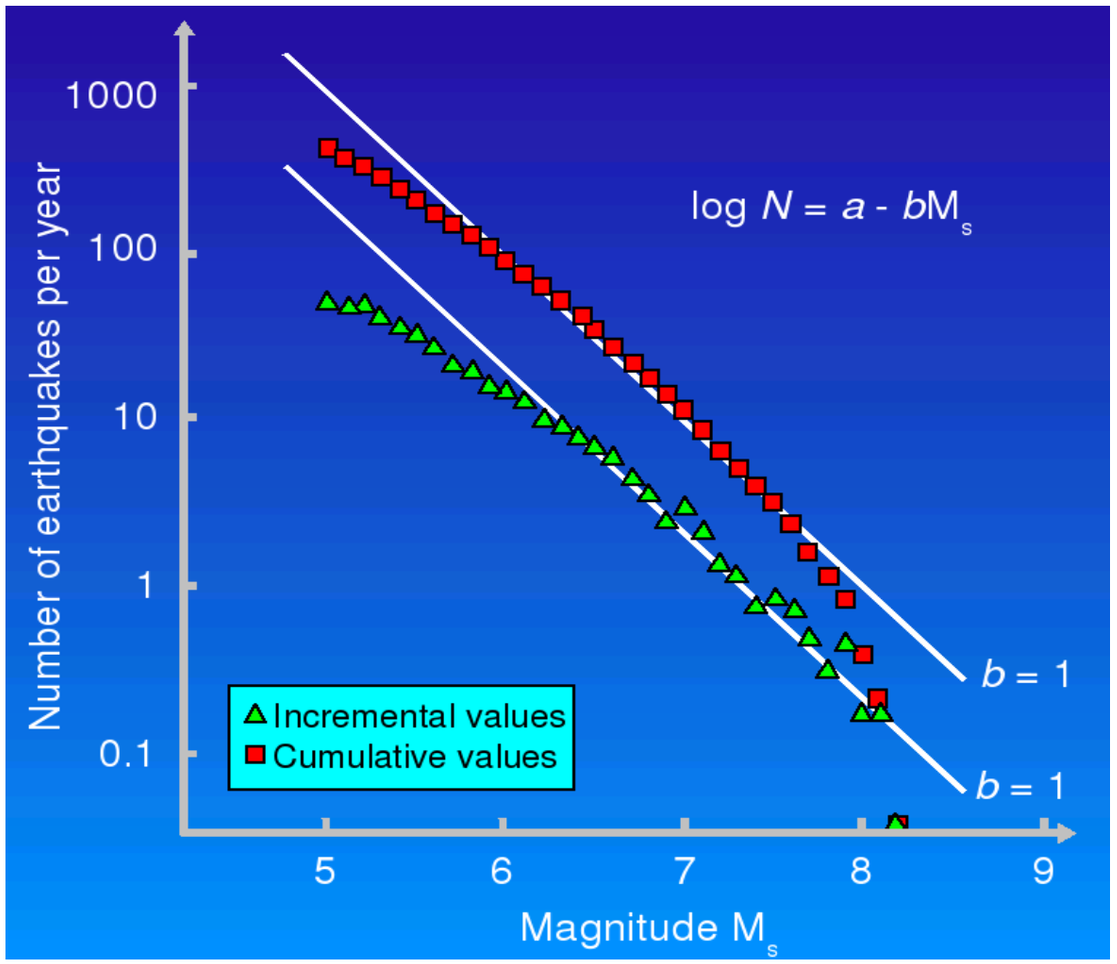

Probabilistic Seismic Hazard Analysis

All possible distances are considered - contribution of each is weighted by its probability of occurrence

$$\lambda_{y^*} = \sum_{i=1}^{N_S} \sum_{j=1}^{N_M} \sum_{k=1}^{N_R} \nu_i \int\int P[Y > y^* \mid m_j, r_k] P[M = m_j] P[R = r_k]$$

All sites are considered

All possible effects are considered - each weighted by its conditional probability of occurrence

All possible magnitudes are considered - contribution of each is weighted by its probability of occurrence

Probabilistic Seismic Hazard Analysis

Seismic Zonation

$$\lambda_{y^*} = \sum_{i=1}^{N_S} \sum_{j=1}^{N_M} \sum_{k=1}^{N_R} \nu_i \int\int P[Y > y^* \mid m_j, r_k] P[M = m_j] P[R = r_k]$$

All sites are considered

Ground Motion Prediction Equations - GMPEs

Seismic Catalogs

Italian building code (NTC08/18)

- Seismic classification

  https://rischi.protezionecivile.gov.it/it/sismico/attivita/classificazione-sismica

- Seismic hazard

  http://esse1.mi.ingv.it

- NTC08 Seismic code (§ 2.*; 3.2; 7.*)

  https://www.gazzettaufficiale.it/eli/id/2008/02/04/08A00368/sg

- NTC18 Seismic code (§ 2.*; 3.2; 7.*)

  https://www.gazzettaufficiale.it/eli/gu/2018/02/20/42/so/8/sg/pdf

  https://www.gazzettaufficiale.it/eli/id/2019/02/11/19A00855/sg

Italian code NTC18 - Seismic Action

L'azione sismica è caratterizzata da 3 componenti traslazionali, due orizzontali contrassegnate da X ed Y ed una verticale contrassegnata da Z, da considerare tra di loro indipendenti. Le componenti possono essere descritte, in funzione del tipo di analisi adottata, mediante una delle seguenti rappresentazioni:

- accelerazione massima in superficie;

- accelerazione massima e relativo spettro di risposta in superficie;

- storia temporale del moto del terreno.

Le due componenti ortogonali indipendenti che descrivono il moto orizzontale sono caratterizzate dallo stesso spettro di risposta o dalle due componenti accelerometriche orizzontali del moto sismico.

Italian code NTC18 - Elastic spectra

Lo spettro di risposta elastico in accelerazione è espresso da una forma spettrale (spettro normalizzato) riferita ad uno smorzamento convenzionale del 5%, moltiplicata per il valore della accelerazione orizzontale massima a_g su sito di riferimento rigido orizzontale.

Sia la forma spettrale che il valore di a_g variano al variare della probabilità di superamento nel periodo di riferimento P_{VR} (vedi § 2.4 e § 3.2.1).

Gli spettri così definiti possono essere utilizzati per strutture con periodo fondamentale minore o uguale a 4,0 s. Per strutture con periodi fondamentali superiori lo spettro deve essere definito da apposite analisi oppure l'azione sismica deve essere descritta mediante storie temporali del moto del terreno.

Italian code NTC18 - Elastic spectra

Lo spettro di risposta (componente orizzontale) è definito a partire dai valori dei seguenti parametri, validi per sito di riferimento su suolo rigido:

- a_g accelerazione orizzontale massima al sito

- F_0 è il fattore che quantifica l'amplificazione spettrale massima, su sito di riferimento rigido orizzontale, ed ha valore minimo pari a 2,2

- T_C^* (valore di riferimento per la determinazione del) periodo di inizio del tratto a velocità costante dello spettro in accelerazione orizzontale.
  Viene quindi definito: $T_C = C_C\ T_C^*$
  dove C_C dipende dalla categoria del sottosuolo

I valori di tali parametri sono forniti dalla NTC18, per tutti i siti considerati, in forma tabellare. Per la pericolosità in particolare (a_g):http://esse1.mi.ingv.it

Italian code NTC18 - Elastic spectra

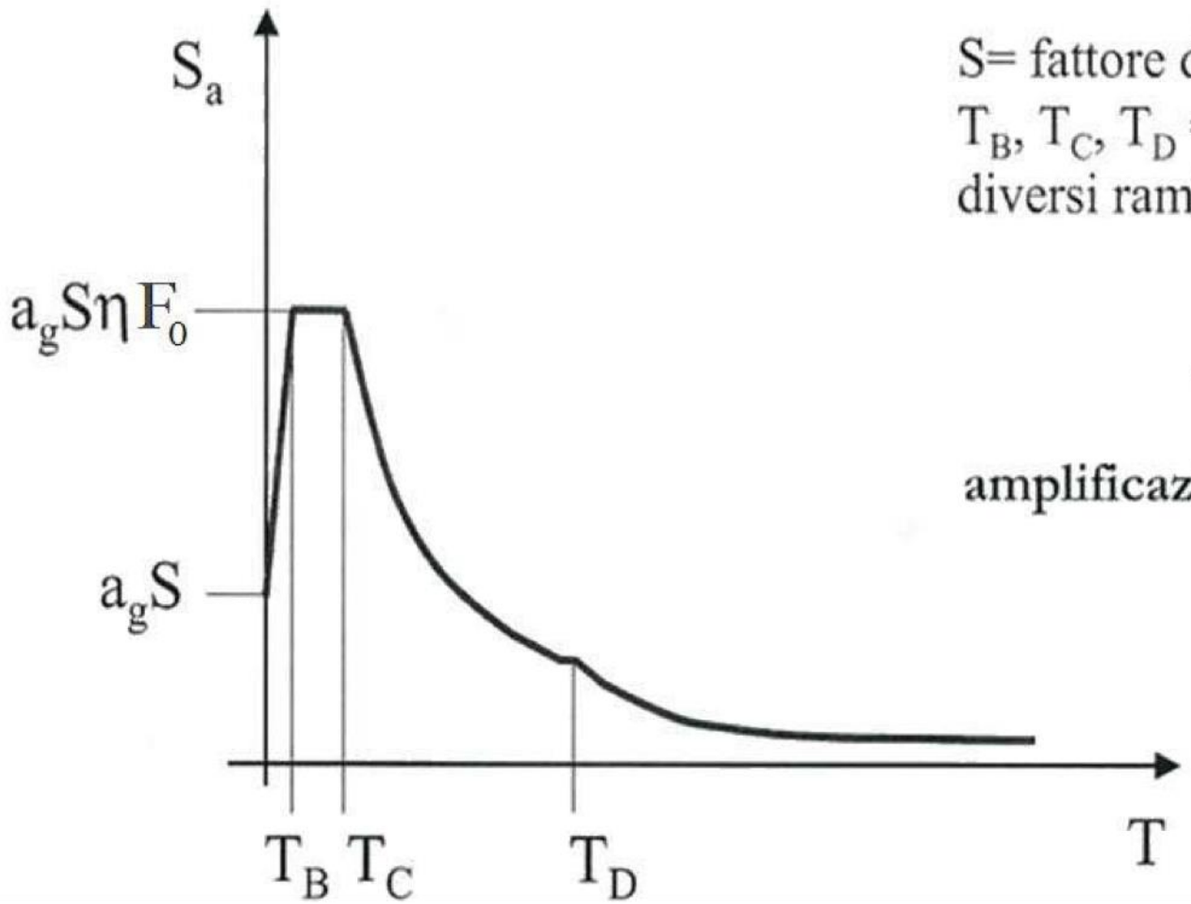

S= fattore di amplificazione
T_B, T_C, T_D = periodo che separano i diversi rami dello spettro

amplificazione del terreno

$$S_e(T) = a_g \cdot S \cdot \eta \cdot F_0 \cdot \left[\frac{T}{T_B} + \frac{1}{\eta \cdot F_0} \cdot \left(1 - \frac{T}{T_B}\right)\right] \qquad S_e(T) = a_g \cdot S \cdot \eta \cdot F_0 \cdot \left(\frac{T_C}{T}\right)$$

$$S_e(T) = a_g \cdot S \cdot \eta \cdot F_0 \qquad S_e(T) = a_g \cdot S \cdot \eta \cdot F_0 \cdot \left(\frac{T_C \cdot T_D}{T^2}\right)$$

- T_B è il periodo corrispondente all'inizio del tratto dello spettro ad accelerazione costante, $T_B = T_C/3$; T_D è il periodo corrispondente all'inizio del tratto a spostamento costante dello spettro, espresso in secondi mediante la relazione: $T_D = 4.0 * a_g/g + 1.6$
- η è il fattore che altera lo spettro elastico per coefficienti di smorzamento viscosi convenzionali ξ diversi dal 5%, ($\eta = [10/(5+\xi)]^{0.5} \geq 0{,}55$), e valutato sulla base di materiali, tipologia strutturale e terreno di fondazione

Italian code NTC18 - from hazard to “design”

- Per ciascun nodo del reticolo di riferimento e per ciascuno dei periodi di ritorno T_R considerati dalla pericolosità sismica, i tre parametri si ricavano riferendosi ai valori corrispondenti al 50–esimo percentile ed attribuendo a F_0 e T_C^* i valori ottenuti imponendo che...

- le forme spettrali in accelerazione, velocità e spostamento previste dalle NTC scartino al minimo dalle corrispondenti forme spettrali previste dalla pericolosità sismica (la condizione di minimo è imposta operando ai minimi quadrati, su spettri di risposta normalizzati ad uno, per ciascun sito e ciascun periodo di ritorno).

Site effects and NTC18 - Elastic spectra & soil

S è il coefficiente che tiene conto della categoria di sottosuolo e delle condizioni topografiche mediante la relazione: $S = S_S \cdot S_T$

S_S è il coefficiente di amplificazione stratigrafica
S_T è il coefficiente di amplificazione topografica

Tab. 3.2.V – *Valori massimi del coefficiente di amplificazione topografica* S_T

Categoria topografica	Ubicazione dell'opera o dell'intervento	S_T
T1	-	1,0
T2	In corrispondenza della sommità del pendio	1,2
T3	In corrispondenza della cresta di un rilievo con pendenza media minore o uguale a 30°	1,2
T4	In corrispondenza della cresta di un rilievo con pendenza media maggiore di 30°	1,4

Tab. 3.2.IV – *Espressioni di* S_S *e di* C_C

Categoria sottosuolo	S_S	C_C
A	1,00	1,00
B	$1,00 \le 1,40 - 0,40 \cdot F_o \cdot \frac{a_g}{g} \le 1,20$	$1,10 \cdot (T_C^*)^{-0,20}$
C	$1,00 \le 1,70 - 0,60 \cdot F_o \cdot \frac{a_g}{g} \le 1,50$	$1,05 \cdot (T_C^*)^{-0,33}$
D	$0,90 \le 2,40 - 1,50 \cdot F_o \cdot \frac{a_g}{g} \le 1,80$	$1,25 \cdot (T_C^*)^{-0,50}$
E	$1,00 \le 2,00 - 1,10 \cdot F_o \cdot \frac{a_g}{g} \le 1,60$	$1,15 \cdot (T_C^*)^{-0,40}$

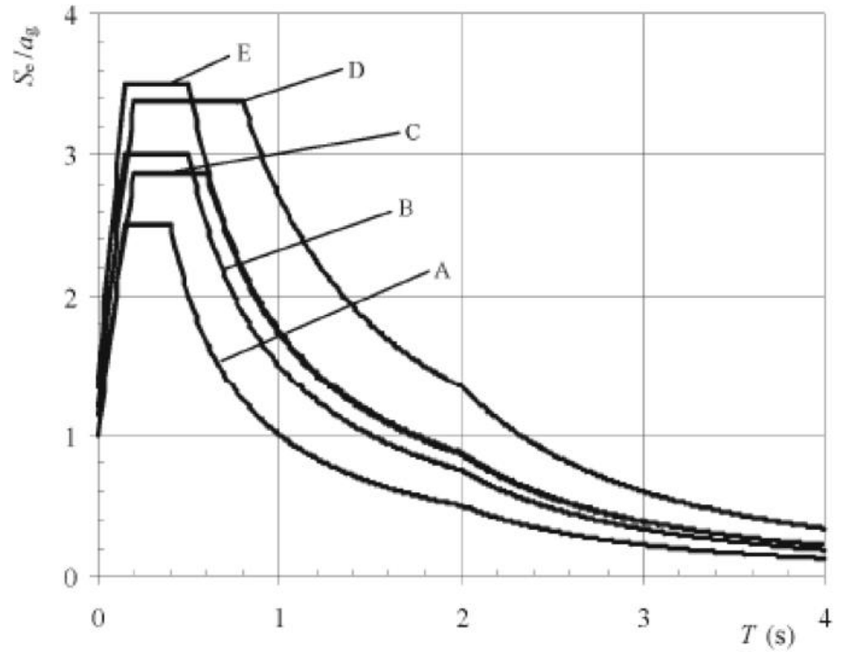

Site effects and NTC18 - Soil classification

3.2.2 CATEGORIE DI SOTTOSUOLO E CONDIZIONI TOPOGRAFICHE

Categorie di sottosuolo

Ai fini della definizione dell'azione sismica di progetto, l'effetto della risposta sismica locale si valuta mediante specifiche analisi, da eseguire con le modalità indicate nel § 7.11.3. In alternativa, qualora le condizioni stratigrafiche e le proprietà dei terreni siano chiaramente riconducibili alle categorie definite nella Tab. 3.2.II, si può fare riferimento a un approccio semplificato che si basa sulla classificazione del sottosuolo in funzione dei valori della velocità di propagazione delle onde di taglio, V_S. I valori dei parametri meccanici necessari per le analisi di risposta sismica locale o delle velocità V_S per l'approccio semplificato costituiscono parte integrante della caratterizzazione geotecnica dei terreni compresi nel volume significativo, di cui al § 6.2.2.

Tab. 3.2.II – *Categorie di sottosuolo che permettono l'utilizzo dell'approccio semplificato.*

Categoria	Caratteristiche della superficie topografica
A	*Ammassi rocciosi affioranti o terreni molto rigidi* caratterizzati da valori di velocità delle onde di taglio superiori a 800 m/s, eventualmente comprendenti in superficie terreni di caratteristiche meccaniche più scadenti con spessore massimo pari a 3 m.
B	*Rocce tenere e depositi di terreni a grana grossa molto addensati o terreni a grana fina molto consistenti*, caratterizzati da un miglioramento delle proprietà meccaniche con la profondità e da valori di velocità equivalente compresi tra 360 m/s e 800 m/s.
C	*Depositi di terreni a grana grossa mediamente addensati o terreni a grana fina mediamente consistenti* con profondità del substrato superiori a 30 m, caratterizzati da un miglioramento delle proprietà meccaniche con la profondità e da valori di velocità equivalente compresi tra 180 m/s e 360 m/s.
D	*Depositi di terreni a grana grossa scarsamente addensati o di terreni a grana fina scarsamente consistenti*, con profondità del substrato superiori a 30 m, caratterizzati da un miglioramento delle proprietà meccaniche con la profondità e da valori di velocità equivalente compresi tra 100 e 180 m/s.
E	*Terreni con caratteristiche e valori di velocità equivalente riconducibili a quelle definite per le categorie C o D,* con profondità del substrato non superiore a 30 m.

Site effects and NTC18 - $V_{S,eq}$

La classificazione del sottosuolo si effettua in base alle condizioni stratigrafiche ed ai valori della velocità equivalente di propagazione delle onde di taglio, $V_{S,eq}$ (in m/s), definita dall'espressione:

$$V_{S,eq} = \frac{H}{\sum_{i=1,N} \frac{h_i}{V_{S,i}}} \quad [m / s]$$

con h_i spessore dell'i-esimo strato; $V_{S,i}$ velocità delle onde di taglio nell'i-esimo strato; N numero di strati; H profondità del substrato, definito come quella formazione costituita da roccia o terreno molto rigido, caratterizzata da V_S non inferiore a 800 m/s.

Per depositi con profondità H del substrato superiore a 30 m, la velocità equivalente delle onde di taglio $V_{S,eq}$ è definita dal parametro $V_{S,30}$, ottenuto ponendo H=30 m nella precedente espressione e considerando le proprietà degli strati di terreno fino a tale profondità.

V_{S30}

Nelle definizioni precedenti Vs_{30} è la velocità media di propagazione dei primi 30 m di profondità delle onde di taglio e viene calcolata con la seguente espressione:

$$V_{S30} = \frac{30}{\sum_{i=1,N} \frac{h_i}{V_i}} \qquad [m / s]$$

dove h_i e V_i indicano lo spessore (in m) e la velocità delle onde di taglio (per deformazioni di taglio $\gamma < 10^{-6}$) dello strato i-esimo, per un totale di N strati presenti nei 30 m superiori.

Site effects and NTC18 - Topography

Per condizioni topografiche complesse è necessario predisporre specifiche analisi di risposta sismica locale. Per configurazioni superficiali semplici si può adottare la seguente classificazione (Tab. 3.2.III):

T1 Superficie pianeggiante, pendii e rilievi isolati con inclinazione media i≤15°

T2 Pendii con inclinazione media i>15°

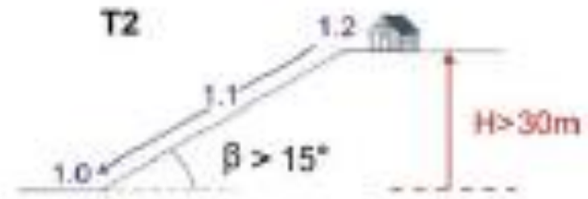

T3 Rilievi con larghezza in cresta molto minore che alla base e inclinazione media 15≤i≤30°

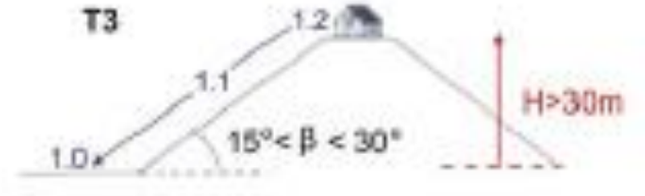

T4 Rilievi con larghezza in cresta molto minore che alla base e inclinazione media i>30°

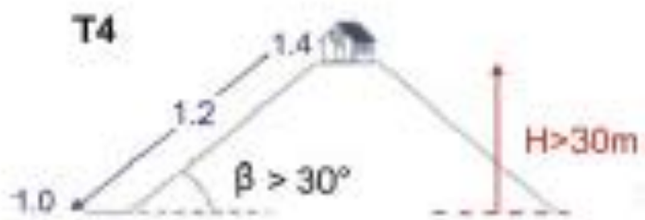

Le su esposte categorie topografiche si riferiscono a configurazioni geometriche prevalentemente bidimensionali, creste o dorsali allungate, e devono essere considerate nella definizione dell'azione sismica se di altezza maggiore di 30 m.

Site effects and NTC18 - Topography

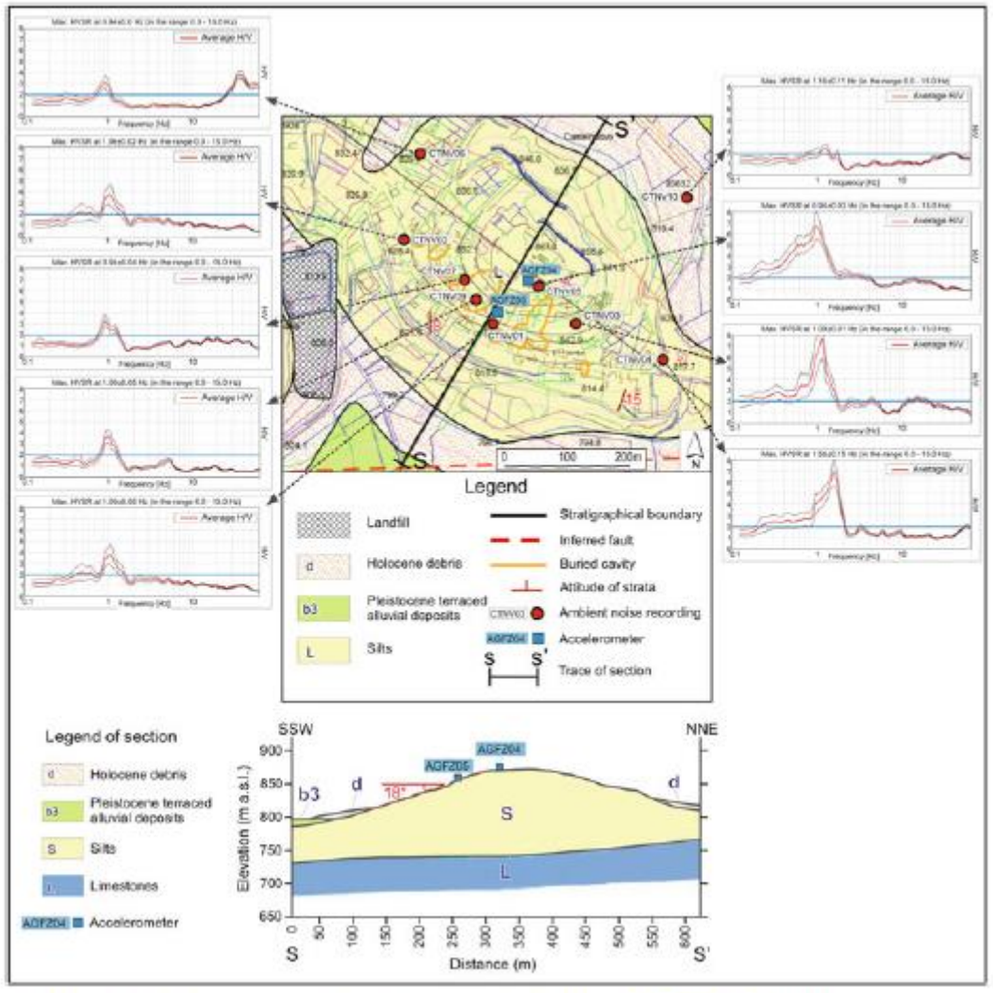

Fig. 2 Geological map and section for Castelnuovo (modified from Gallipoli et al. 2011)

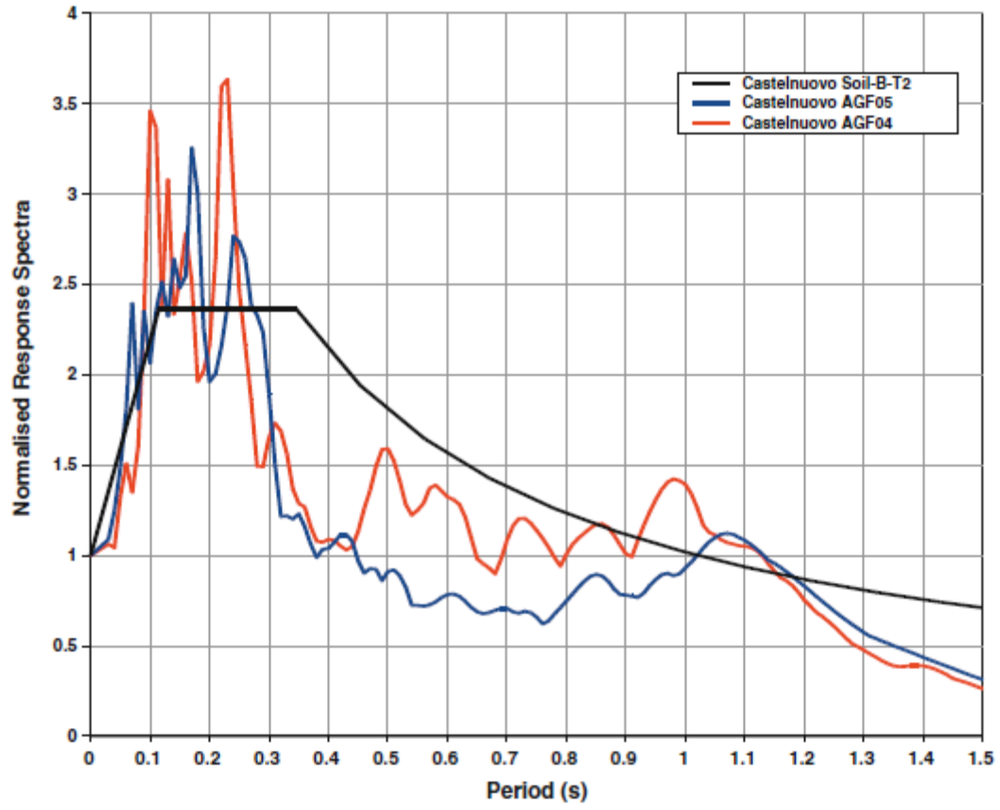

Fig. 5 Normalised Response spectra of the M 5.1 event of April 9, 2009 recorded at two sites in Castelnuovo compared with code provision

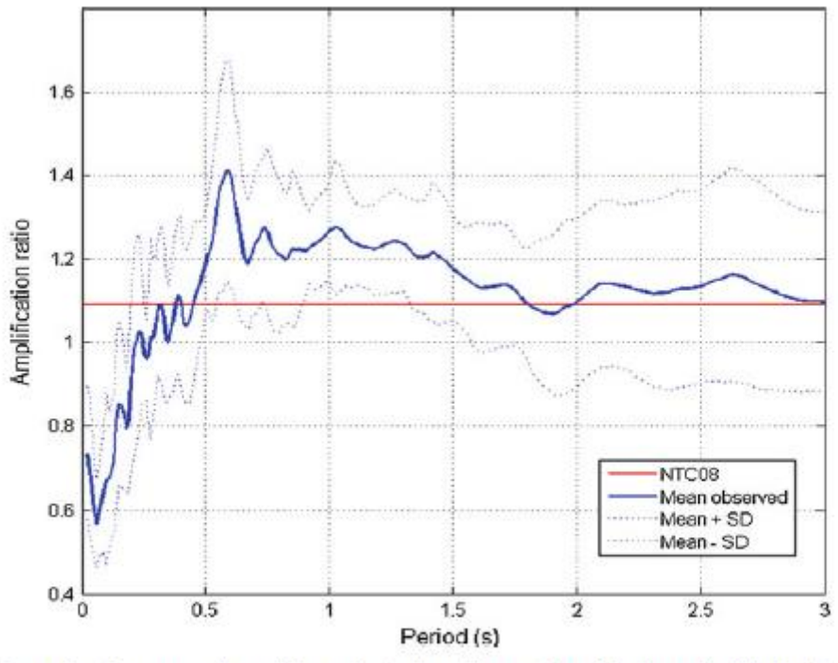

Fig. 6 Comparison between code provisions ratio (*red*) and observed amplification ratio (*blue*) in Castelnuovo

Site effects and NTC18 - Topography

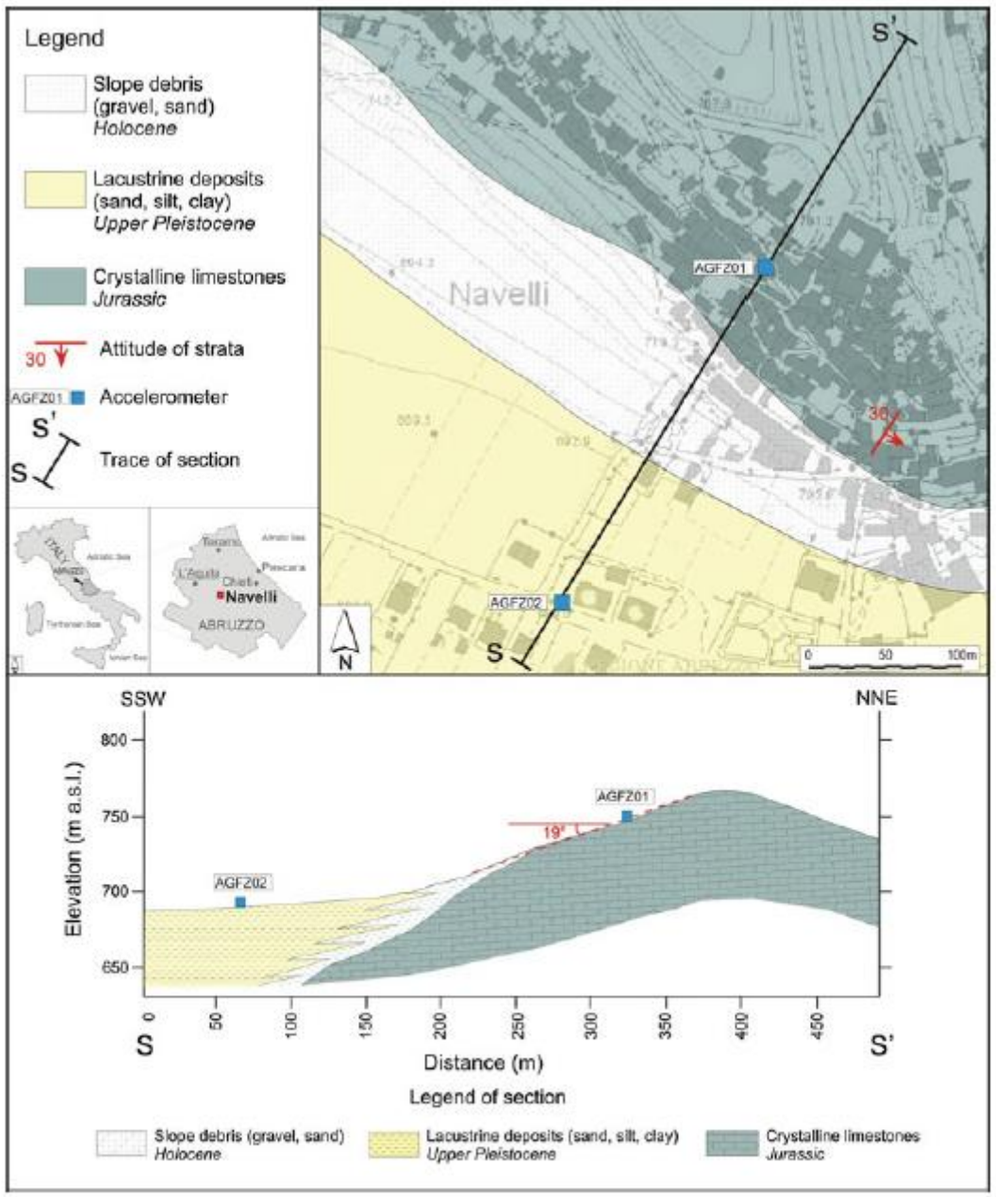

Fig. 7 Geological map and section for Navelli

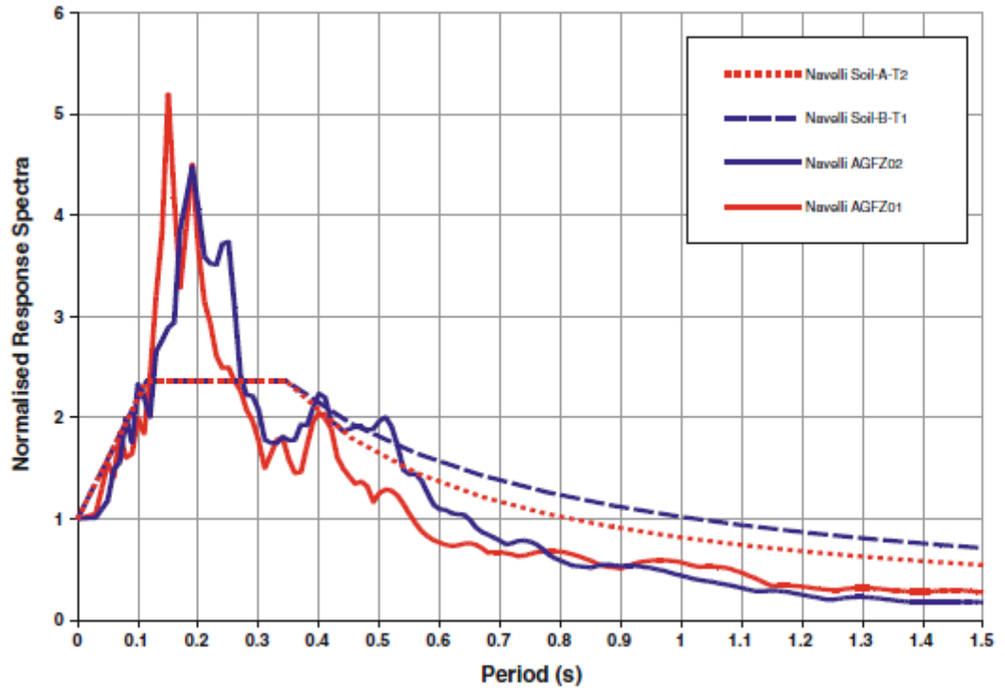

Fig. 10 Normalised Response spectra of the M 5.1 event of April 9, 2009 recorded at two sites in Navelli compared with code provision

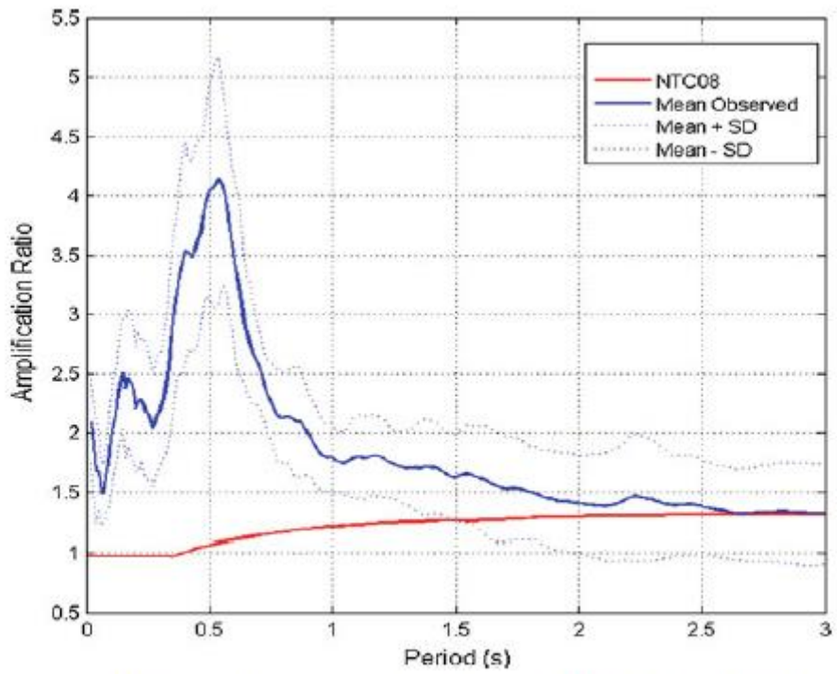

Fig. 11 Comparison between code provisions (*red*) and observed amplification ratio (*blue*) in Navelli

NTC18 - Time histories (3.2)

Gli stati limite, ultimi e di esercizio, possono essere verificati mediante l'uso di storie temporali del moto del terreno artificiali o naturali...
L'uso di storie temporali del moto del terreno artificiali non è ammesso nelle analisi dinamiche di opere e sistemi geotecnici.

L'uso di storie temporali del moto del terreno generate mediante simulazione del meccanismo di sorgente e della propagazione è ammesso a condizione che siano adeguatamente giustificate le ipotesi relative alle caratteristiche sismogenetiche della sorgente e del mezzo di propagazione e che, negli intervalli di periodo sopraindicati, l'ordinata spettrale media non presenti uno scarto in difetto superiore al 20% rispetto alla corrispondente componente dello spettro elastico.

L'uso di storie temporali del moto del terreno naturali o registrate è ammesso a condizione che la loro scelta sia rappresentativa della sismicità del sito e sia adeguatamente giustificata in base alle caratteristiche sismogenetiche della sorgente, alle condizioni del sito di registrazione, alla magnitudo, alla distanza dalla sorgente e alla massima accelerazione orizzontale attesa al sito.

NTC18 - Space variability (3.2.4.1)

Nei punti di contatto con il terreno di opere con sviluppo planimetrico significativo, il moto sismico può avere caratteristiche differenti, a causa del carattere asincrono del fenomeno di propagazione, delle disomogeneità e delle discontinuità eventualmente presenti, e della diversa risposta locale del terreno.

Degli effetti sopra indicati deve tenersi conto quando essi possono essere significativi e in ogni caso quando le condizioni di sottosuolo siano così variabili lungo lo sviluppo dell’opera da richiedere l’uso di accelerogrammi o di spettri di risposta diversi.

NTC18 - Local response (7.11.3)

Il moto generato da un terremoto in un sito dipende dalle particolari condizioni locali, cioè dalle caratteristiche topografiche e stratigrafiche del sottosuolo e dalle proprietà fisiche e meccaniche dei terreni e degli ammassi rocciosi di cui è costituito. Alla scala della singola opera o del singolo sistema geotecnico, l'analisi della risposta sismica locale consente quindi di definire le modifiche che il segnale sismico di ingresso subisce, a causa dei suddetti fattori locali.

...

Nelle analisi di risposta sismica locale, l'azione sismica di ingresso è descritta in termini di storia temporale dell'accelerazione (accelerogrammi) su di un sito di riferimento rigido ed affiorante con superficie topografica orizzontale.

L'applicazione del metodo richiede la valutazione dell'accelerazione critica, che deve essere valutata con i valori caratteristici dei parametri di resistenza, e dell'azione sismica di progetto, che deve essere rappresentata mediante storie temporali delle accelerazioni. Gli accelerogrammi impiegati nelle analisi, in numero non inferiore a 7, devono essere rappresentativi della sismicità del sito e la loro scelta deve essere adeguatamente giustificata (vedi § 3.2.3.6). Non è ammesso l'impiego di accelerogrammi artificiali.

SURFACE TOPOGRAPHY EFFECTS

(convexity) sensitivity to:
a) type of wavefield
b) angle of incidence
c) shape and sharpness

GROUNDSHAKING SITE EFFECTS

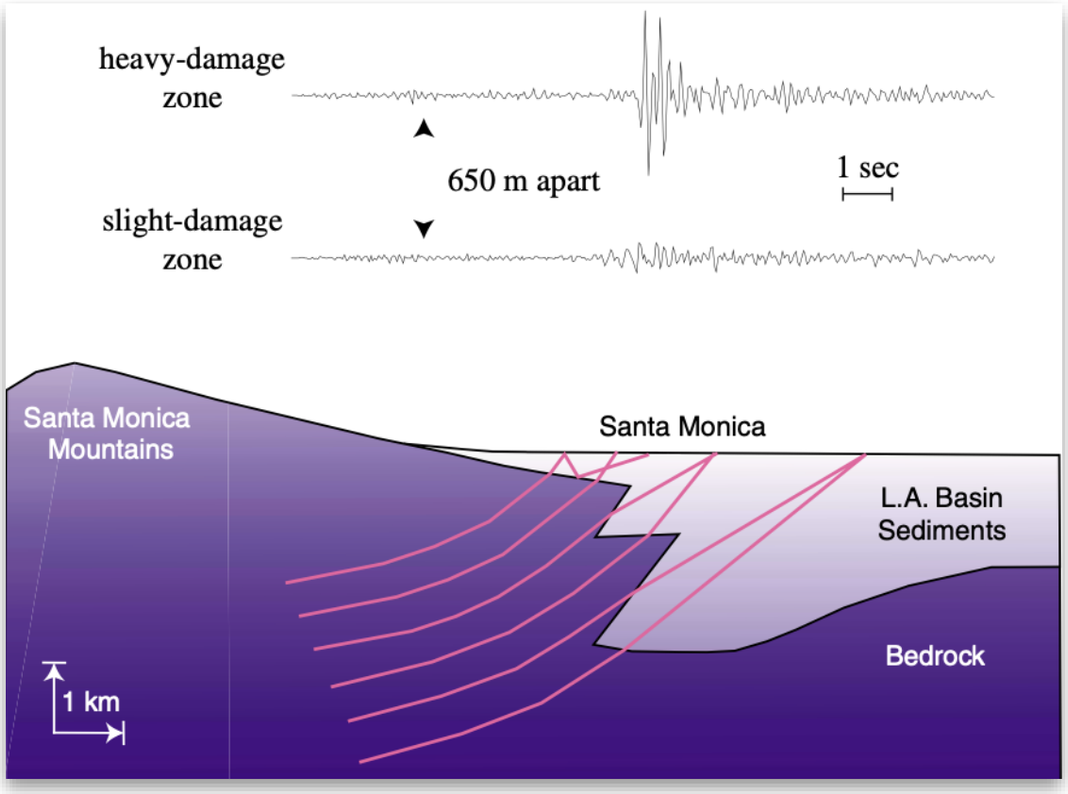

SOFT SURFACE LAYERING

a) 1-D: trapping of waves for impedance contrast; vertical resonances

$f_n=[(2n+1)\beta]/4H$; $A\approx(\rho_2 v_2)/(\rho_1 v_1)$

b) 2-D, 3-D: complex energy focusing; diffraction effects; basin edge waves

Effetti di sito 1D

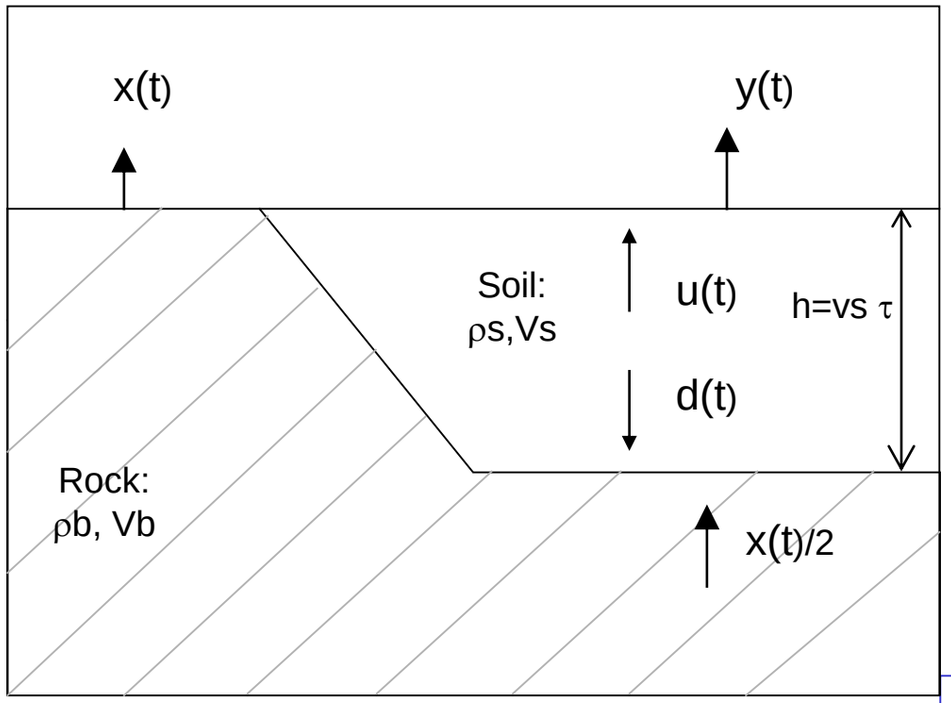

$$|H(f)| = \left(\frac{(1+r)^2}{1+2r\cos(4\pi f \tau)+r^2} \right)^{1/2}$$

$$r = \frac{p_b V_b - p_s V_s}{p_b V_b + p_s V_s} = \frac{c-1}{1+c}$$

$\tau = h/V_s$

f_o=400/(4*100)=1Hz

$$C = \left(\frac{2800*1200}{2600*400} \right) \sim 3.23$$

$|H(f)|$ Massimo per f=f_o
Tale che $\cos(4\pi f\tau)=-1$ ⇒ $f_o = \frac{1}{4\tau} = \frac{V_s}{4h}$

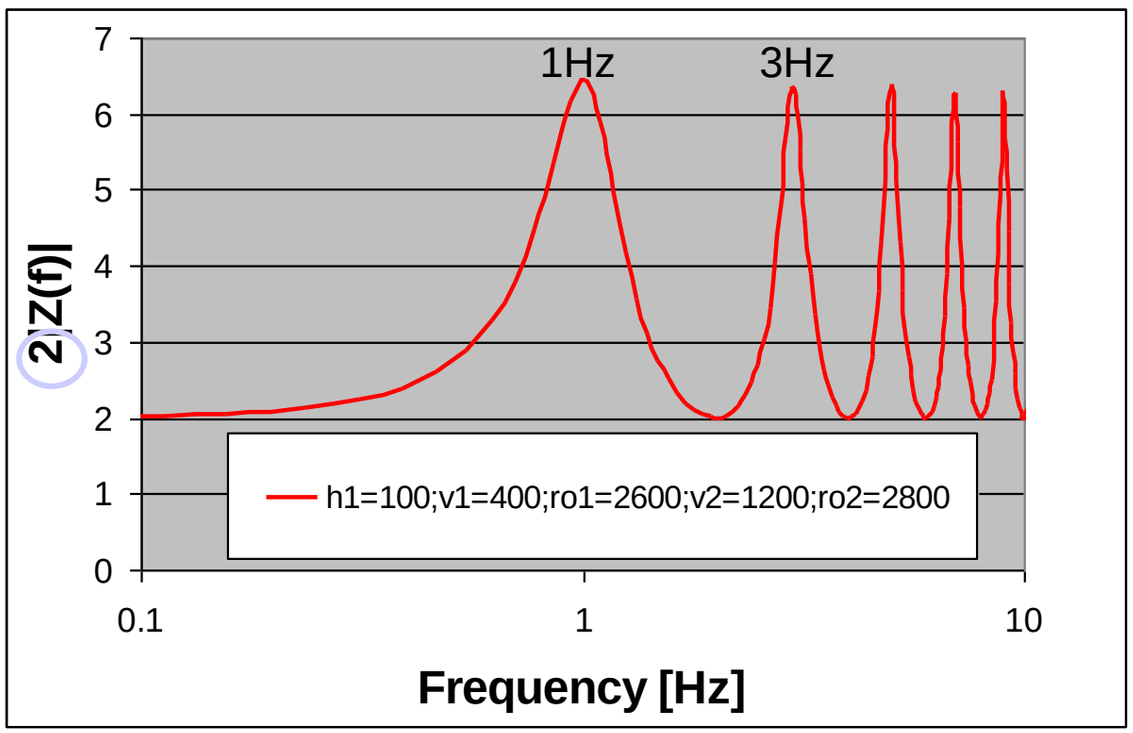

Esistono diversi massimi a frequenze:

$$f_n = \frac{V_s}{4h}(2n+1) \quad \text{with } n = 0,1,2,3,\ldots$$

(n=0 modo fondamentale
n>0 modi superiori)

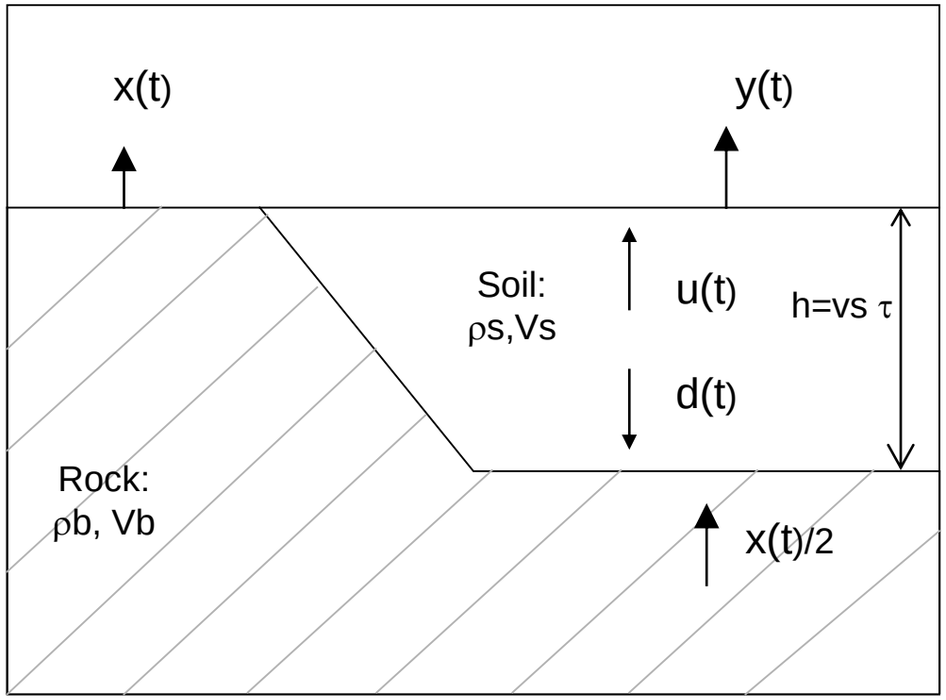

$$|H(f)| = \left(\frac{(1+r)^2}{1+2r\cos(4\pi ft)+r^2} \right)^{1/2}$$

Per f=f_n $|H(f)|$ diventa

f_o=400/(4*100)=1Hz

$$C = \left(\frac{2800*1200}{2600*400} \right) \sim 3.23$$

$$|H(f_n)| = \left(\frac{(1+r)^2}{1-2r+r^2} \right)^{1/2} = \frac{1+r}{1-r} = c$$

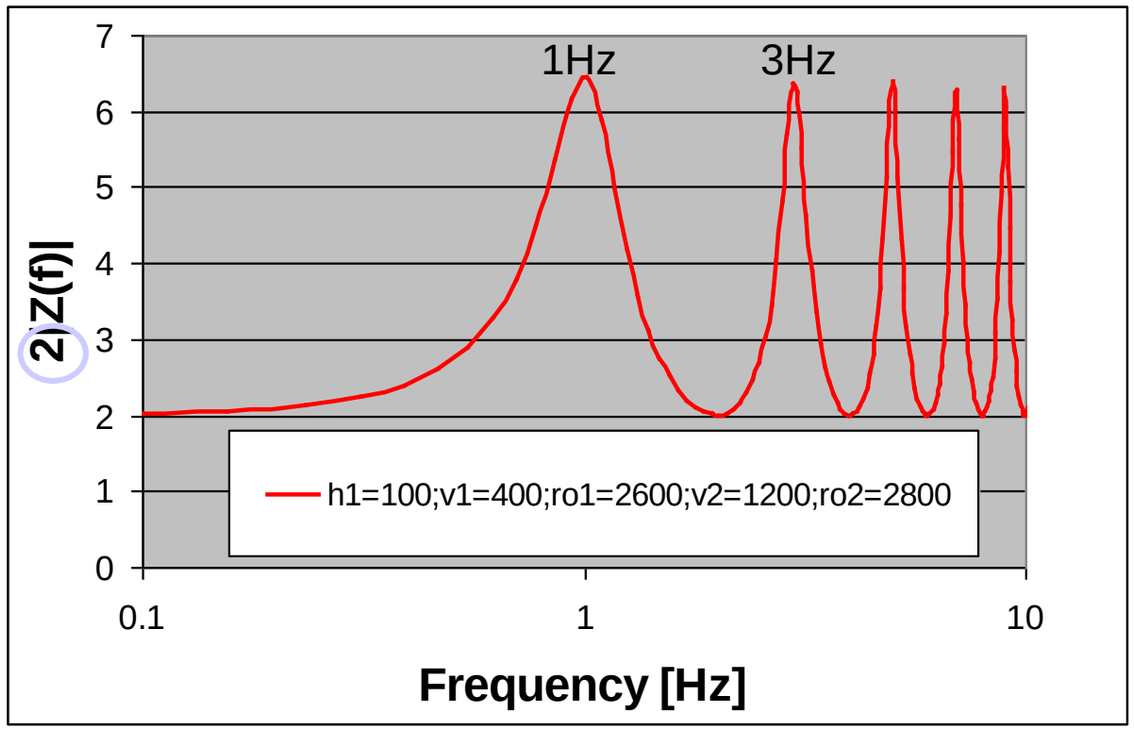

Il contrasto di impedenza determina l'ampiezza del picco (modello elastic)

1D site effects

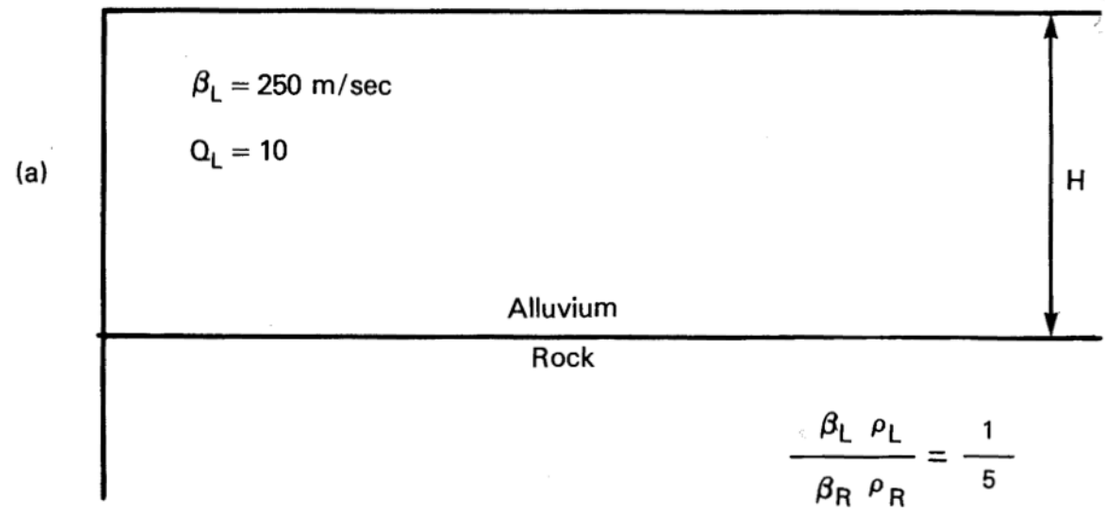

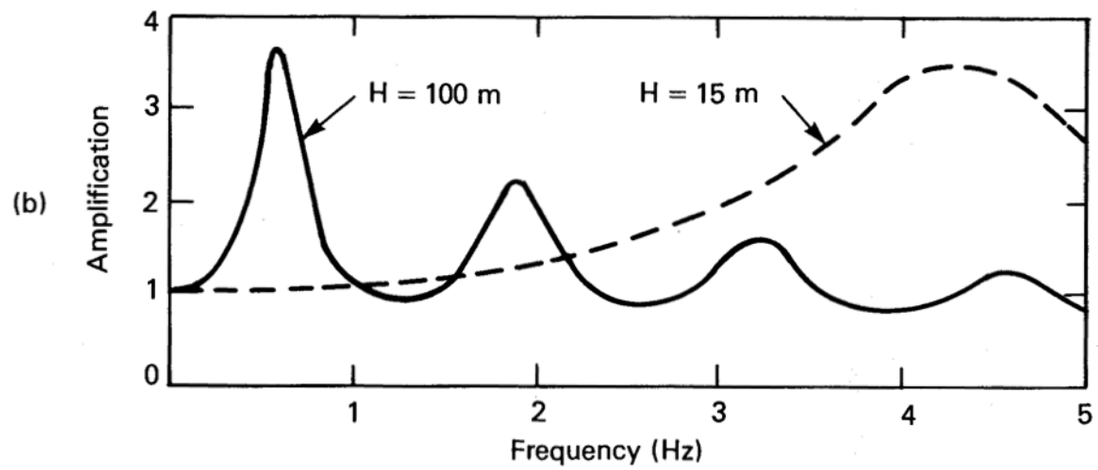

FIGURE 8.2 Model of site amplification. (a) Crossection of alluvial layer of thickness H overlying rock. Impedance of rock is five times impedance of alluvium. (b) Amplification factors in the frequency domain for two thicknesses of alluvium (after Murphy and O'Brien 1978).

$$\left|U_L(\omega)\right| = 2.0\left[\cos^2(k_L H) + \left(\frac{\rho_L v_L}{\rho_H v_H}\right)\sin^2(k_L H)^2\right]^{-1/2}$$

Site effect estimation

1) <u>Direct methods</u>:

Earthquake based:

<u>With reference site</u>: Standard Spectral Ratio (SSR), Generalised Inversion Technique (GIT),

<u>Without a reference site</u>: Horizontal-to-Vertical Spectral Ratio (H/V)

Seismic noise based:

<u>With reference site</u>: Standard Spectral Ratio (SSR), Spectra analysis,

<u>Without a reference site</u>: Horizontal-to-Vertical Spectral Ratio (H/V)

2) ***<u>Indirect methods</u>***: active (SASW, MASW) and passive (seismic noise) array analysis. Numerical simulations

EMPIRICAL TECHNIQUES FOR SITE EFFECT ESTIMATION

WEAK (AND STRONG) MOTION

a) S/B spectral ratio (Borcherdt, 1970)

b) generalized inversion scheme (Andrews, 1986)

c) coda waves analysis (Margheriti et al., 1994)

d) parametrized source and path inversion (Boatwright et al., 1991)

e) H/V spectral ratio (receiver function) (Lermo et al., 1993)

$$R_{ij}(\omega) = E_i(\omega) \cdot P_{ij}(\omega) \cdot S_j(\omega)$$

MICROTREMORS

a) peak frequencies examination

b) S/B spectral ratio

c) H/V spectral ratio (Nagoshi, 1971; Nakamura, 1989)

d) array analysis (Malagnini et al., 1993)

Earthquake based Reference Site methods

1) *Standard spectral ratio*: spectral ratio between the same ground motion components of 2 close stations

2) *Generalized inversion techniques*: a spectral inversion is performed in order to correct for the path effects if the reference station is faraway from the actual one.

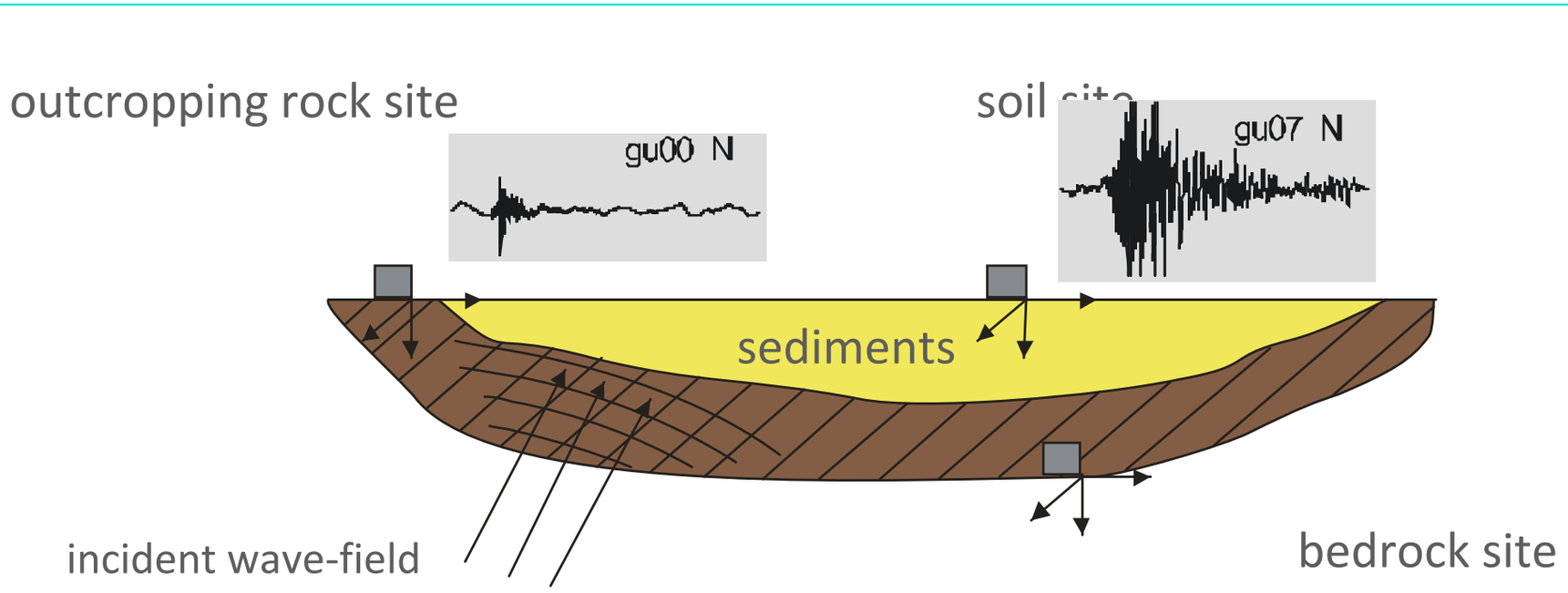

Fourier Amplitude Spectra A(f)

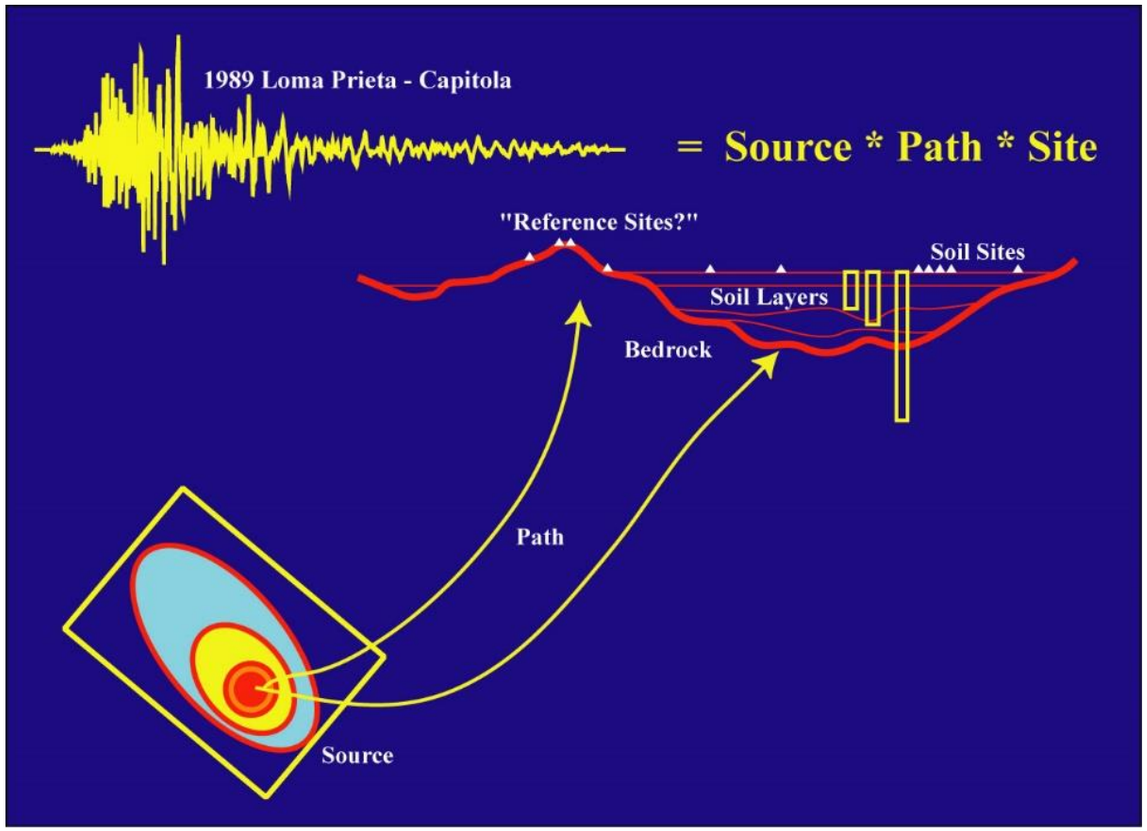

Amplitude

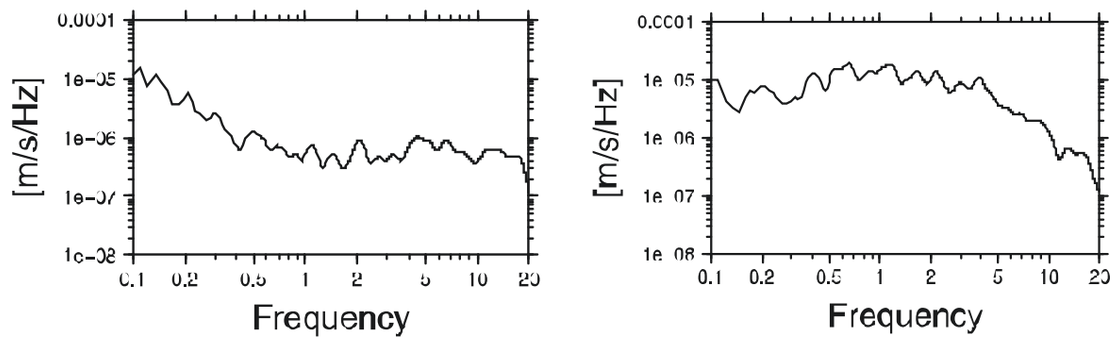

Amplification function

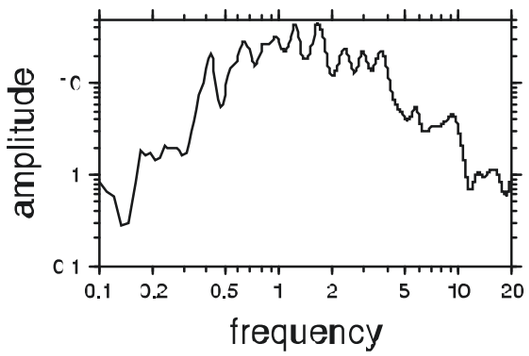

$$\frac{A_{soil}(f)}{A_{rock}(f)} = \frac{Source_{soil}\, Path_{soil}\, Site_{soil}}{Source_{rock}\, Path_{rock}\, Site_{rock}} = \frac{Path_{soil}\, Site_{soil}}{Path_{rock}} = Site_{soil}$$

=1

(reference)

Window selection in time domain

Fourier amplitude and smoothing

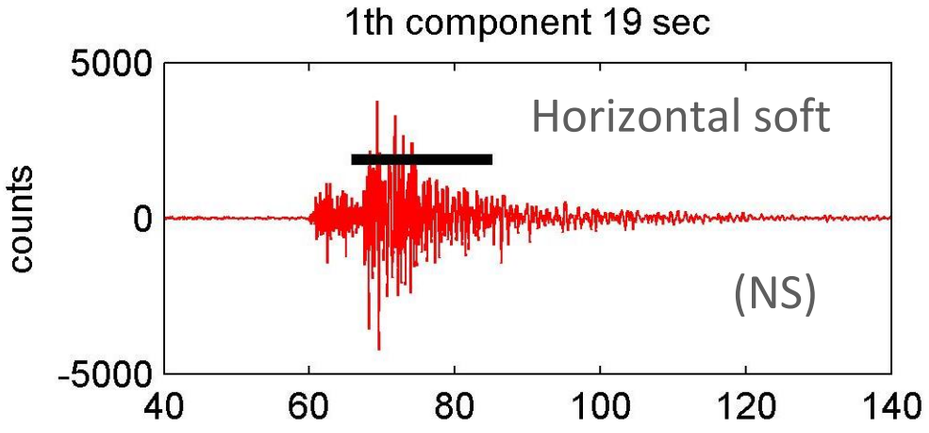

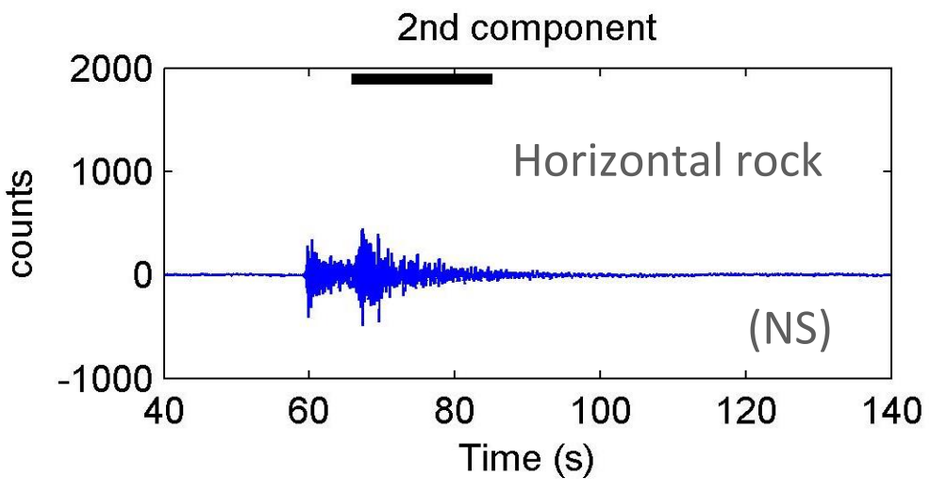

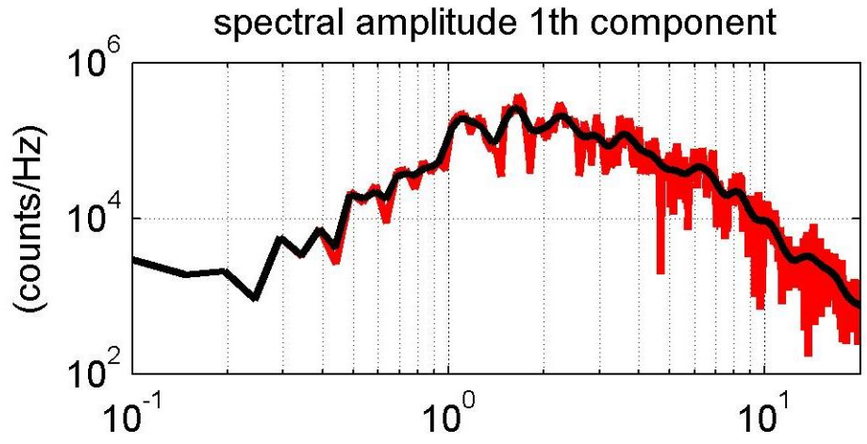

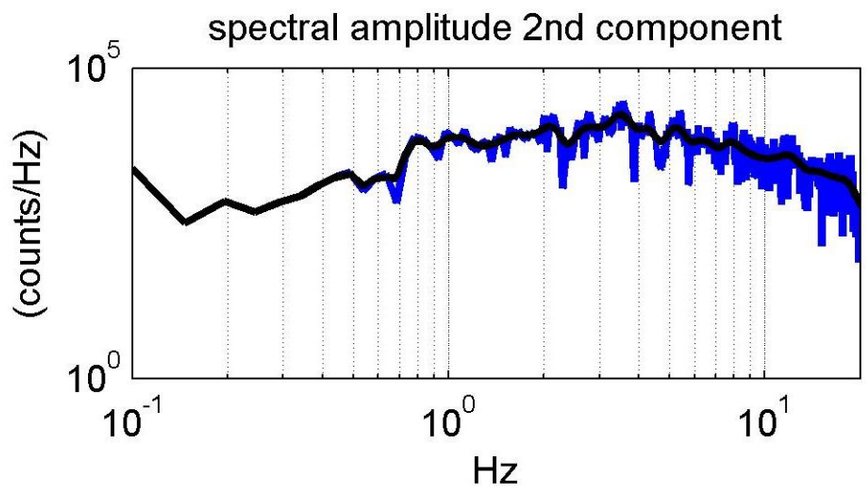

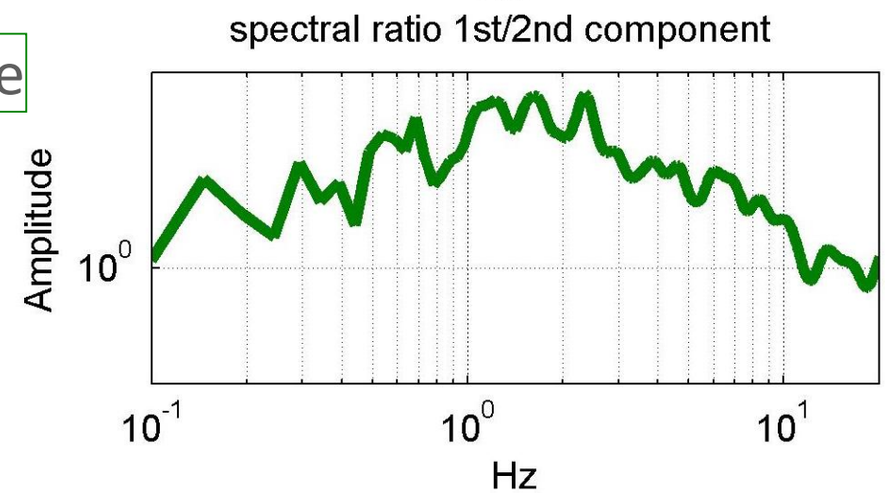

Average

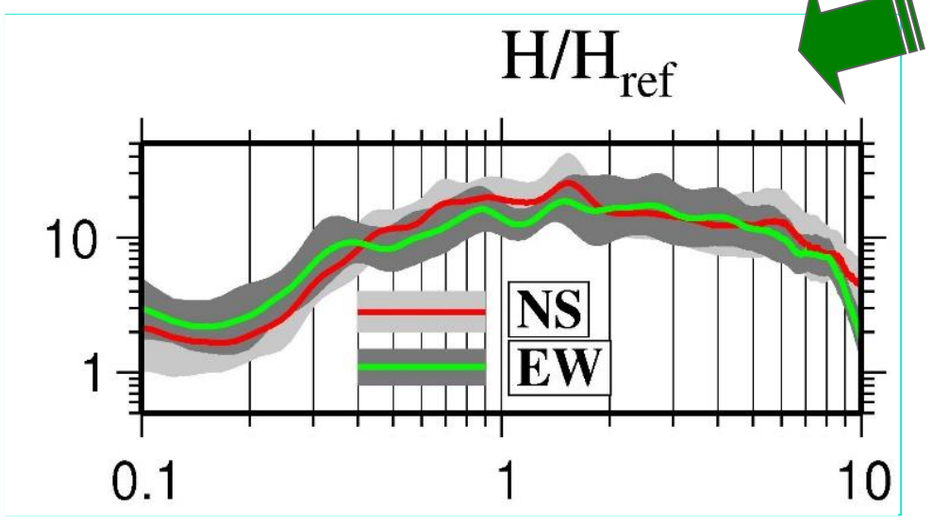

H(f)

H(f)

=

|SSR(f)|

UNIVERSITÀ DEGLI STUDI DI TRIESTE

Standard spectral ratios: the example of Gubbio basin (Italy)

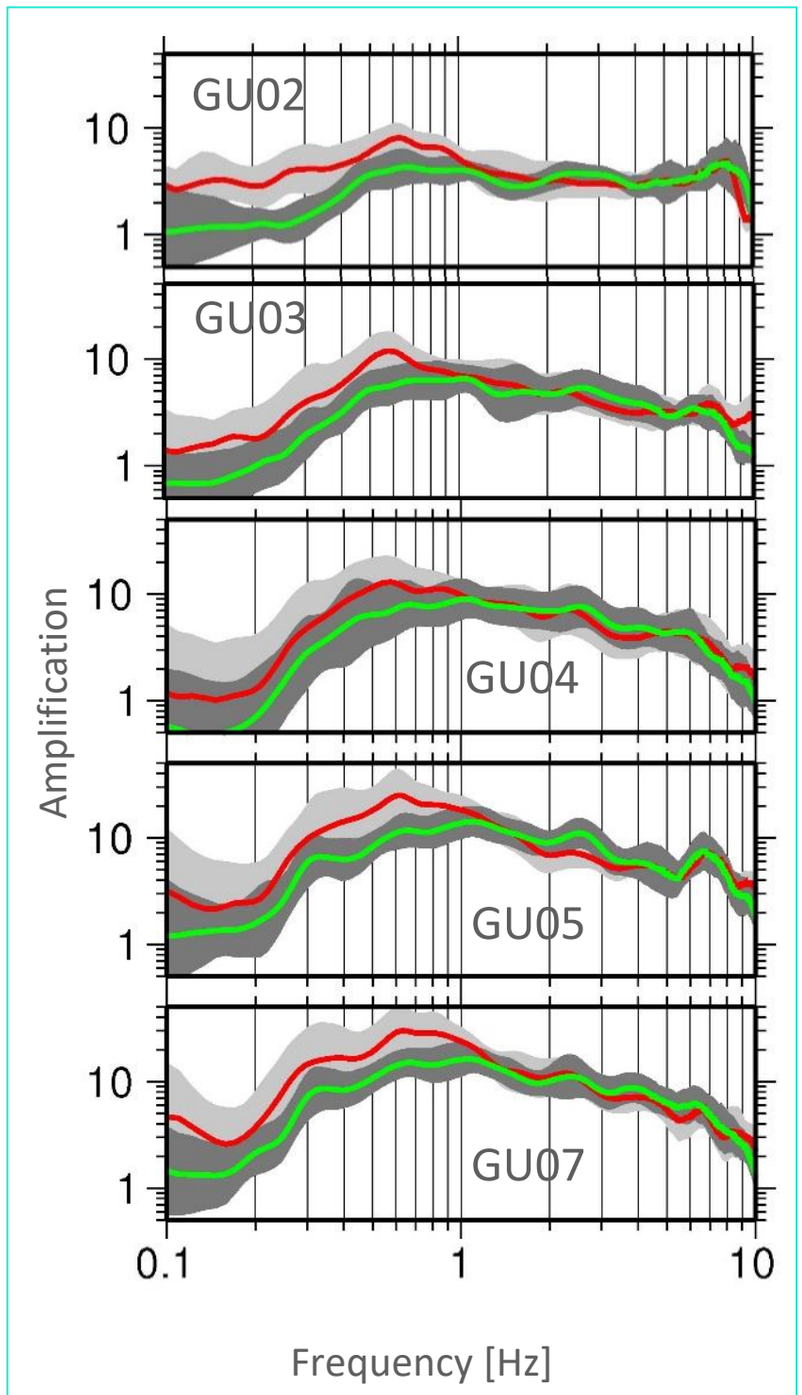

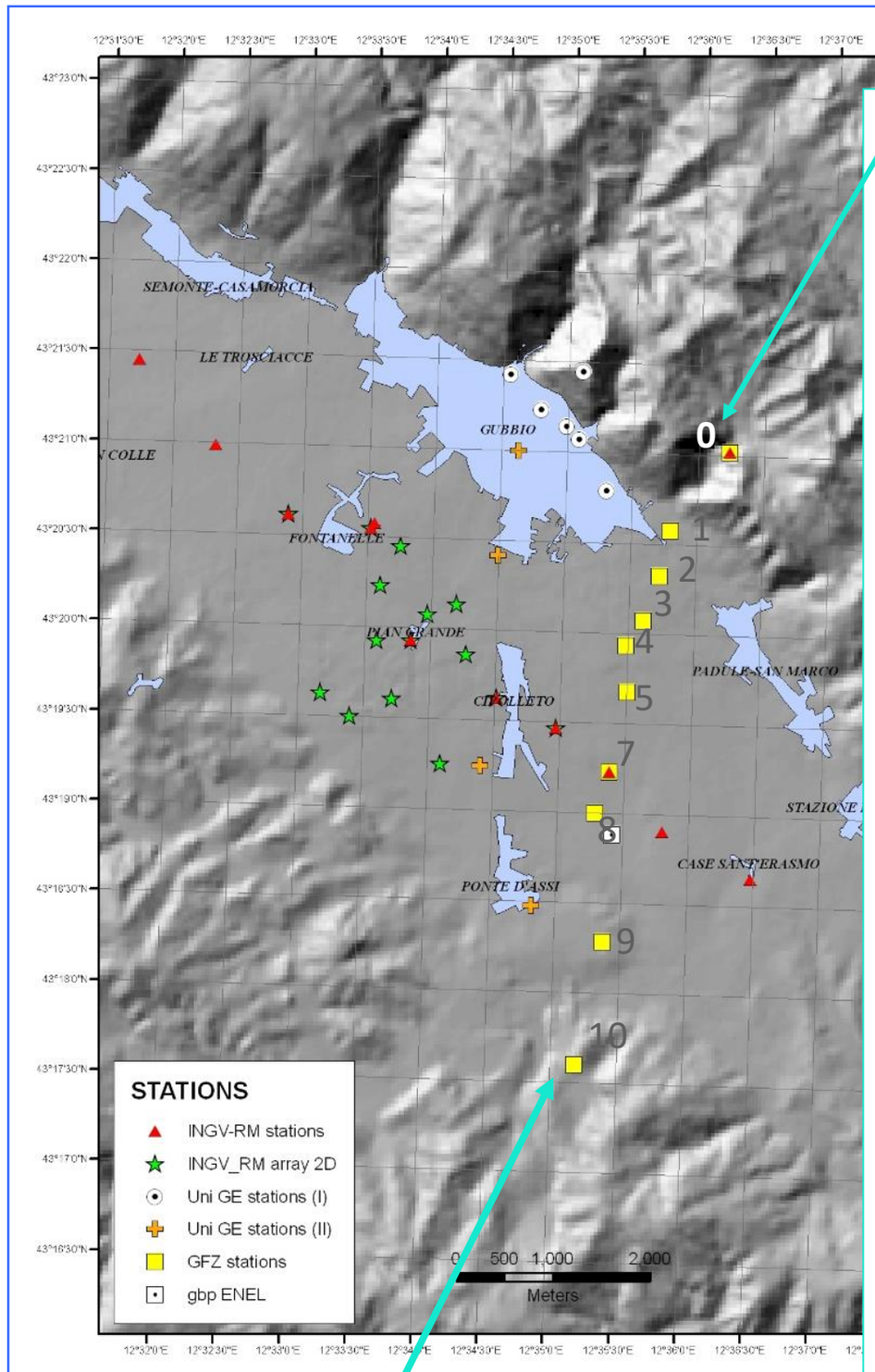

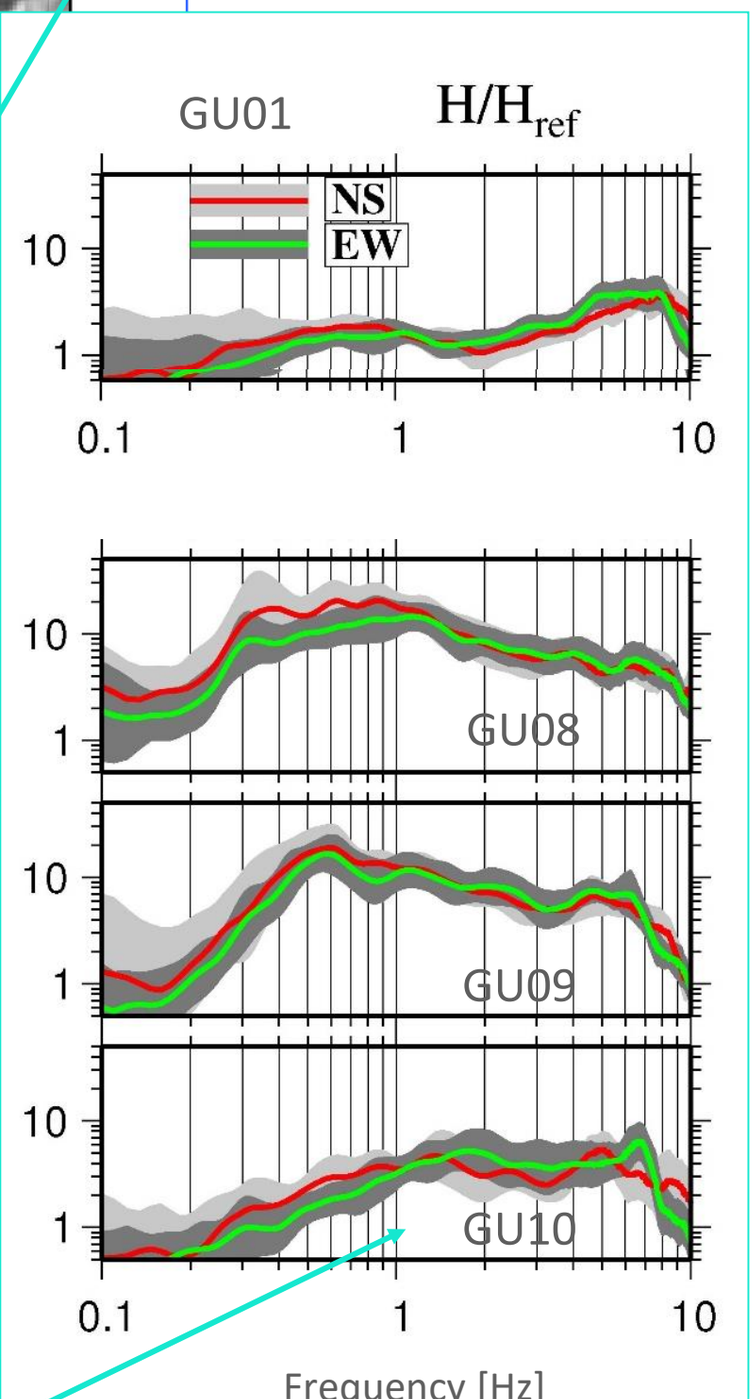

another rock station but ……

Bindi et al. (2009)

Important issues in SRE

- Near surface effects: impedance contrast, velocity
  - geological maps, V_{S30}
  - Basin effects
  - Basin-edge induced waves
  - Subsurface focusing

In SHA the site effect should be defined as the average behavior, relative to other sites, given all potentially damaging earthquakes.

This produces an intrinsic variability with respect to different earthquake locations, that cannot exceed the difference between sites

Amplification patterns...

....may vary greatly among the earthquake scenarios, considering different source locations (and rupture ...)

SCEC Phase 3 Report

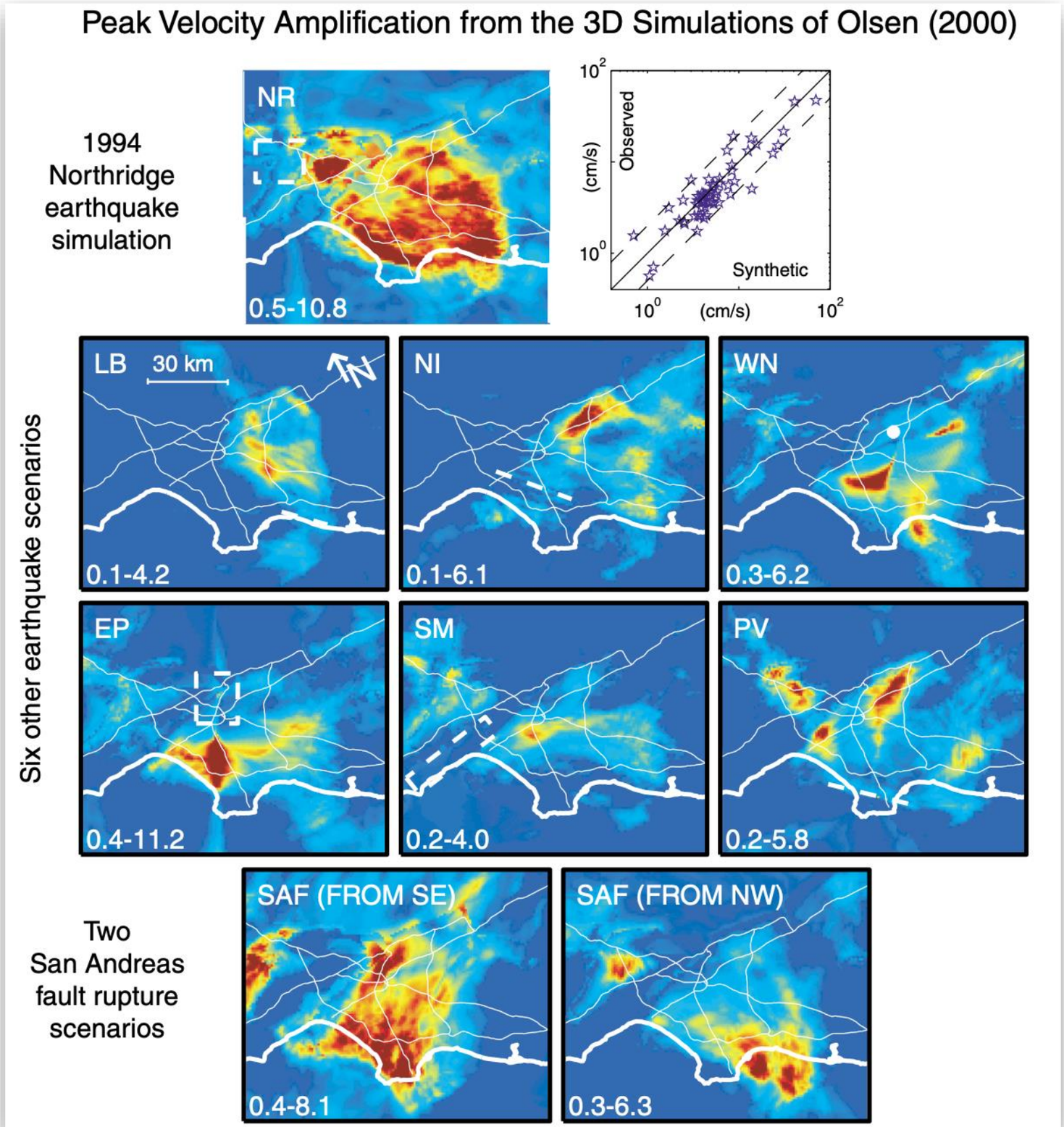

Seismic Source effects

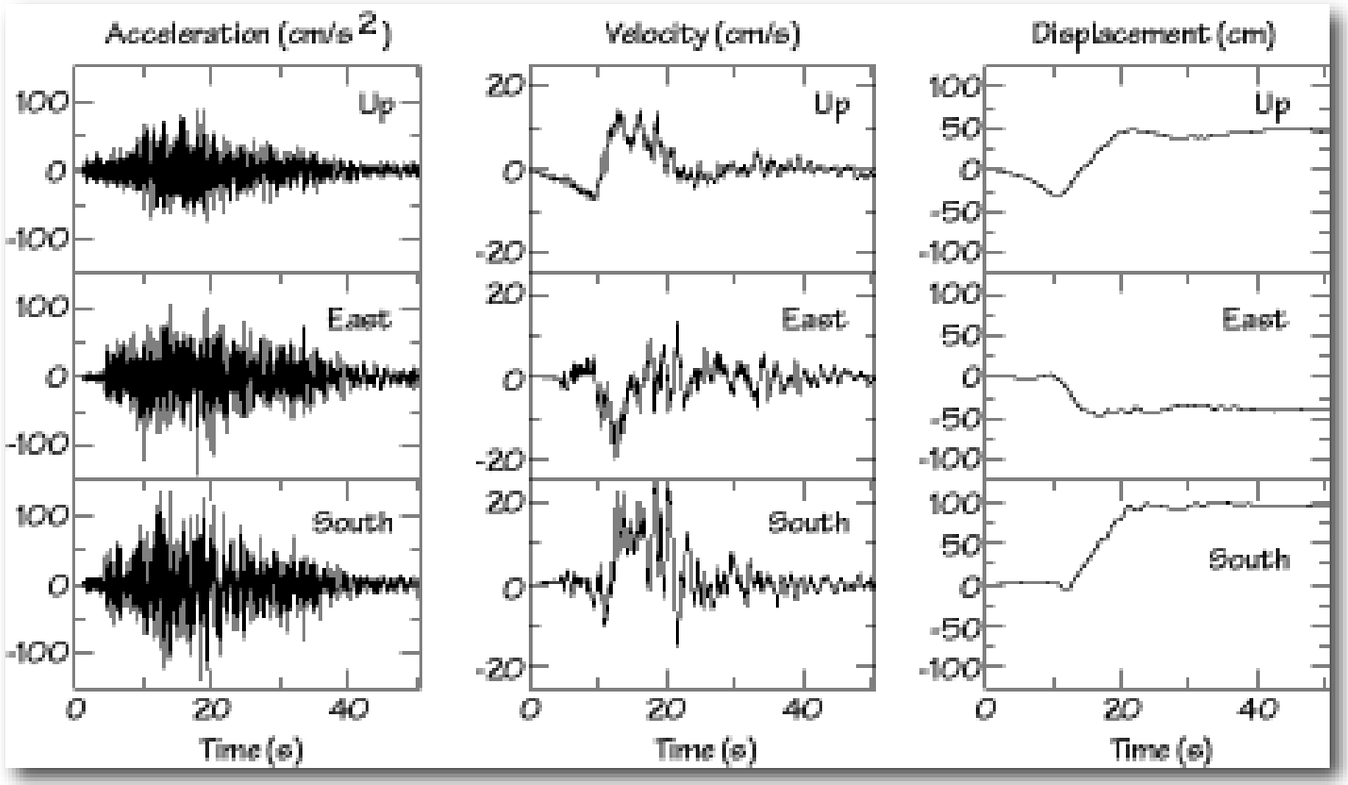

Michoacan, 1985

Fling & Directivity

aka

Near-field & Near-source

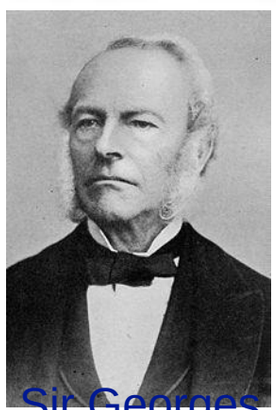

Sir Georges Stokes

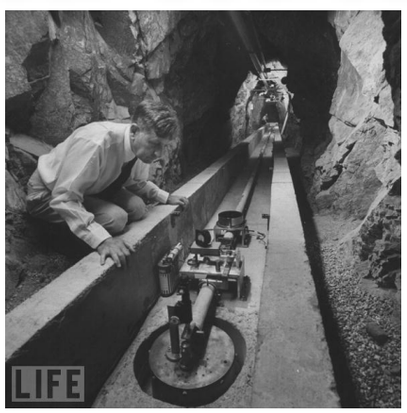

Hugo Benioff

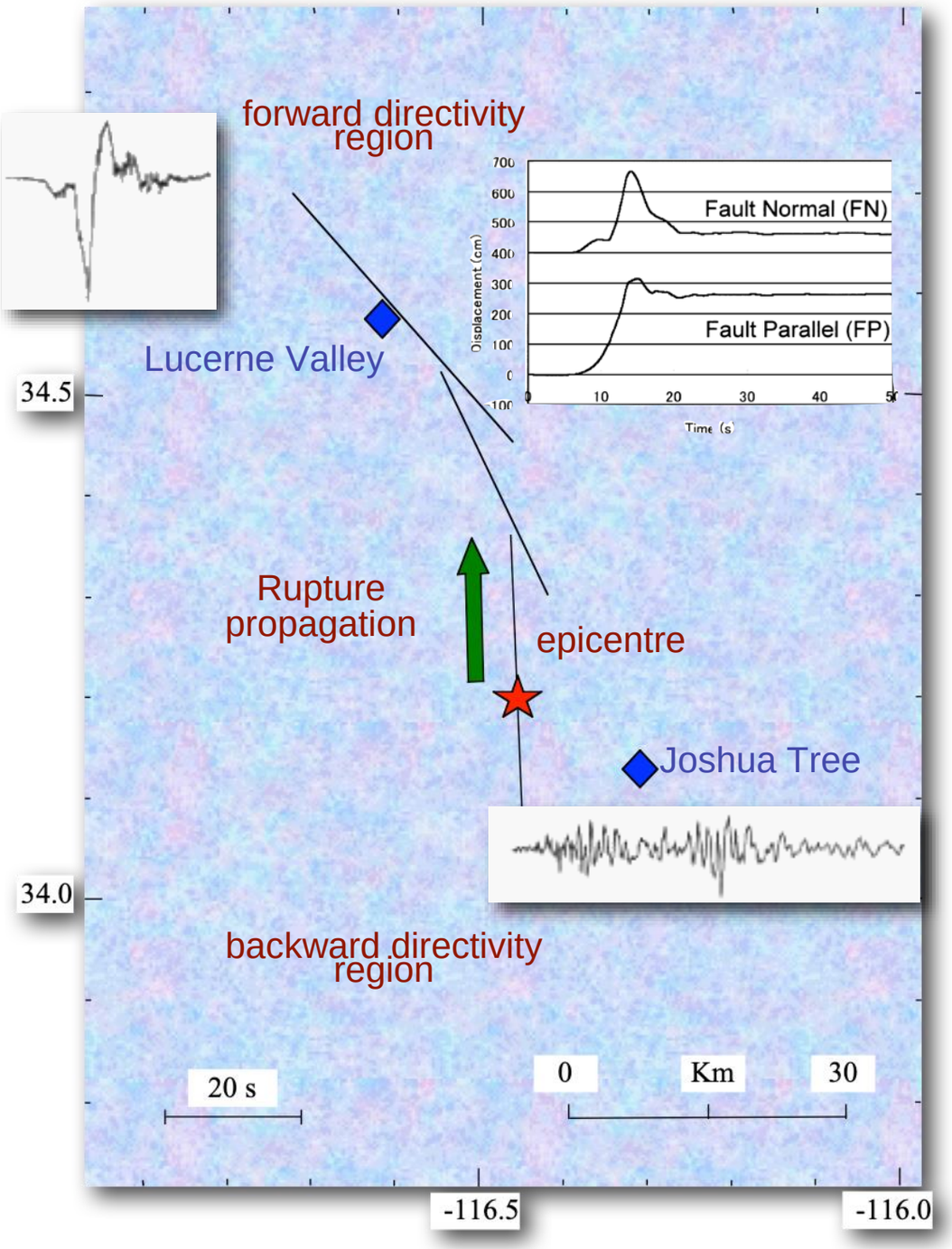

Landers, 1992

Seismic source: Friction & Stresses

A number of factors can control friction: temperature, slip rate and slip history. Many materials become weaker with repeated slip (slip weakening).
They may exhibit an inverse dependence of friction on slip velocity (velocity weakening).
Stick slip behaviour is observed only at temperatures below 300°C.

Anderson's theory of faulting: he recognized that principal stress orientations could vary among geological provinces within the upper crust of the earth. He deduced the connection between three common fault types: normal, strike-slip, and thrust and the three principal stress systems arising as a consequence of the assumption that one principal stress must be normal to the earth's surface.

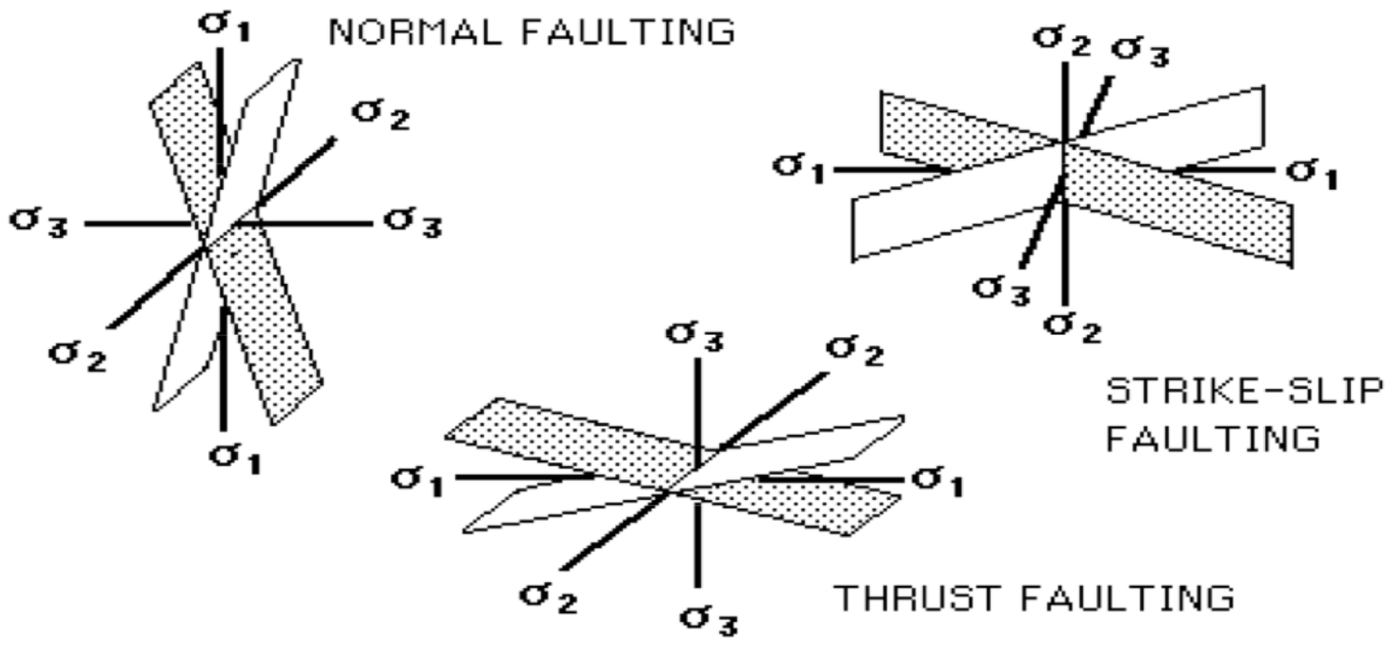

Rupture process

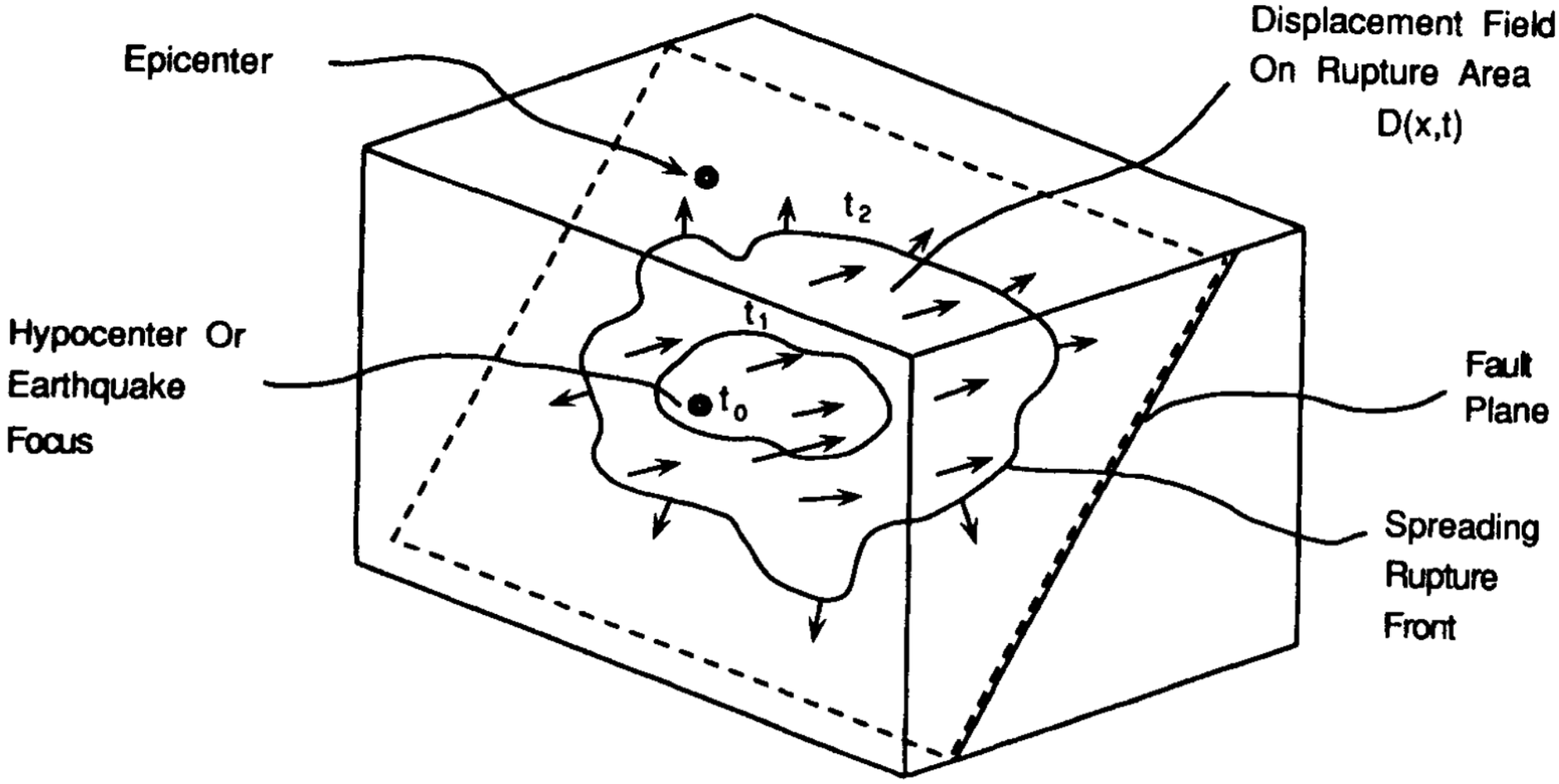

Schematic diagram of rupture on a fault plane. Slipping points radiate outgoing P- and S-waves. In general, rupture wavefront is not regular and slip vector, as well as slipping time, is different for the points on the fault.

Fault slip involves three main stages:

1) initiation of fault sliding
2) rupture front expansion
3) termination of rupture process.

Equivalent Forces

The observable seismic radiation is through energy release as the fault surface moves: formation and propagation of a crack. This complex dynamical problem can be studied by kinematical equivalent approaches.

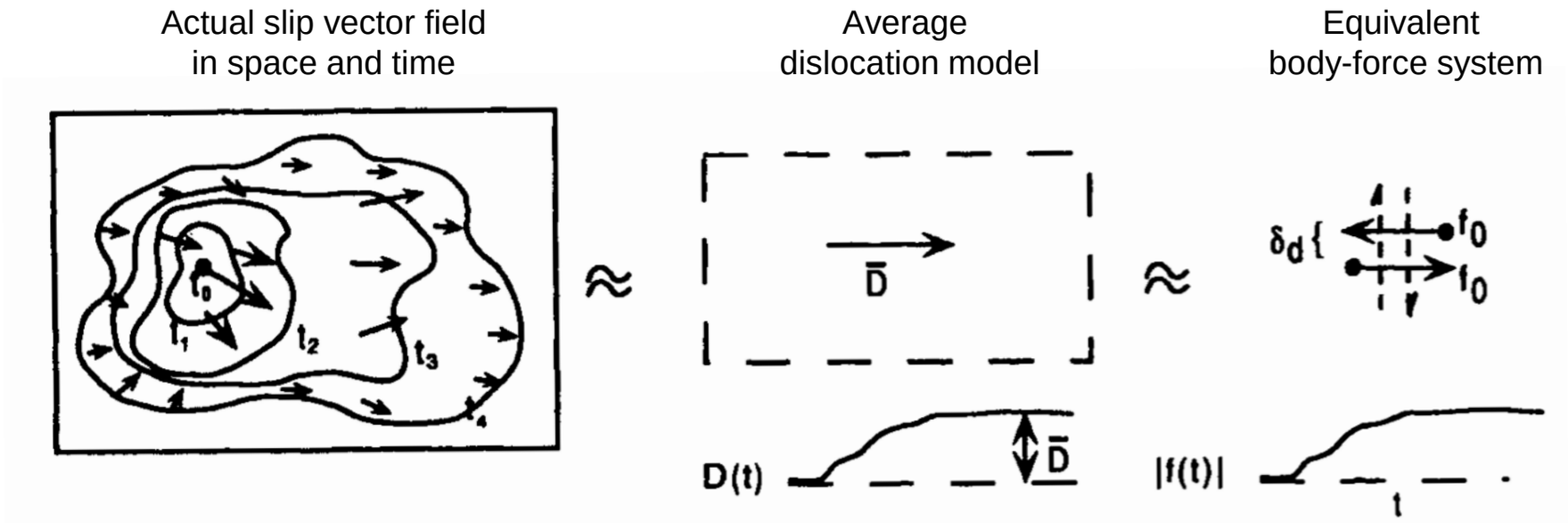

The scope is to develop a representation of the displacement generated in an elastic body in terms of the quantities that originated it: body forces and applied tractions and displacements over the surface of the body.

The actual slip process will be described by superposition of equivalent body forces acting in space (over a fault) and time (rise time).

Fundamental papers

- Maruyama T. (1963). On the force equivalents of dynamical elastic dislocations with reference to the earthquake mechanism. Bulletin of the Earthquake Research Institute 41: 467–486.

- Burridge R. and Knopoff L. (1964). Body force equivalents for seismic dislocations. Bulletin of the Seismological Society of America 54: 1875–1878.

“An explicit expression is derived for the body force to be applied in the absence of a dislocation, which produces radiation identical to that of the dislocation. This equivalent force depends only upon the source and the elastic properties of the medium in the immediate vicinity of the source and not upon the proximity of any reflecting surfaces. The theory is developed for dislocations in an anisotropic inhomogeneous medium; in the examples isotropy is assumed. For displacement dislocation faults, the double couple is an exact equivalent body force.”

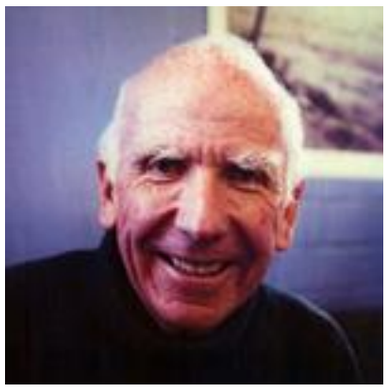

Leon Knopoff

Fault plane and slip vector

Figure 4.2-2: Fault geometry used in earthquake studies.

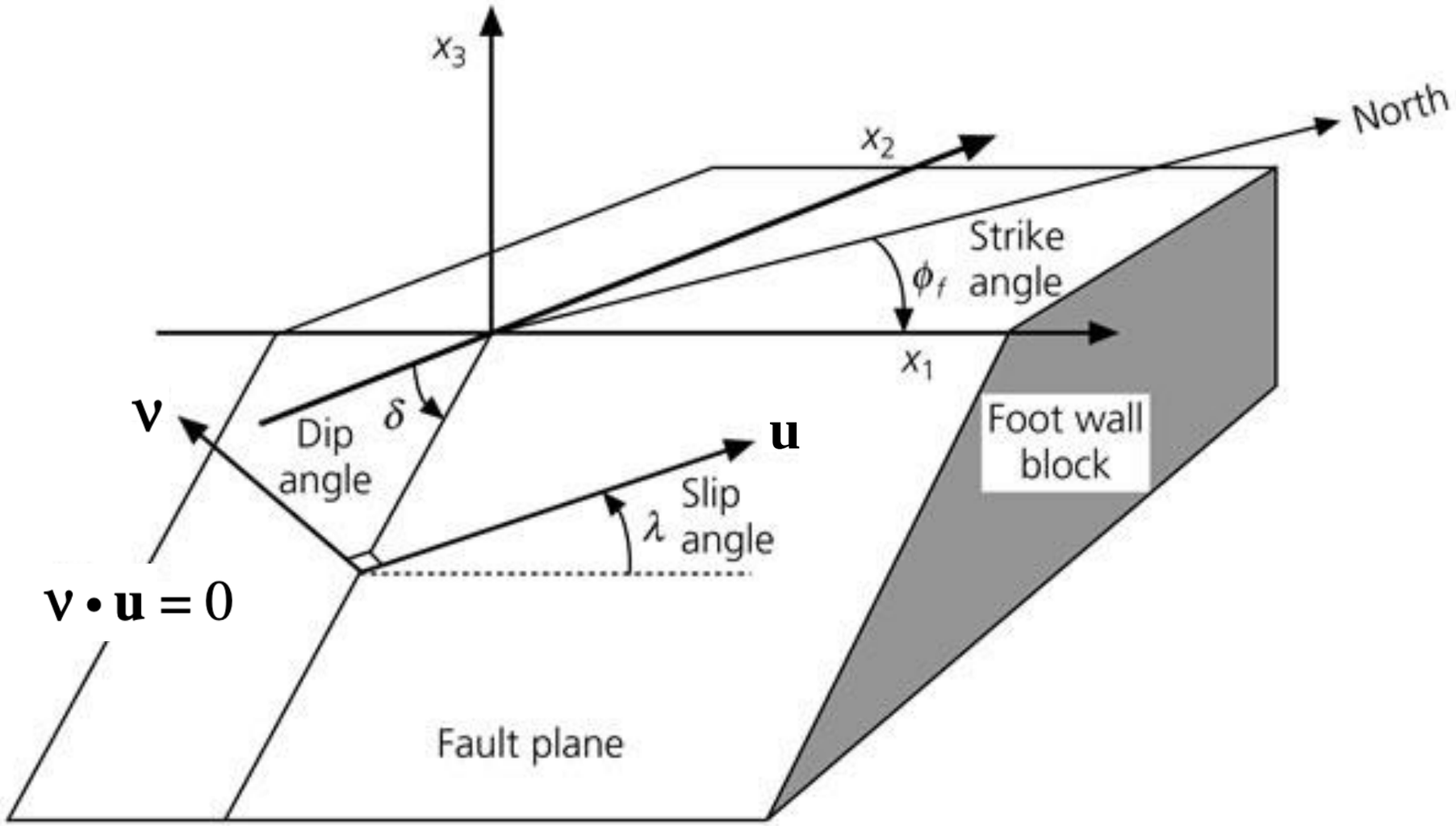

Final (point) source representation

And if the source can be considered a point-source (for distances greater than fault dimensions), the contributions from different surface elements can be considered in phase.

Thus for an effective point source, one can define the moment tensor, to be convolved with the (spatially derived) Green's function of the medium:

$$u_n(x,t) = M_{pq} * G_{np,q}$$

For a shear dislocation, the equivalent point force is a **double-couple**, since internal faulting implies that the total force $\mathbf{f}^{[u]}$ and its total moment are null. The seismic moment has a **null trace** and **one of the eigenvalues is 0**.

$$M_{pq}(\text{doublecouple}) = \begin{pmatrix} M_0 & 0 & 0 \\ 0 & 0 & 0 \\ 0 & 0 & -M_0 \end{pmatrix} \quad \text{with } M_0 = \mu A[\bar{u}]$$

M_0 is called **seismic moment**, a scalar quantity related to the area of the fault and to the slip, averaged over the fault plane.

Moment tensor components

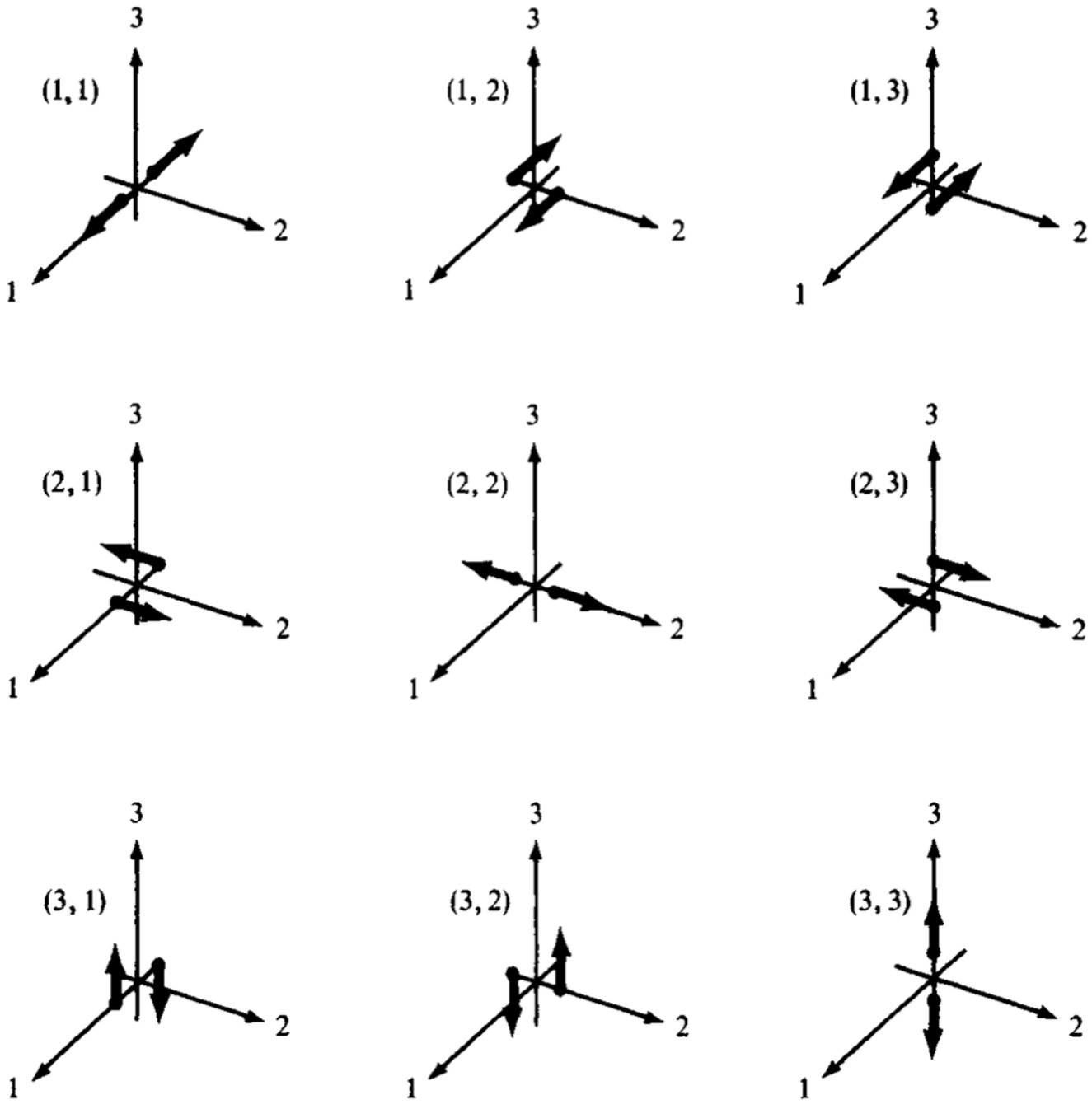

The nine possible couples that are required to obtain equivalent forces for a generally oriented displacement discontinuity in anisotropic media.

Point sources can be described by the seismic moment tensor **Mpq**, whose elements have clear physical meaning of **forces acting on particular planes**.

The Principal Focal Mechanisms

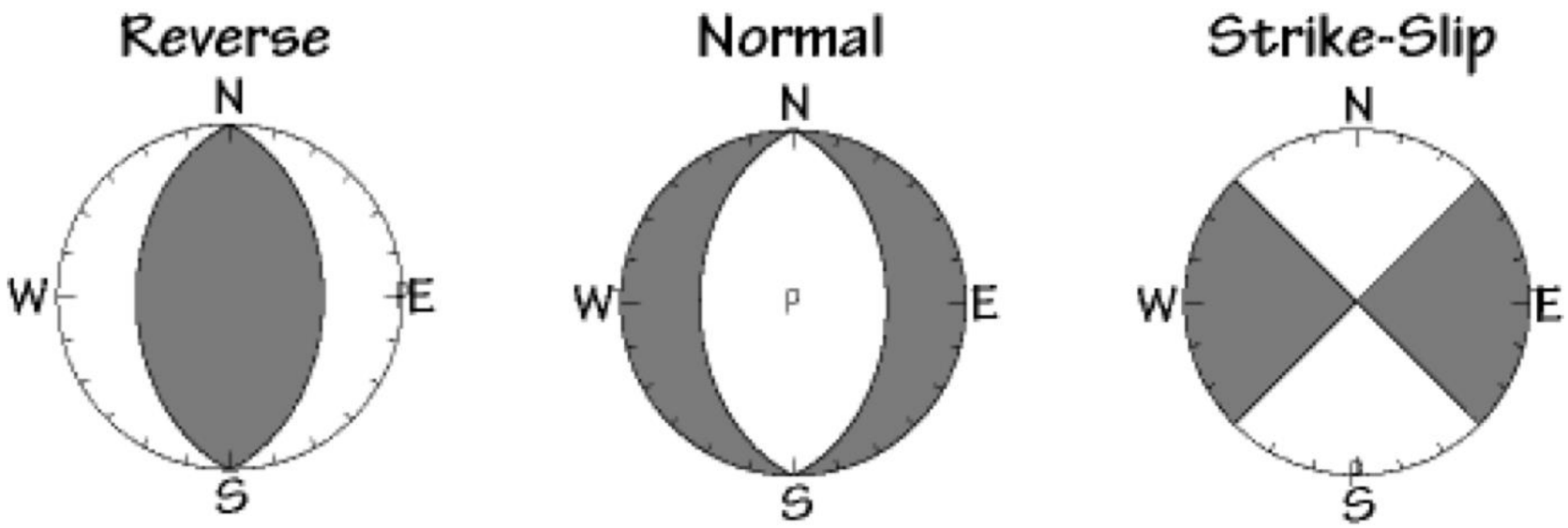

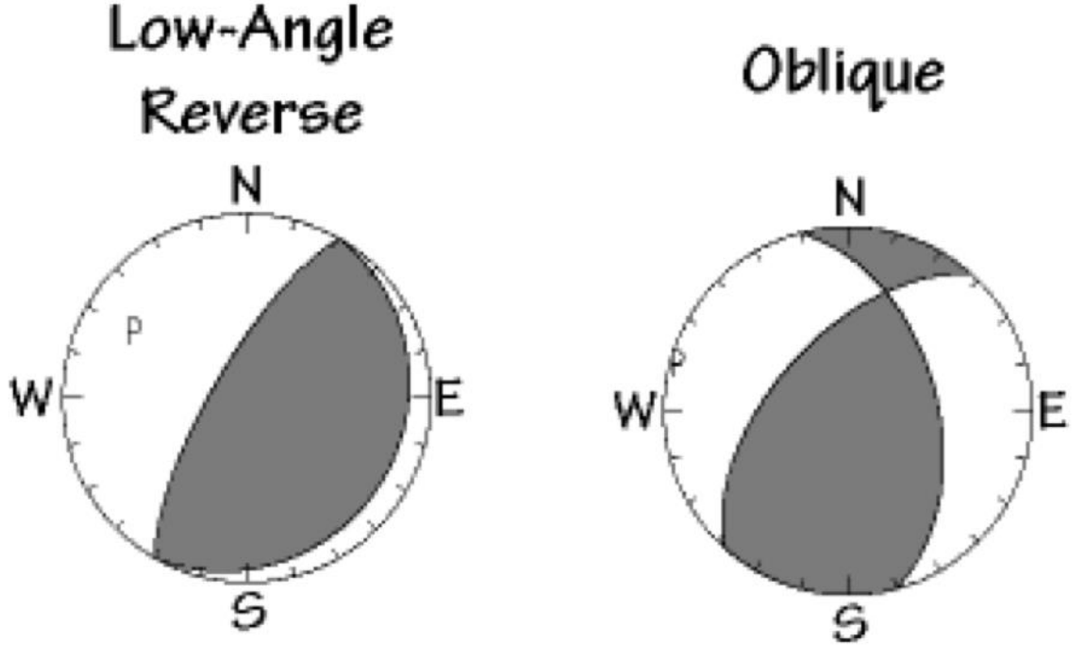

FM & stress axes

Figure 4.2-16: Relation between fault planes and stress axes.

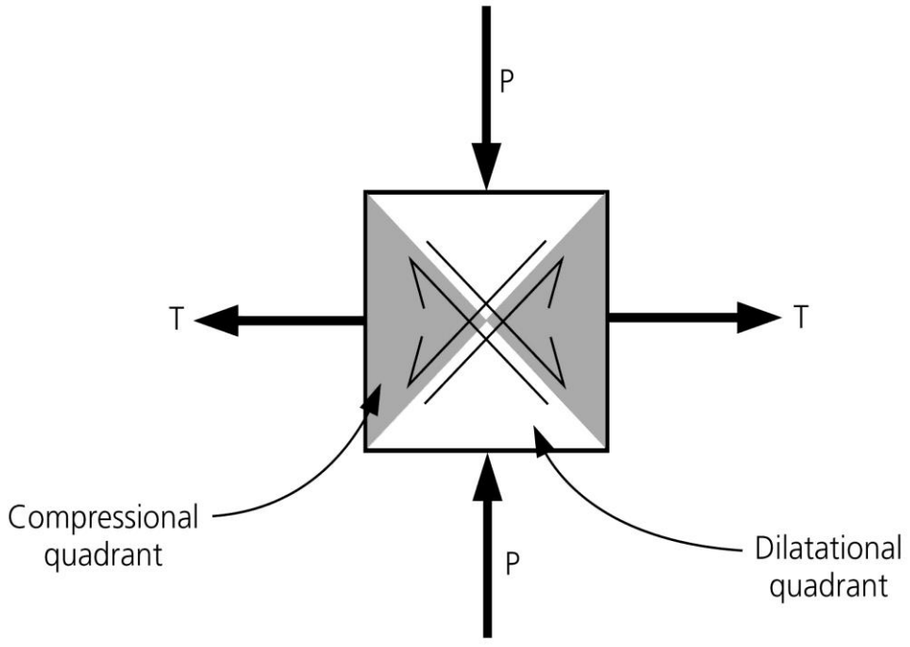

Faults

45° Dipping thrust

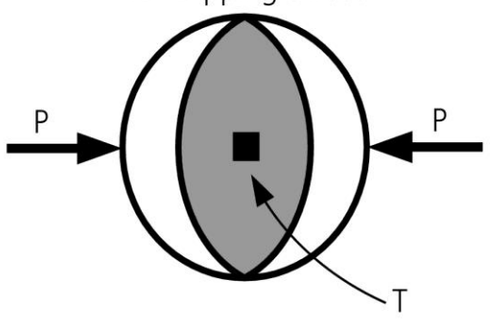

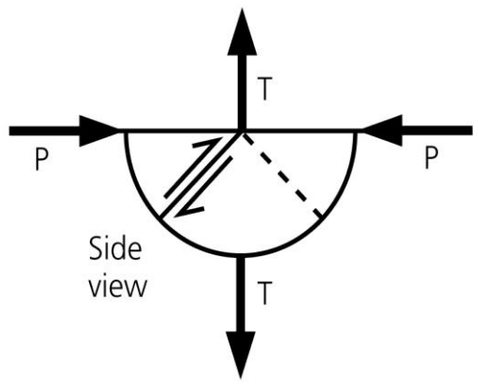

45° Dipping normal

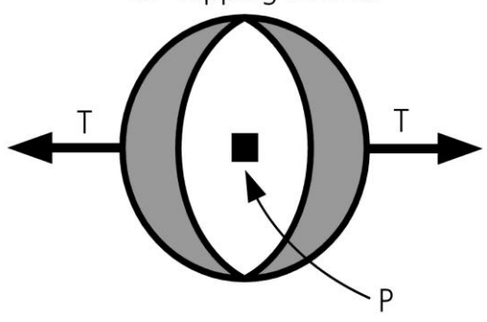

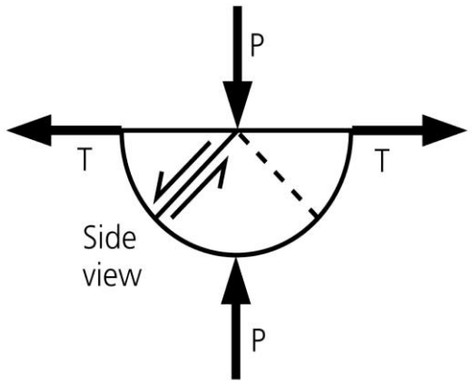

To obtain P and T axes:

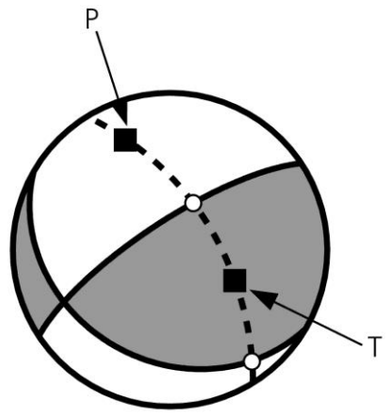

On the meridian connecting the poles, the points half-way between the nodal planes are the **P** and **T** axes

Radiation pattern & surface waves

Figure 4.3-12: Surface wave amplitude radiation patterns for several focal mechanisms.

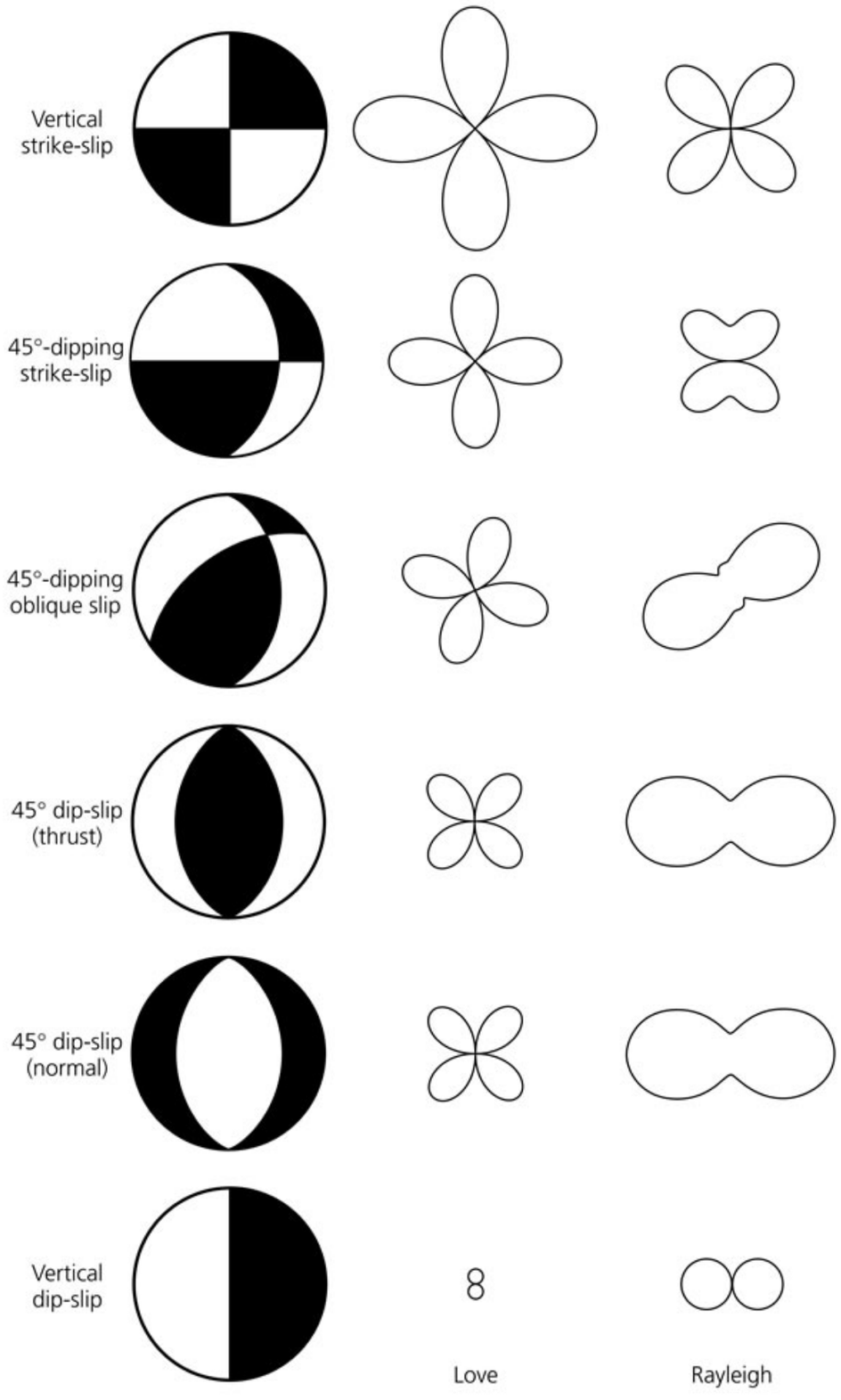

Haskell dislocation model

Haskell N. A. (1964). Total energy spectral density of elastic wave radiation from propagating faults, Bull. Seism. Soc. Am. **54**, 1811-1841

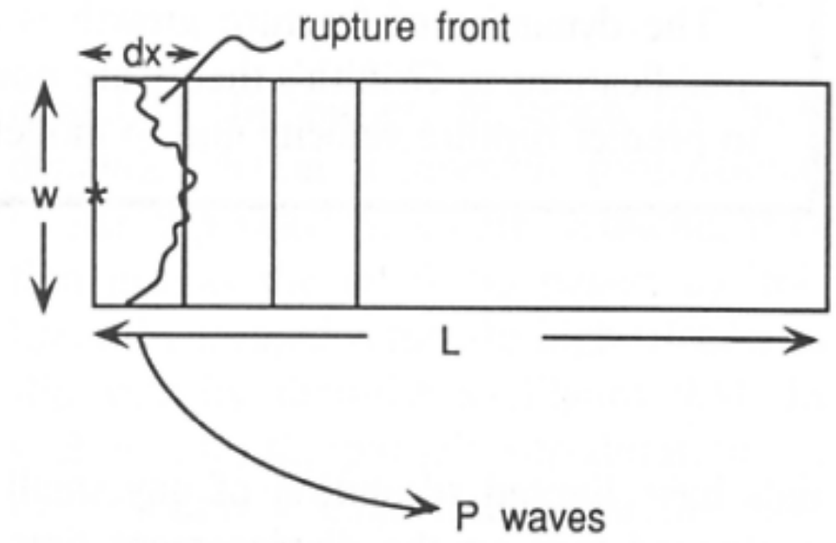

FIGURE 9.5 Geometry of a one-dimensional fault of width w and length L. The individual segments of the fault are of length dx, and the moment of a segment is $m\,dx$. The fault ruptures with velocity v_r.

Sumatra earthquake, Dec 26, 2004

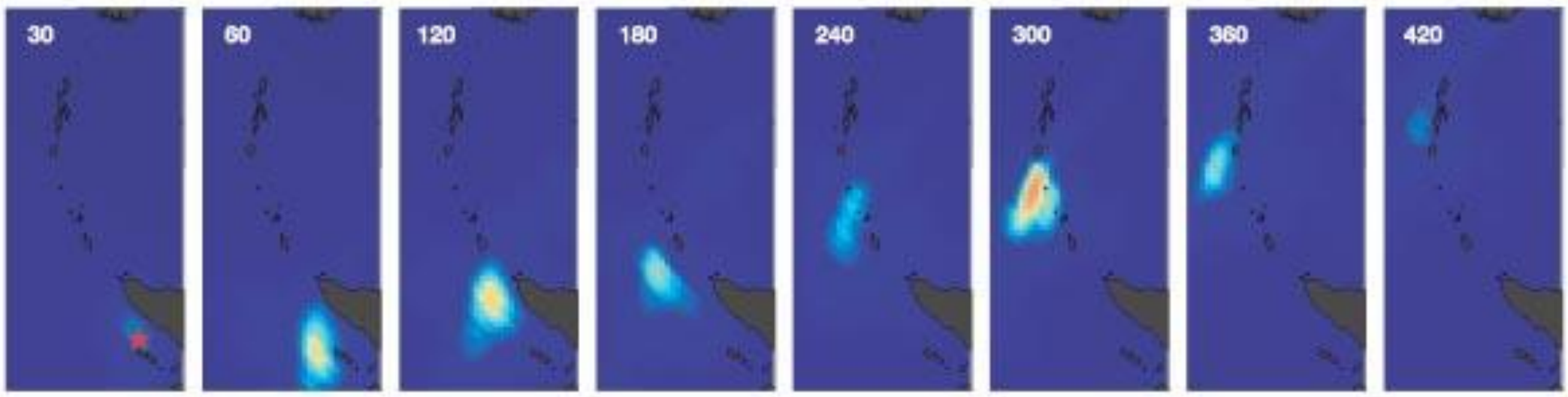

Ishii et al., Nature 2005 doi:10.1038/nature03675

Haskell source model: far field

resulting in the convolution of two boxcars: the first with duration equal to the rise time and the second with duration equal to the **rupture time** (L/v_r)

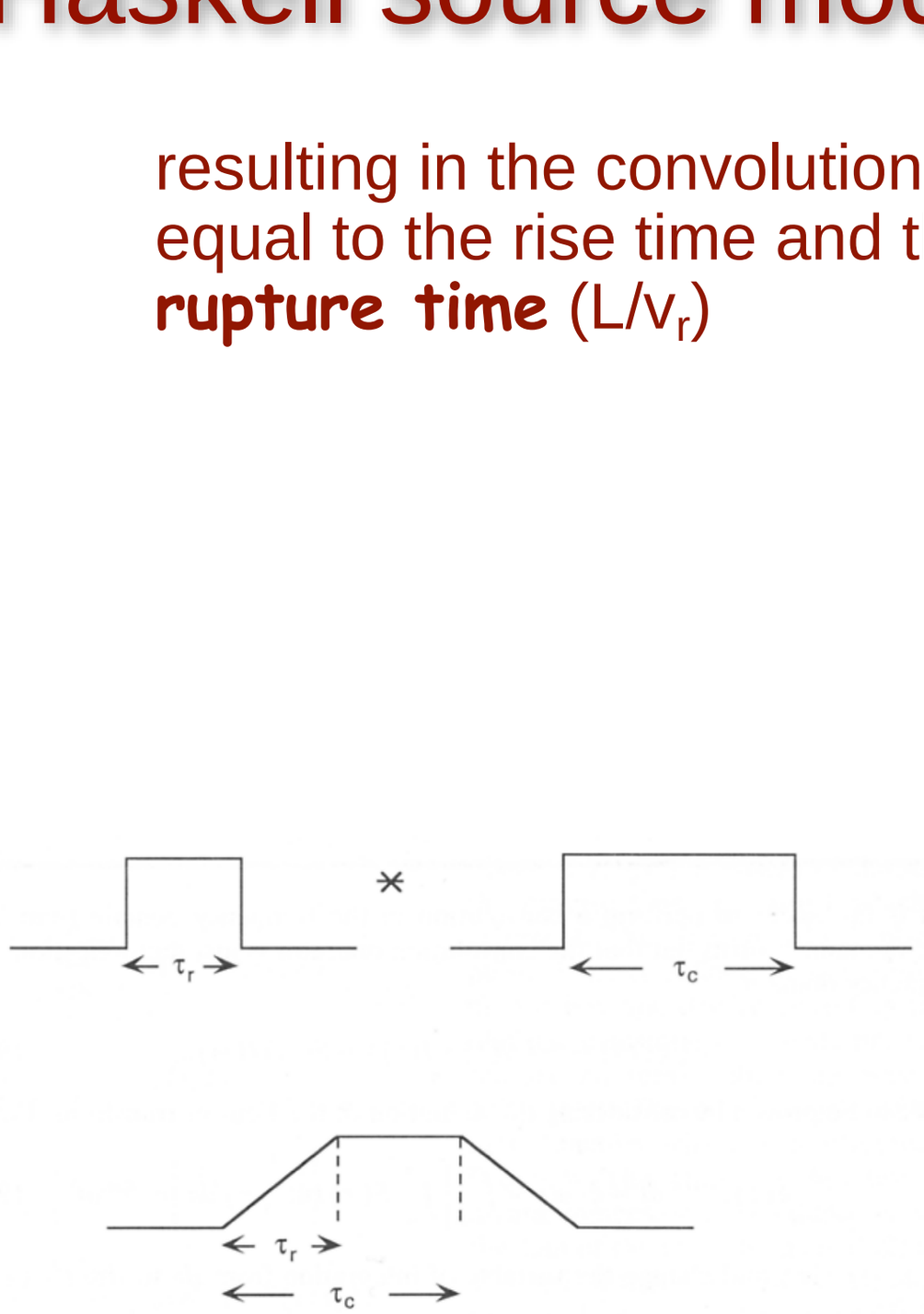

FIGURE 9.6 The convolution of two boxcars, one of length τ_r and the other of length τ_c ($\tau_c > \tau_r$). The result is a trapezoid with a rise time of τ_r, a top of length $\tau_c - \tau_r$, and a fall of width τ_r.

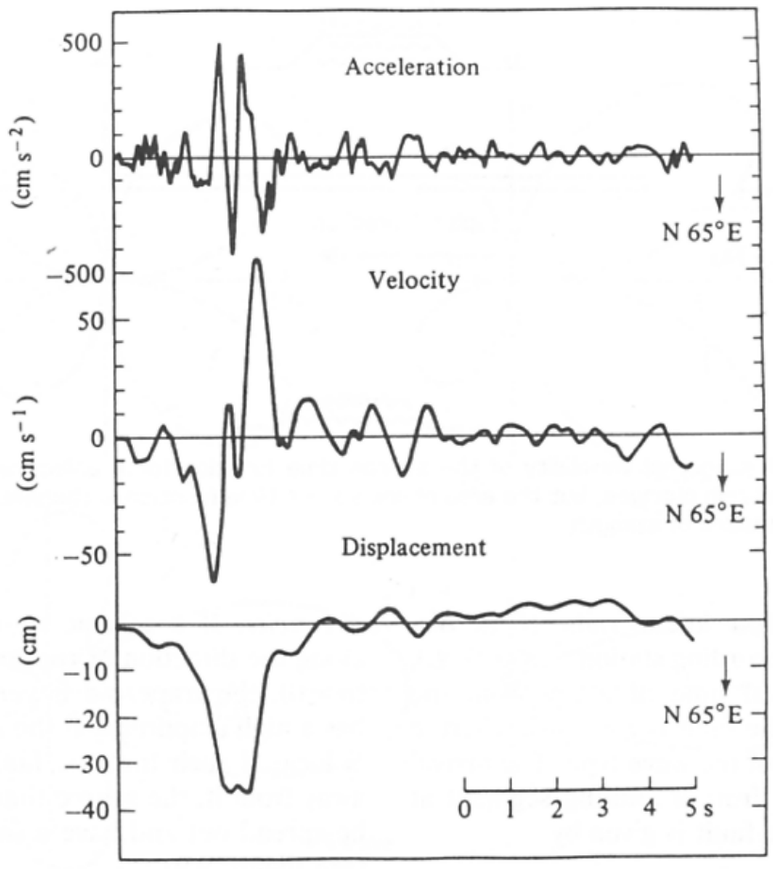

FIGURE 9.7 A recording of the ground motion near the epicenter of an earthquake at Parkfield, California. The station is located on a node for *P* waves and a maximum for *SH*. The displacement pulse is the *SH* wave. Note the trapezoidal shape. (From Aki, *J. Geophys. Res.* 73, 5359–5375, 1968; © copyright by the American Geophysical Union.)

Haskell source model: directivity

The body waves generated from a breaking segment will arrive at a receiver before than those that are radiated by a segment that ruptures later.

If the path to the station is not perpendicular, the waves generated by different segments will have different path lengths, and then unequal travel times.

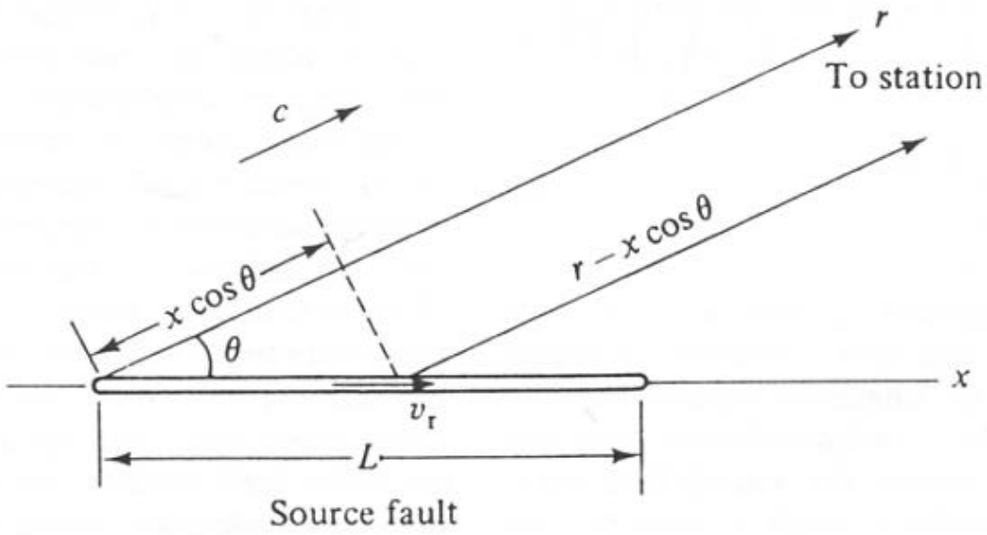

FIGURE 9.8 Geometry of a rupturing fault and the path to a remote recording station. (From Kasahara, 1981.)

$$T_r = \left[\frac{L}{v_r} + \left(\frac{r - L\cos\theta}{c}\right)\right] - \frac{r}{c} =$$

$$= \frac{L}{v_r} - \left(\frac{L\cos\theta}{c}\right) = \frac{L}{v_r}\left(1 - \frac{v_r}{c}\cos\theta\right)$$

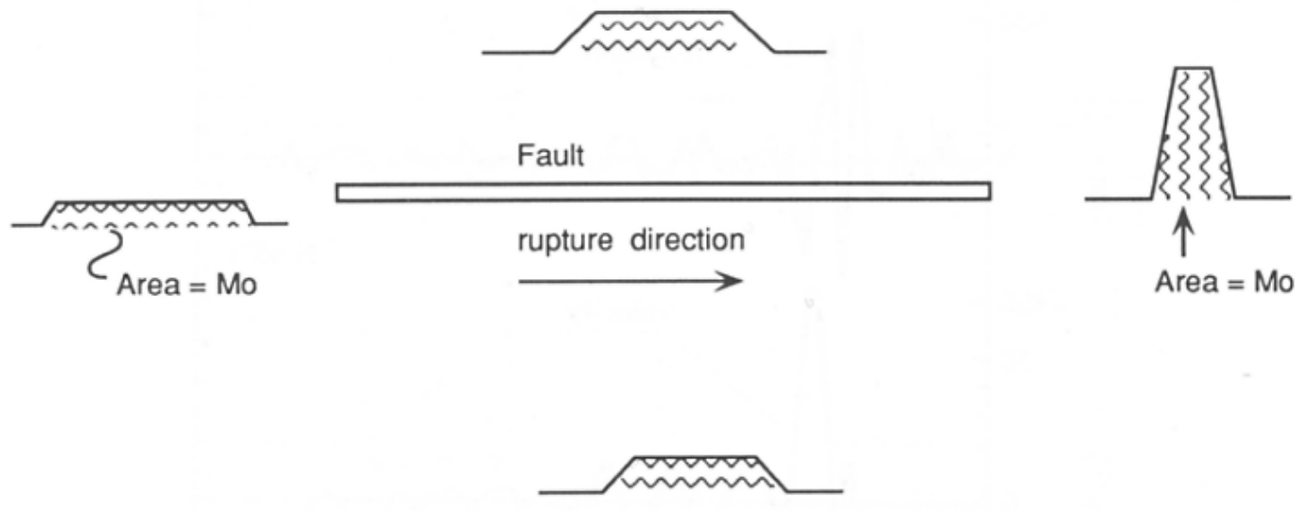

FIGURE 9.9 Azimuthal variability of the source time function for a unilaterally rupturing fault. The duration changes, but the area of the source time function is the seismic moment and is independent of azimuth.

Directivity example

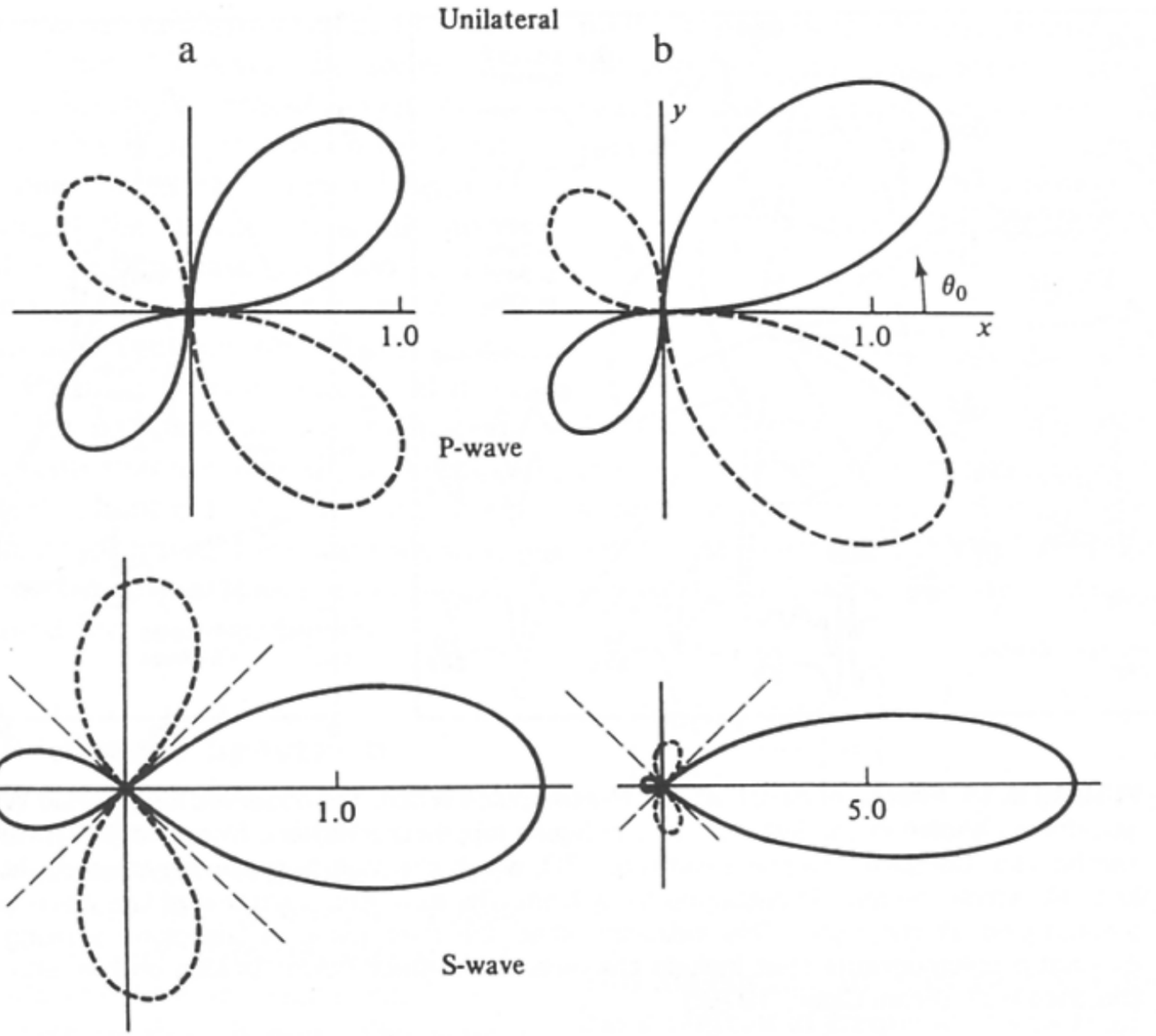

FIGURE 9.10 The variability of *P*- and *SH*-wave amplitude for a propagating fault (from left to right). For the column on the left $v_r/v_s = 0.5$, while for the column on the right $v_r/v_s = 0.9$. Note that the effects are amplified as rupture velocity approaches the propagation velocity. (From Kasahara, 1981.)

Source spectrum (amplitude)

The displacement pulse, corrected for the geometrical spreading and the radiation pattern can be written as:

$$U(\omega) \approx \begin{cases} M_0 & \omega < \dfrac{2}{T_r} \\ \dfrac{2M_0}{\omega T_R} & \dfrac{2}{T_r} < \omega < \dfrac{2}{\tau} \\ \dfrac{4M_0}{\omega^2 \tau T_R} & \omega > \dfrac{2}{\tau} \end{cases}$$

Figure 4.6-4: Approximation of the (sin *x*)/*x* function, and derivation of corner frequencies.

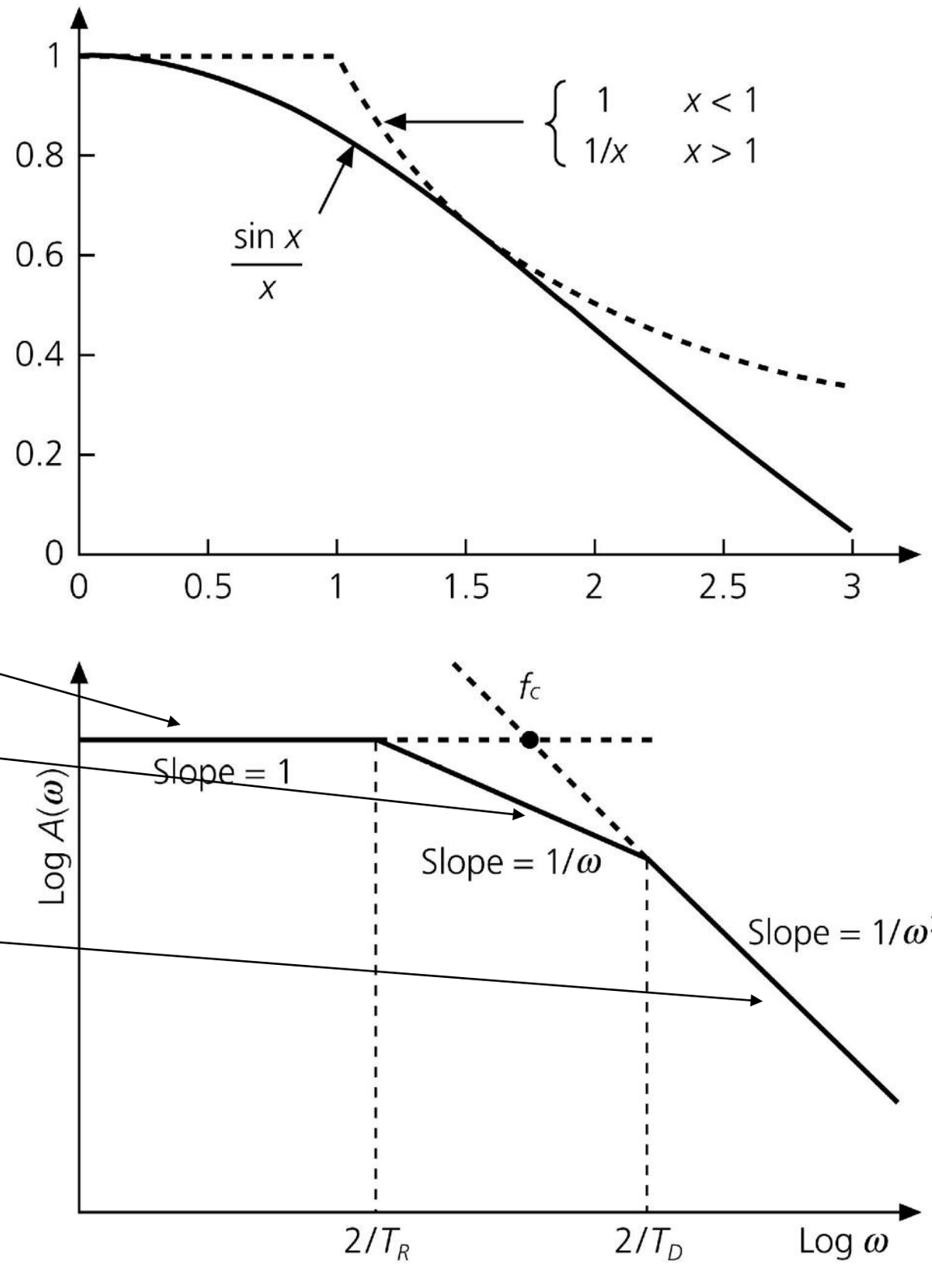

Magnitude Scales - Richter

The concept of magnitude was introduced by Richter (1935) to provide an objective instrumental measure of the size of earthquakes. Contrary to seismic intensity, I, which is based on the assessment and classification of shaking damage and human perceptions of shaking, the magnitude M uses instrumental measurements of earth ground motion adjusted for epicentral distance and source depth.

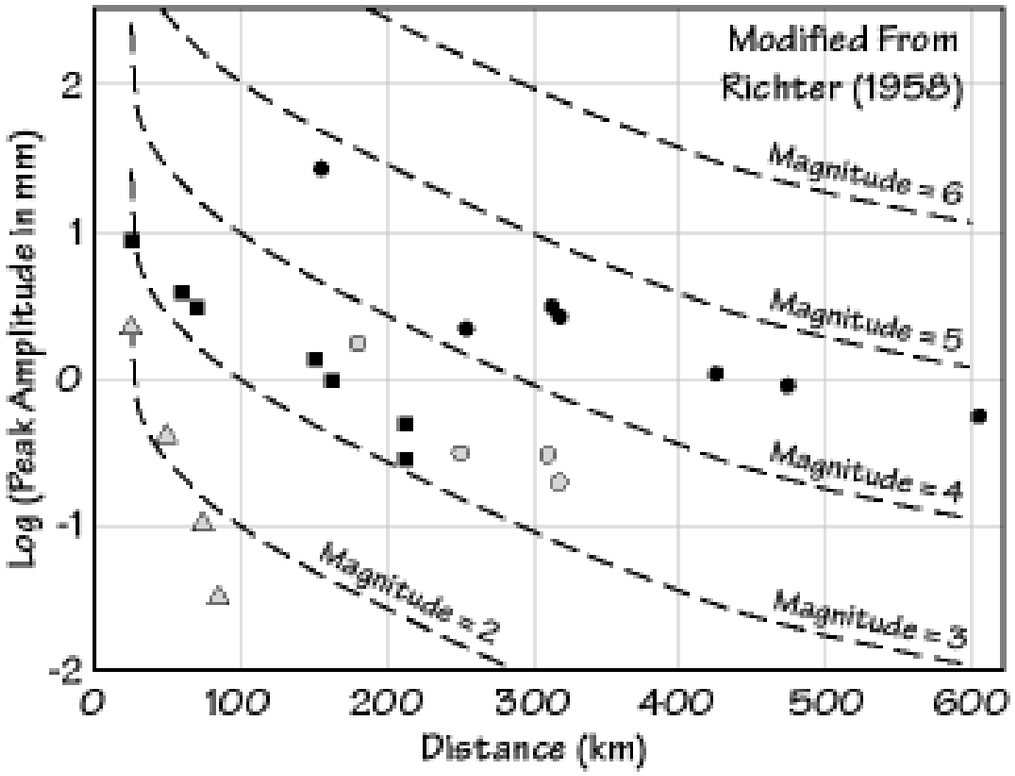

The original Richter scale was based on the observation that the amplitude of seismic waves systematically decreases with epicentral distance.

Data from local earthquakes in California

The relative size of events is calculated by comparison to a reference event, with M_L=0, such that A_0 was 1 μm at an epicentral distance, Δ, of 100 km with a Wood-Anderson instrument:

$$\mathbf{M_L=\log(A/A_0)=\log A-2.48+2.76\Delta}.$$

Magnitude Scales - Richter

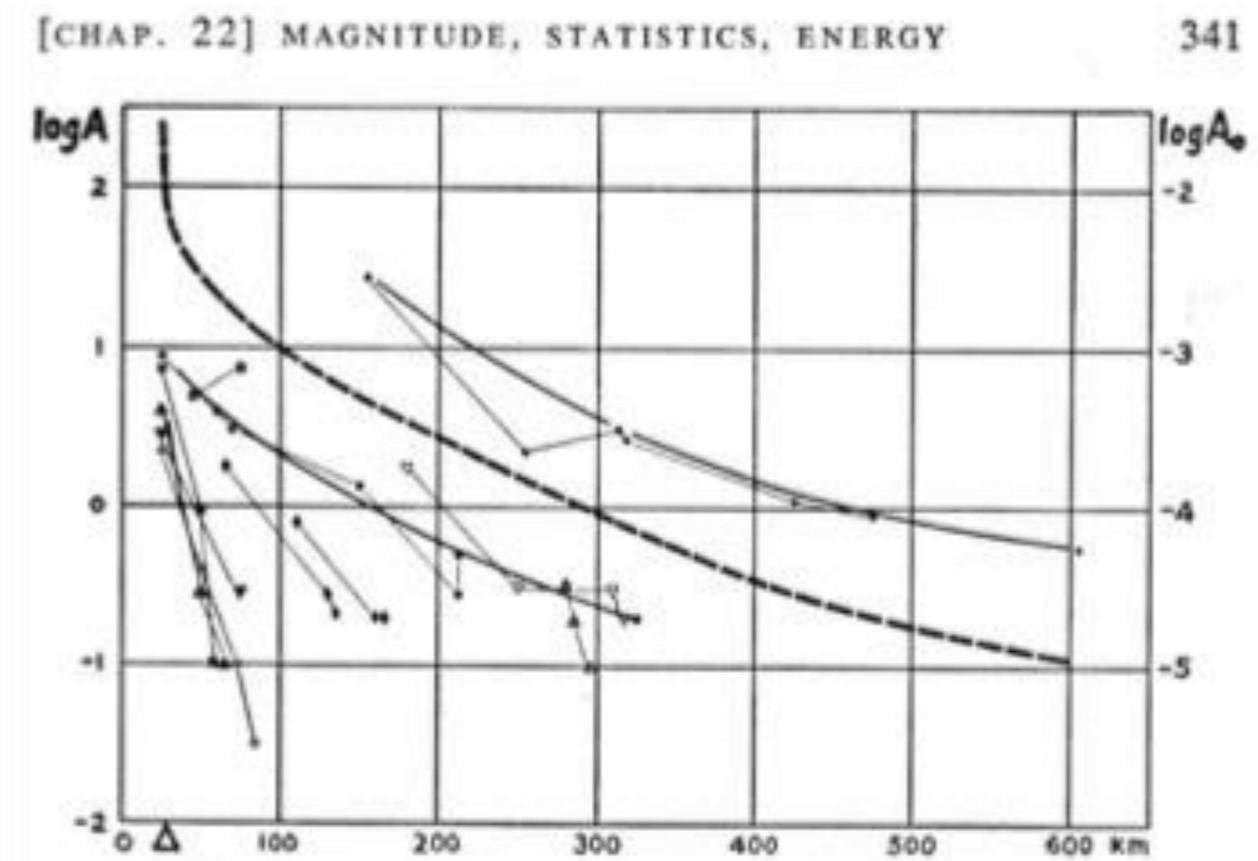

FIGURE 22-2 *Origin of the magnitude scale. Data for Southern California earthquakes of January, 1932. [Redrafted from the original notes.]*

"I found a paper by Professor K. Wadati of Japan in which he compared large earthquakes by plotting the maximum ground motion against distance to the epicenter. I tried a similar procedure for our stations, but the range between the largest and smallest magnitudes seemed unmanageably large. Dr. Beno Gutenberg then made the natural suggestion to plot the amplitudes logarithmically. I was lucky because **logarithmic plots are a device of the devil**. I saw that I could now rank the earthquakes one above the other. Also, quite unexpectedly the attenuation curves were roughly parallel on the plot. By moving them vertically, a representative mean curve could be formed, and individual events were then characterized by individual logarithmic differences from the standard curve. This set of logarithmic differences thus became the numbers on a new instrumental scale. Very perceptively, Mr. Wood insisted that this new quantity should be given a distinctive name to contrast it with the intensity scale. My amateur interest in astronomy brought out the term "magnitude," which is used for the brightness of a star."

Charles F. Richter - An Interview by Henry Spall, Earthquake Information Bulletin. Vol. 12, No. 1, January - February, 1980

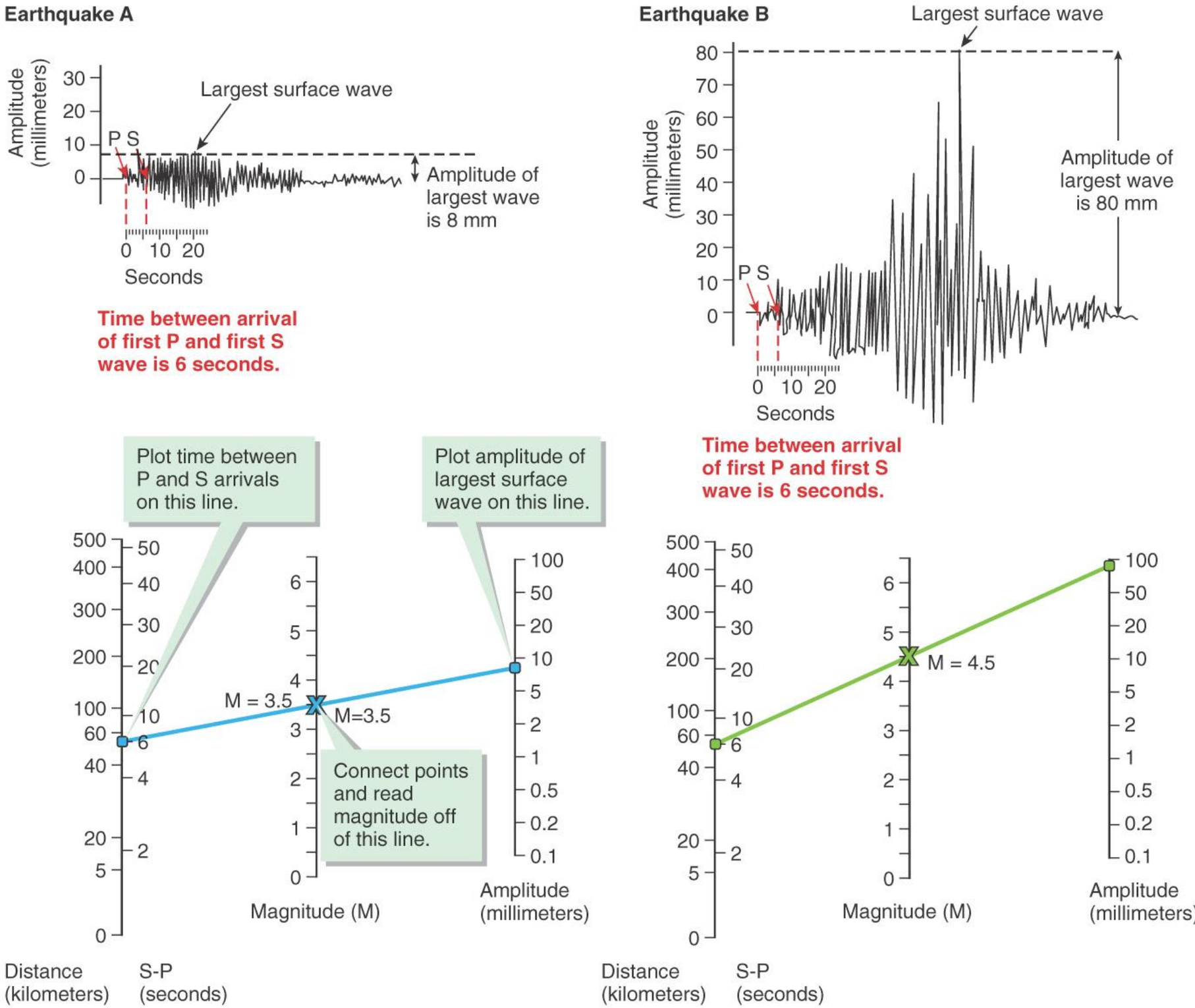

Wood-Anderson Seismometer

Richter also tied his formula to a specific seismic instrument.

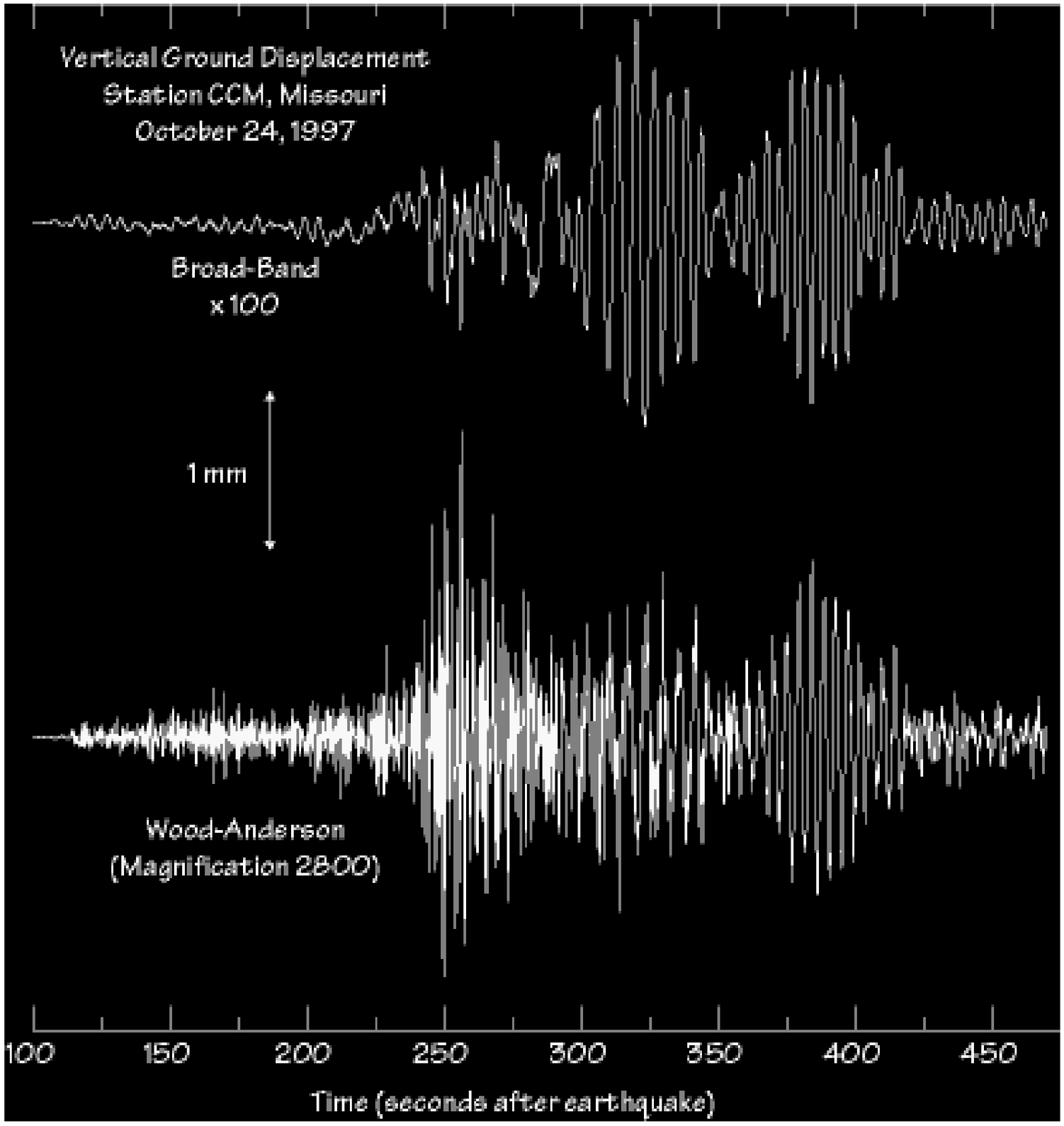

Magnitude Scales

The original M_L is suitable for the classification of local shocks in Southern California only since it used data from the standardized short-period Wood-Anderson seismometer network. The magnitude concept has then been extended so as to be applicable also to ground motion measurements from medium- and long-period seismographic recordings of both surface waves (M_s) and different types of body waves (m_b) in the teleseismic distance range.
The general form of all magnitude scales based on measurements of ground displacement amplitudes A and periods T is:

$$M = \log\left(\frac{A}{T}\right) + f(\Delta, h) + C_r + C_s$$

M seismic magnitude
A amplitude
T period
f correction for distance and depth
C_s correction for site
C_r correction for source region

M_L **Local magnitude**
m_b **body-wave magnitude** (1s)
M_s **surface wave magnitude** (20s)

Teleseismic M_S and mb

The two most common modern magnitude scales are:

- M_S, Surface-wave magnitude (Rayleigh Wave, 20s)
- m_b, Body-wave magnitude (P-wave)

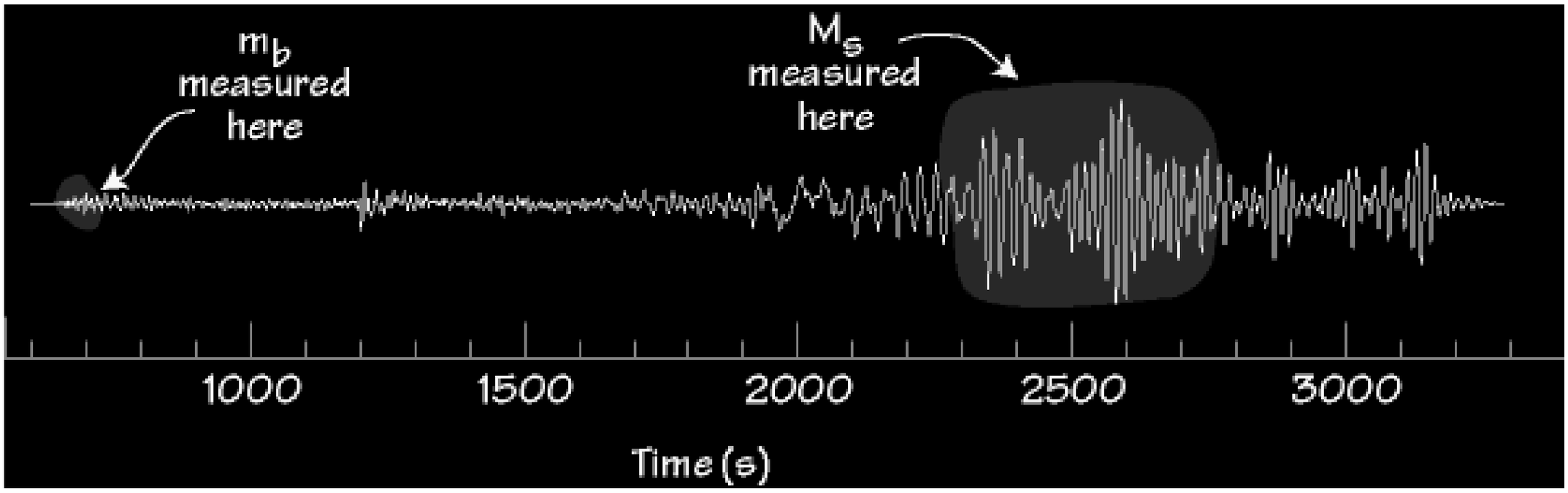

Example: m_b “Saturation”

m_b seldom gives values above 6.7 - it “saturates”.

m_b must be measured in the first 5 seconds - that’s the rule.

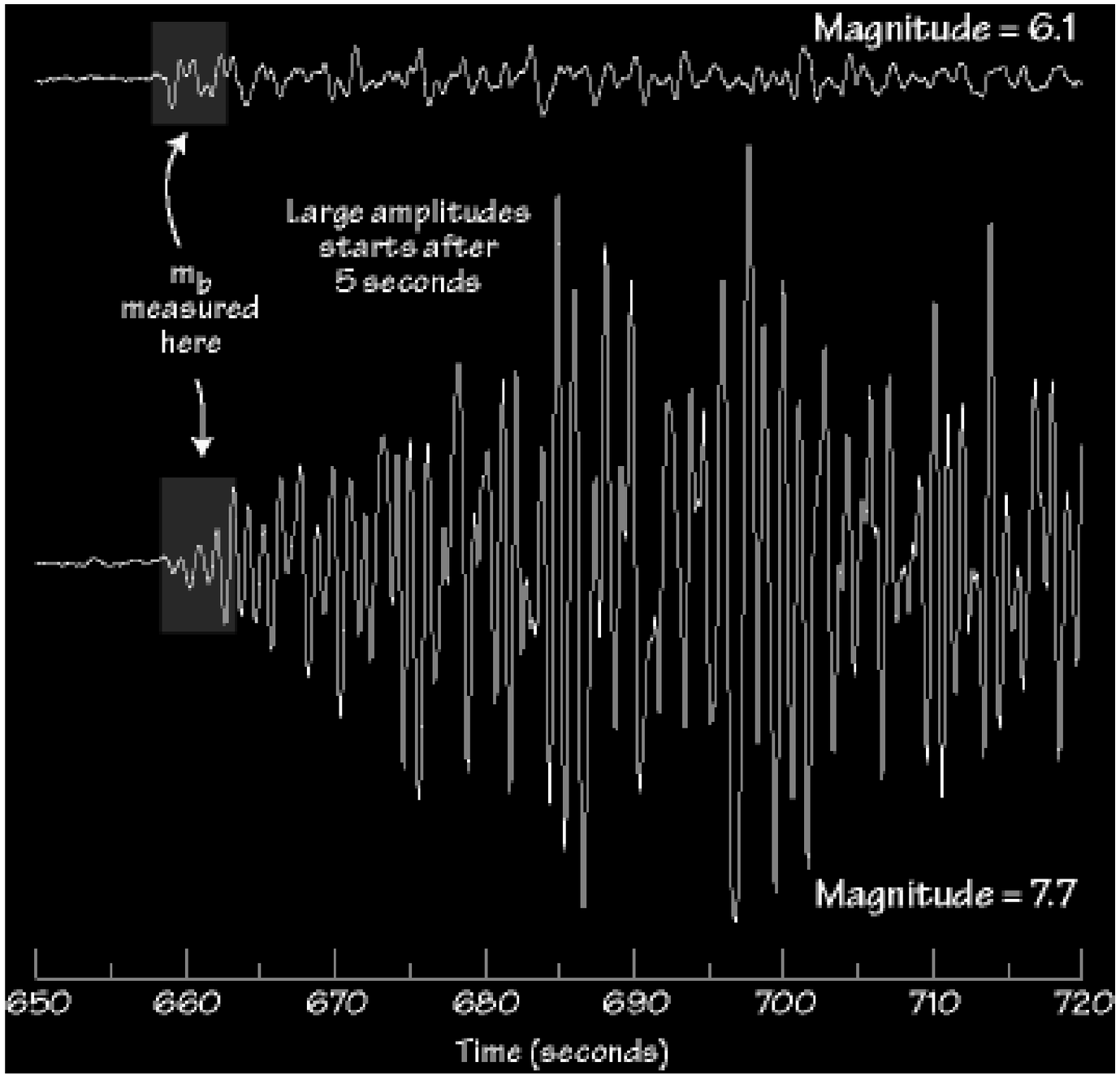

Saturation

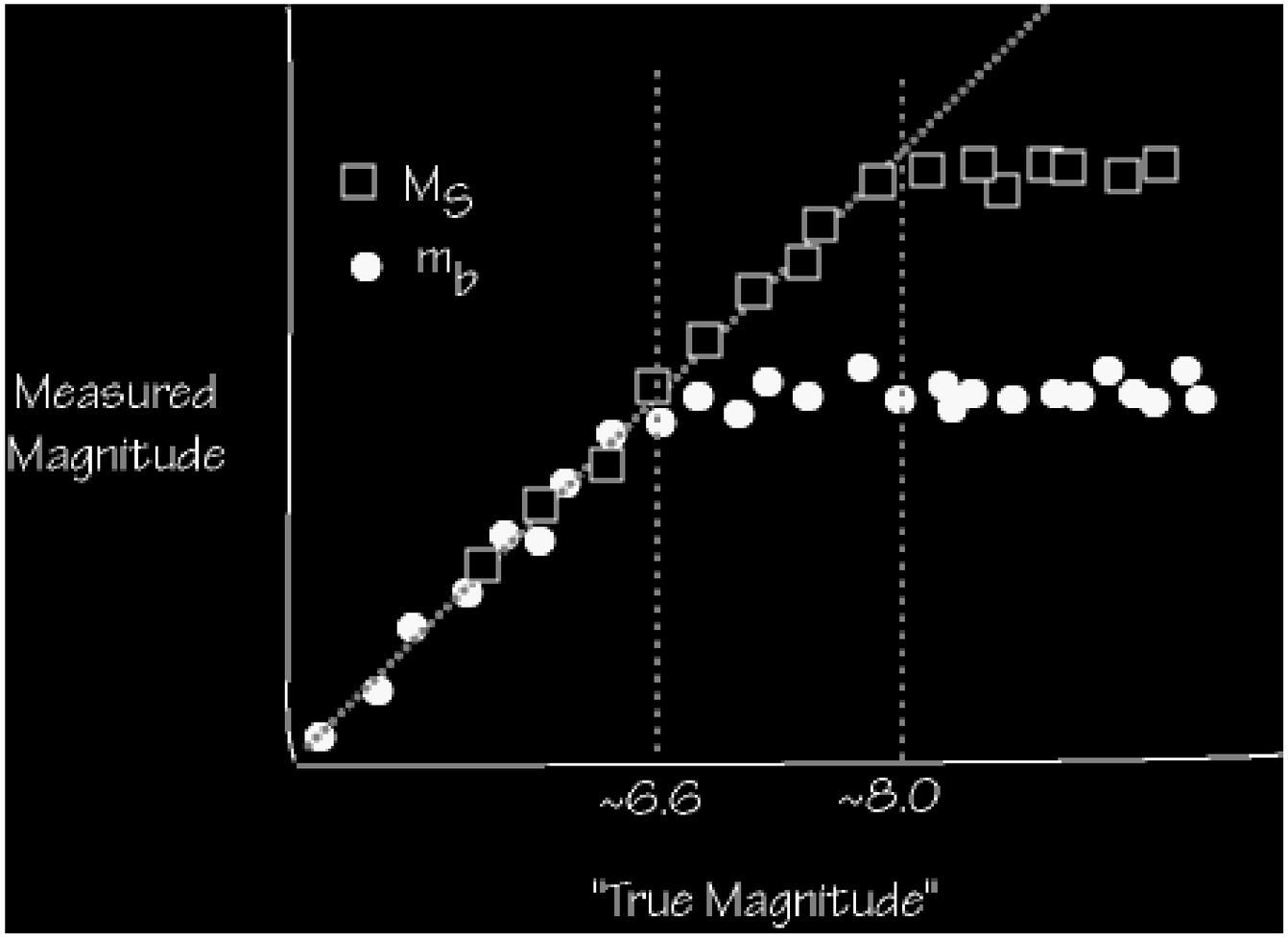

Magnitude saturation

Nature limits the maximum size of tectonic earthquakes which is controlled by the maximum size of a brittle fracture in the lithosphere. A simple seismic shear source with linear rupture propagation has a typical "source spectrum".

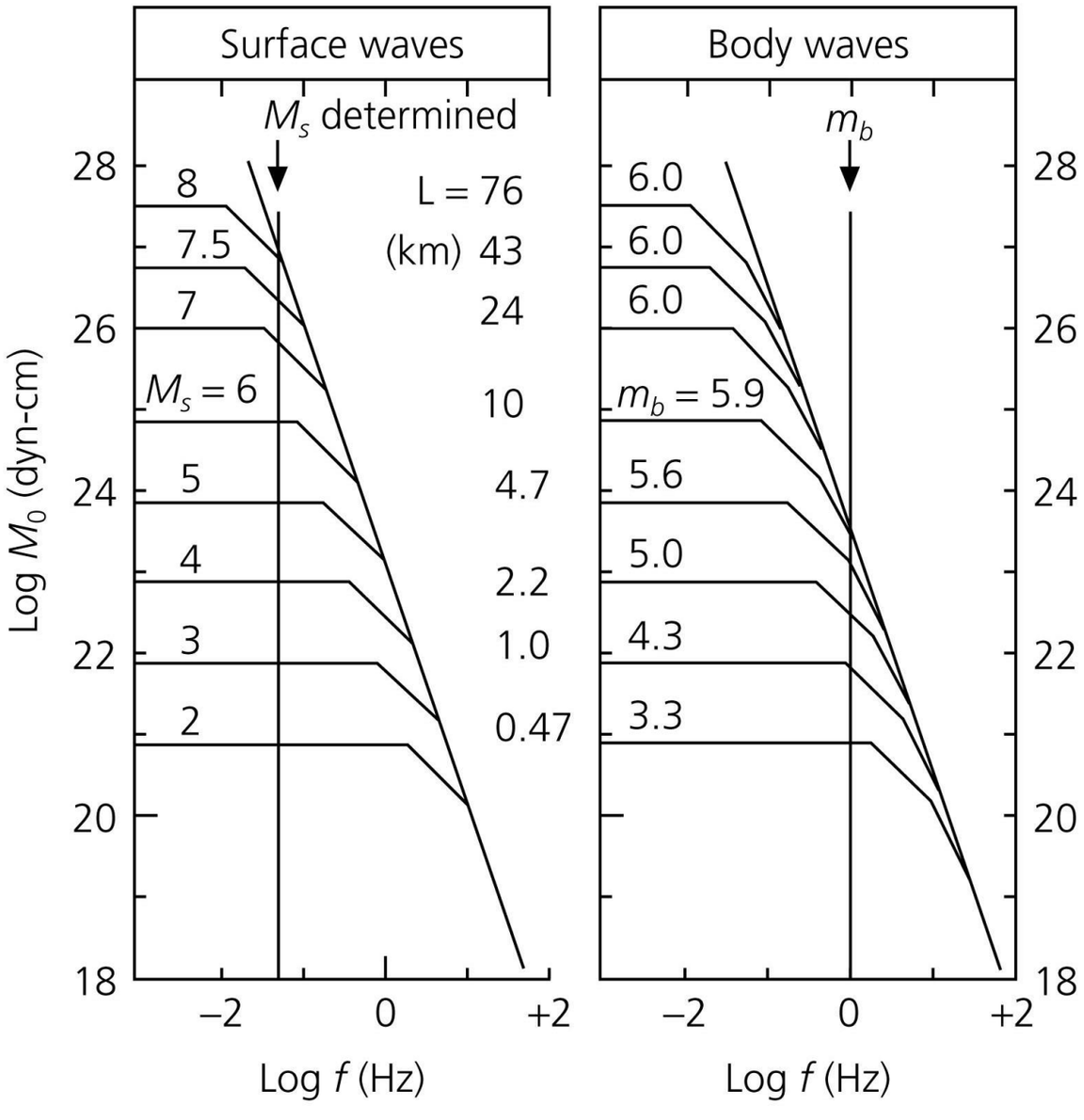

Ms is not linearly scaled with M_0 for $M_s > 6$ due to the beginning of the so-called saturation effect for spectral amplitudes with frequencies $f > f_c$. This saturation occurs already much earlier for m_b which are determined from amplitude measurements around 1 Hz.

Moment magnitude

Empirical studies (Gutenberg & Richter, 1956; Kanamori & Anderson, 1975) lead to a formula for the released seismic energy (in Joule), and for moment, with magnitude:

$\log E = 4.8 + 1.5 M_s \quad \log M_0 = 9.1 + 1.5 M_s$

resulting in

$$M_w = 2/3 \log M_0 - 6.07$$

when the Moment is measured in N·m (otherwise the intercept becomes 10.73); it is related to the final static displacement after an earthquake and consequently to the tectonic effects of an earthquake.

$$u(x,t) = A\cos\left(\frac{2\pi t}{T}\right) \Rightarrow v(x,t) \propto \frac{A}{T}u$$

$$\Rightarrow e \propto v^2 \propto \left(\frac{A}{T}\right)^2 \Rightarrow \log E = C + 2\log\left(\frac{A}{T}\right)$$

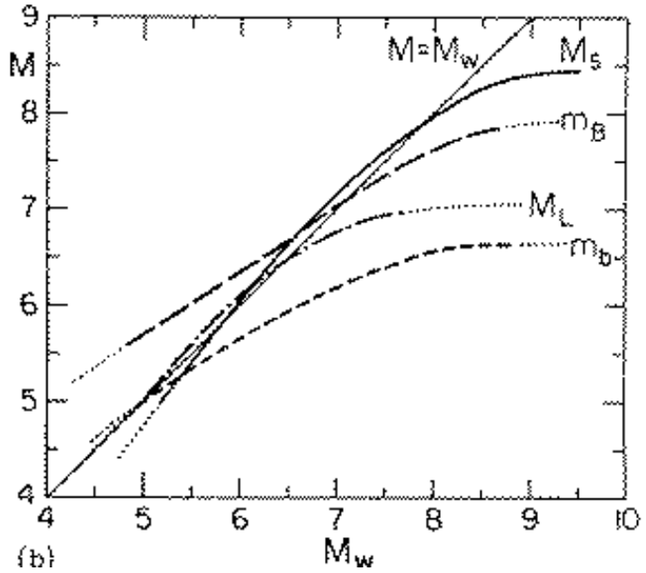

Earthquake	Body wave magnitude m_b	Surface wave magnitude M_s	Fault area (km^2) length × width	Average dislocation (m)	Moment (dyn-cm) M_0	Moment magnitude M_w
Truckee, 1966	5.4	5.9	10 × 10	0.3	8.3×10^{24}	5.8
San Fernando, 1971	6.2	6.6	20 × 14	1.4	1.2×10^{26}	6.7
Loma Prieta, 1989	6.2	7.1	40 × 15	1.7	3.0×10^{26}	6.9
San Francisco, 1906		8.2	320 × 15	4	6.0×10^{27}	7.8
Alaska, 1964	6.2	8.4	500 × 300	7	5.2×10^{29}	9.1
Chile, 1960		8.3	800 × 200	21	2.4×10^{30}	9.5

Seismic moment (1)

Remember . . . the displacement equation for the P and S wave radiation patterns:

$$u_r = \frac{1}{4\pi\alpha^3 r}\,\dot{M}\left(t - r/\alpha\right)\,\sin\left(2\theta\right)\cos\left(\varphi\right)$$ e.g. P waves

Amplitude term

Source time function

Describes the pattern

Considering the ***seismic moment rate function*** or ***source time function***

$$\dot{M}\left(t - r/v\right)$$

which is the time derivative of the ***seismic moment function***

$$M(t) = \mu D(t) S(t)$$

where μ is rigidity, and *D(t)* and *S(t)* are the slip and fault area histories, respectively.

(*Lay & Wallace, 1995; Stein & Wysession, 2003*)

Seismic moment (2)

This leads to the best measure of an earthquake's size and energy,

$$M(t) = \mu D_{av} S$$

the ***seismic moment***, where D_{av} is the average slip or dislocation and S is the fault area.

which in turn gives the ***moment magnitude*** M_w

$$M_w = \frac{\log M_o}{1.5} - 10.73$$

where M_o is in dyn-cm.

and which we will discuss again with respect to other magnitude scales.

(*Lay & Wallace, 1995; Stein & Wysession*

Importance of comparing Mw and Me

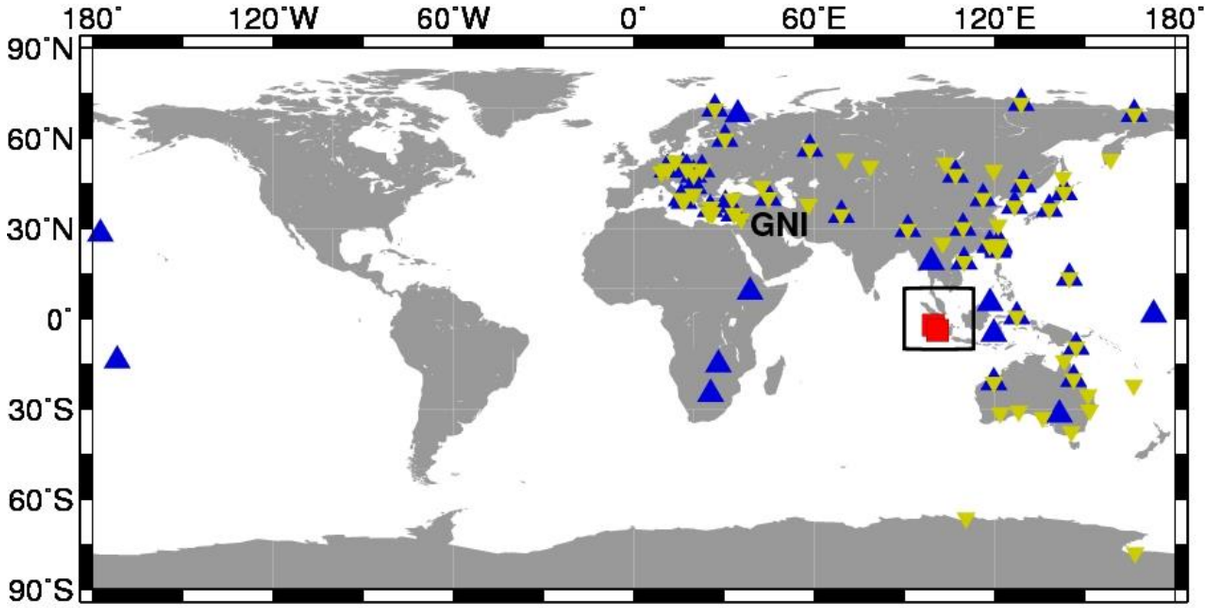

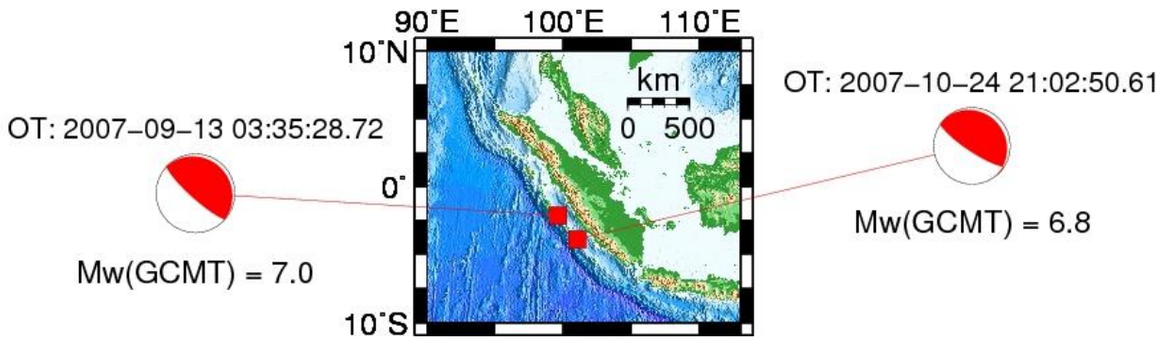

Mw(GCMT) = 7.0
Me(GFZ) = 7.1

Mw(GCMT) = 6.8
Me(GFZ) = 6.4

The locations differ by about 250 km and the moment magnitudes Mw and the fault plane solutions are very similar.

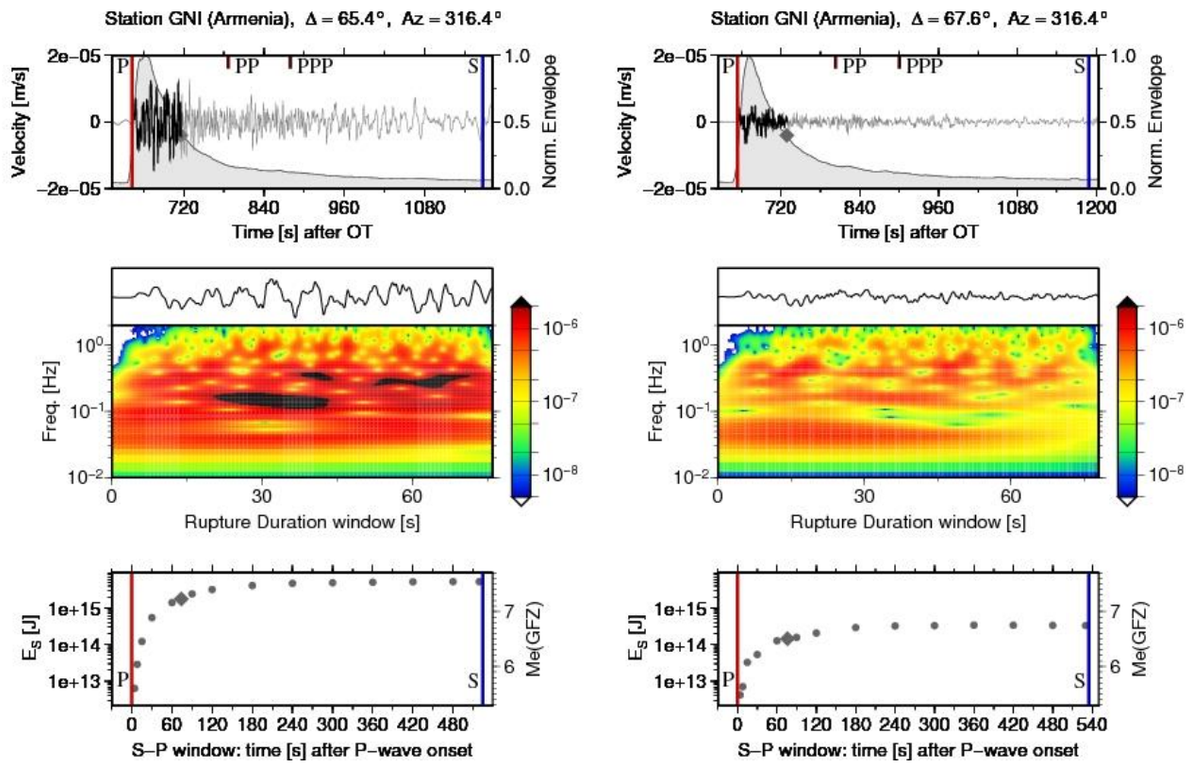

However, the high frequency content observed in the seismograms is significantly different and cannot be explained by Mw only.

Di Giacomo and Bindi (2009)

Importance of comparing Mw and Me

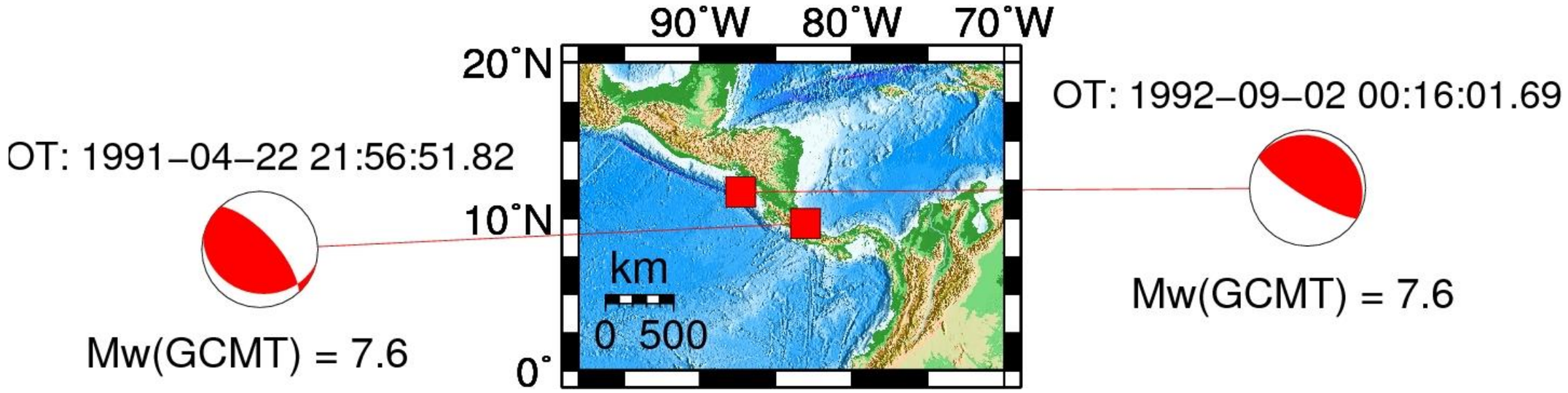

Station CCM (USA), Δ = 29.2°, Az = 346.7°

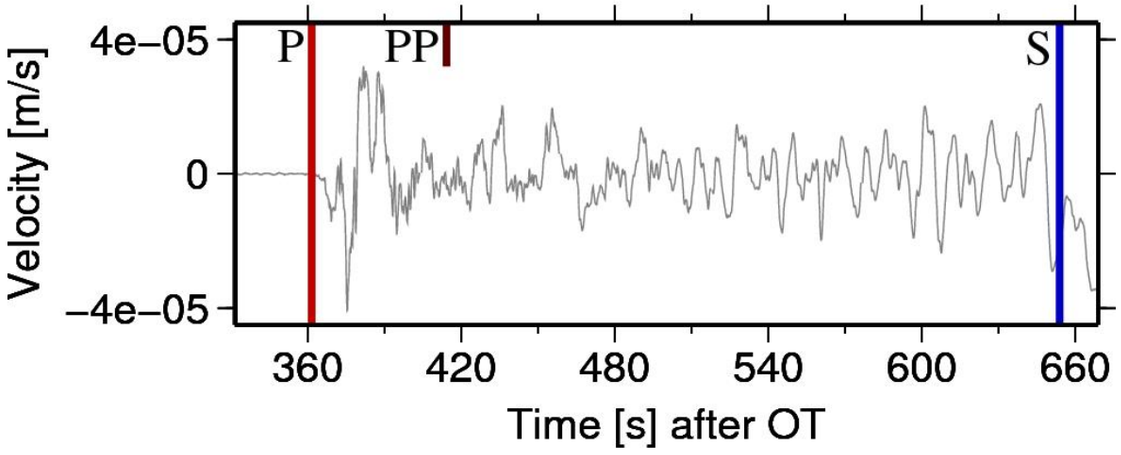

Mw(GCMT) = 7.6, Me(GFZ) = 7.19

Station CCM (USA), Δ = 26.4°, Az = 353.2°

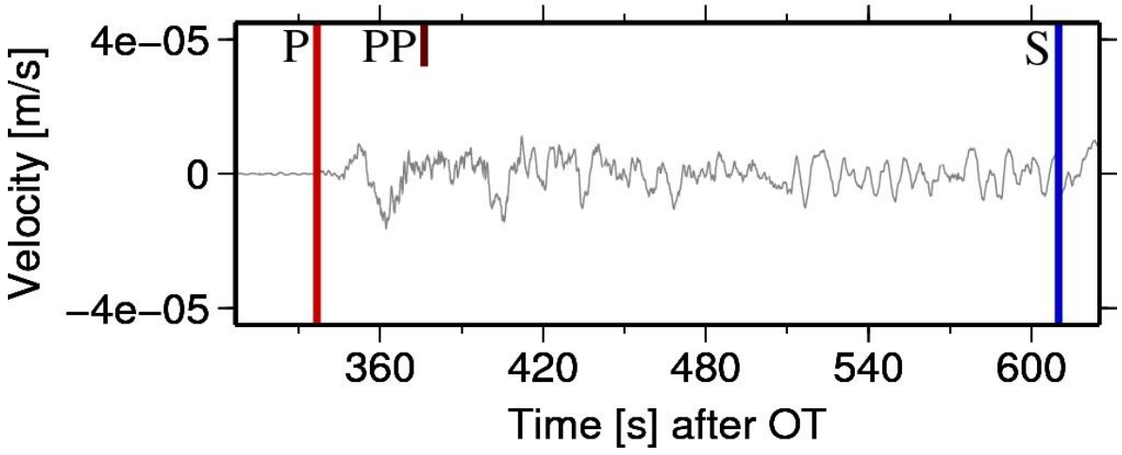

Mw(GCMT) = 7.6, Me(GFZ) = 6.75

The locations differ by about 500 km and the moment magnitudes Mw are nearly identical, therefore the differences in the high frequency content observed in the seismograms can be attributed to different source characteristics.

Di Giacomo and Bindi (2009)

Strong motion seismology

- Strong ground motion is an event in which an earthquake cause the ground to shake at least strongly enough for people to feel the motion or to damage or destroy man-made structures.

- The goal of strong motion seismology is to be able to understand and predict seismic motions sufficiently well that the predictions can be used for engineering applications

- The field of strong-motion seismology could initially be identified with a type of instrument, designed to remain on-scale and record the ground motion with fidelity under the conditions of the strongest ground motions experienced in earthquakes.

Anderson J.G Physical Processes That Control Strong Ground Motion. In: Gerald Schubert (editor-in-chief) Treatise on Geophysics, 2nd edition, Vol 4. Oxford: Elsevier; 2015. p. 505-557.

Strong motion seismology

- Early instruments were typically designed so that ground motions up to the acceleration of gravity (1g) would be on-scale.

- The lower limit of ground motion considered by the early strong motion seismology studies was roughly defined by the thickness of the light beam read until the edge of a recorded film. The minimum acceleration resolved is somewhat less than 0.01g, that approximately coincided with minimum ground motions that humans are able to feel.

- Since much smaller ground motions can be recorded on modern instruments, the distinction between strong-motion seismology and traditional seismology is blurred.

Example of Recordings

Ground acceleration, velocity and displacement, recorded at a strong-motion seismometer that was located directly above the part of a fault that ruptured during the 1985 Mw = 8.1, Michaocan, Mexico earthquake.

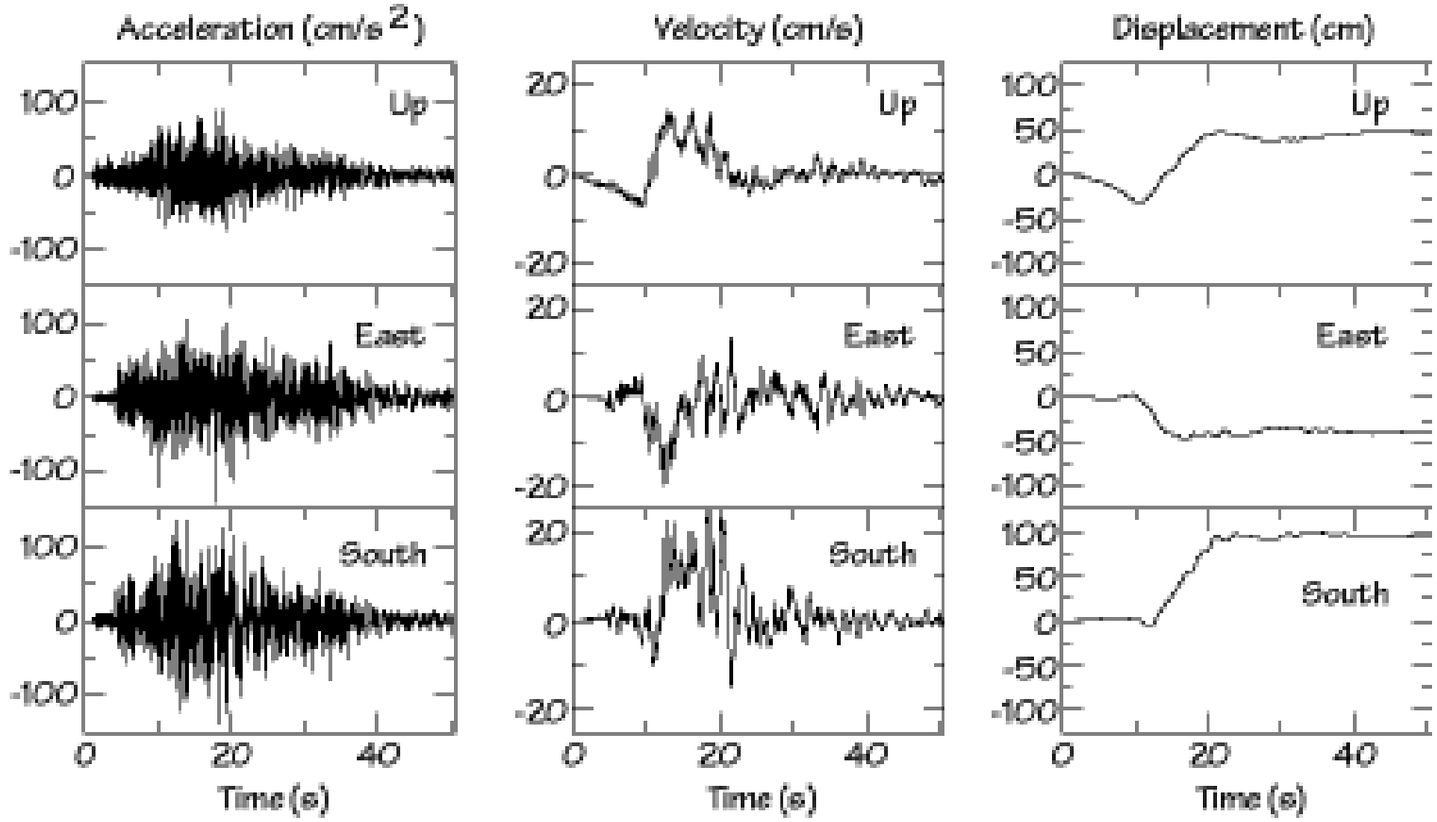

The left panel is a plot of the three components of acceleration: strong, high-frequency shaking lasted almost a minute and the peak acceleration was about 150 cm/s^2 (or about 0.15g). The middle panel shows the velocity of ground movement: the peak velocity for this site during that earthquake was about 20-25 cm/sec. Integrating the velocity, we can compute the displacement, which is shown in the right-most panel: the permanent offsets near the seismometer were up, west, and south, for a total distance of about 125 centimeters.

Maximum Intensity

Maximum Intensity is used to estimate the size of historical earthquakes, but suffers from dependence on depth, population, construction practices, site effects, regional geology, etc.

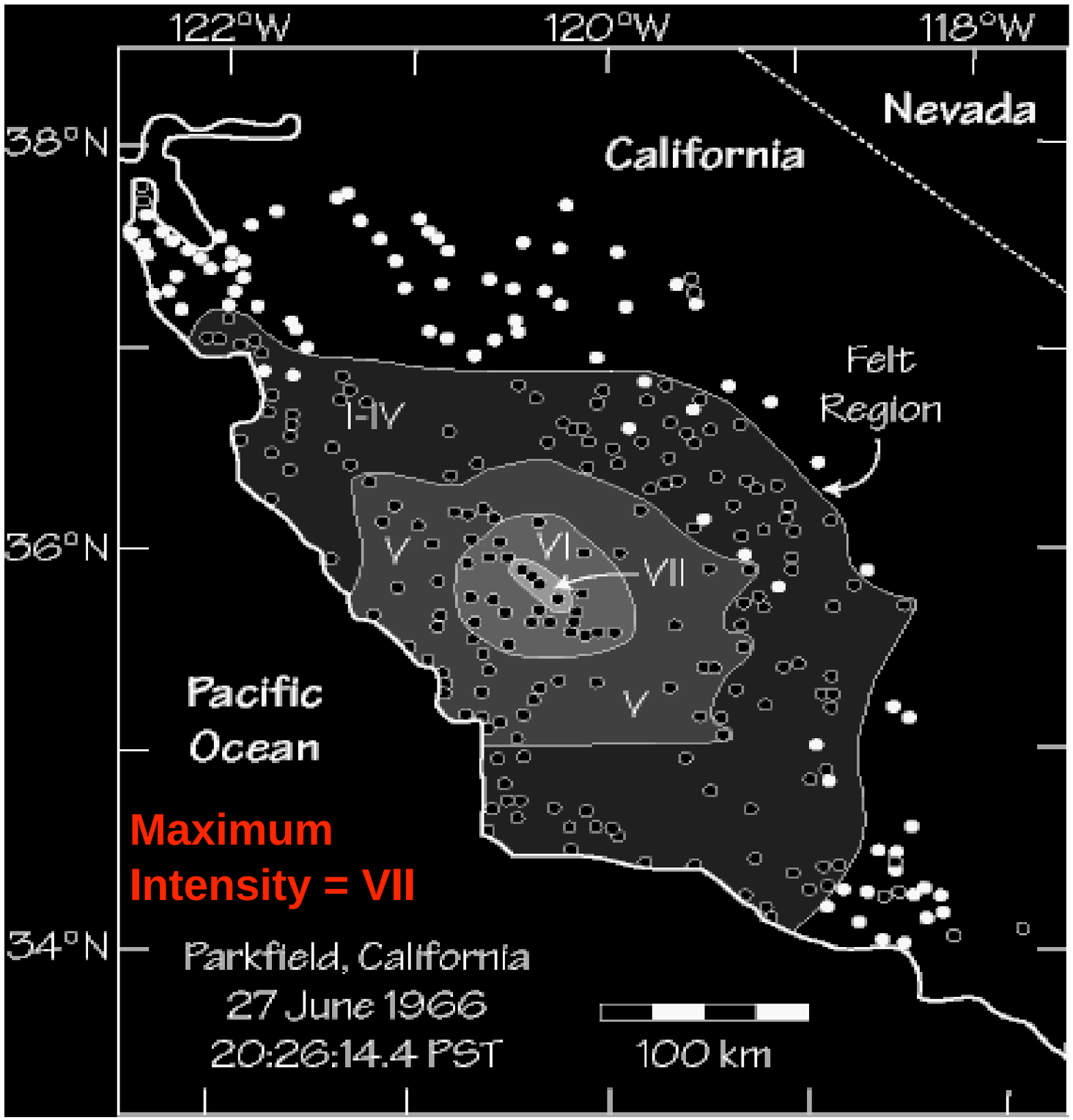

1906 SF and 1811-12 New Madrid

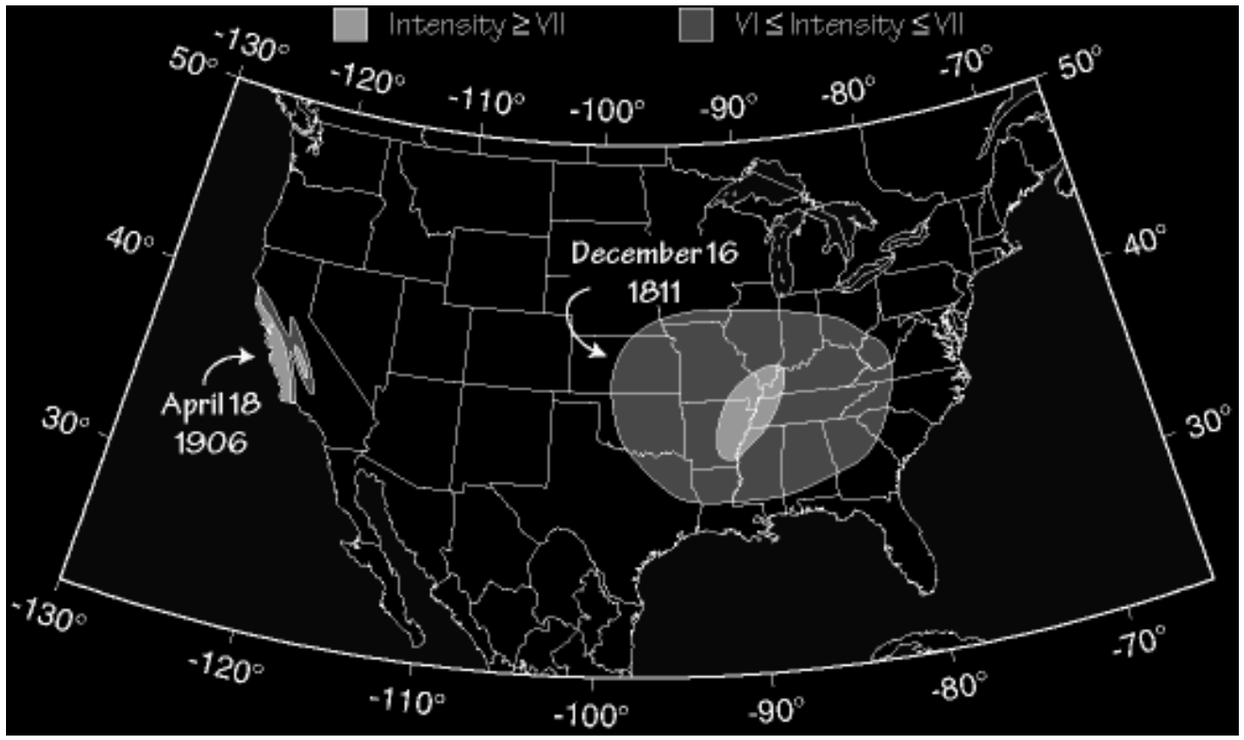

These earthquakes were roughly the same size, but the intensity patterns in the east are broader than in the west (wait for Q...)

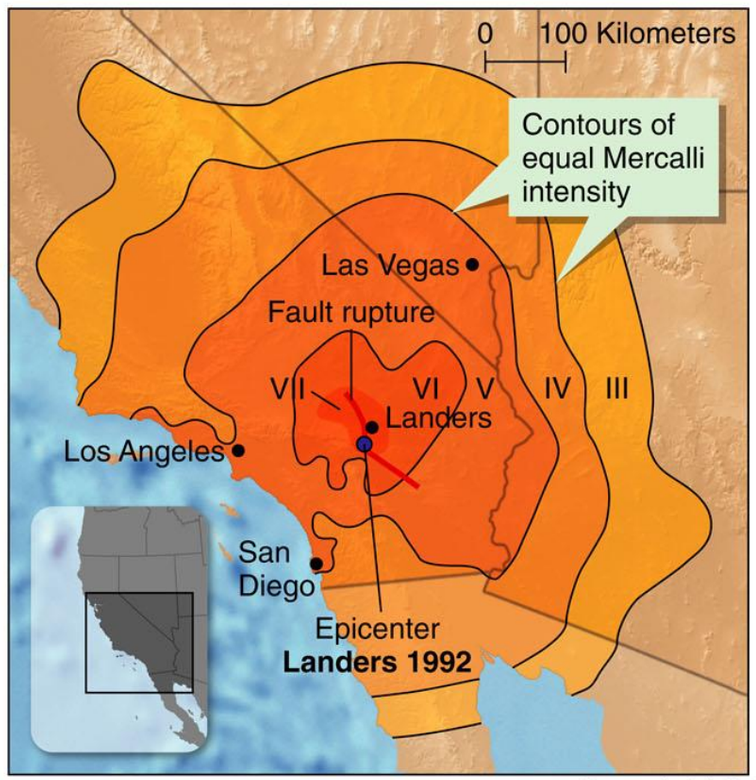

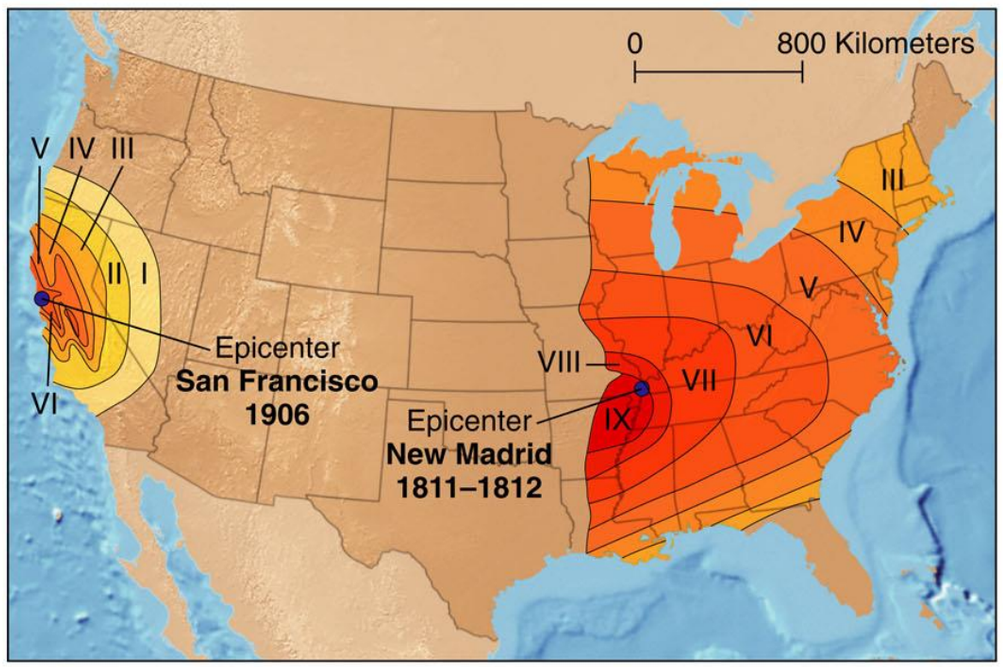

Mercalli Intensity and Richter Magnitude

Magnitude	Intensity	Description
1.0-3.0 **Micro**	**I**	**I.** Not felt except by a very few under especially favorable conditions.
3.0 - 3.9 **Minor**	**II - III**	**II.** Felt only by a few persons at rest, especially on upper floors of buildings. **III.** Felt quite noticeably by persons indoors, especially on upper floors of buildings. Many people do not recognize it as an earthquake. Standing motor cars may rock slightly. Vibrations similar to the passing of a truck. Duration estimated.
4.0 - 4.9 **Light**	**IV - V**	**IV.** Felt indoors by many, outdoors by few during the day. At night, some awakened. Dishes, windows, doors disturbed; walls make cracking sound. Sensation like heavy truck striking building. Standing motor cars rocked noticeably. **V.** Felt by nearly everyone; many awakened. Some dishes, windows broken. Unstable objects overturned. Pendulum clocks may stop.
5.0 - 5.9 **Moderate**	**VI - VII**	**VI.** Felt by all, many frightened. Some heavy furniture moved; a few instances of fallen plaster. Damage slight. **VII.** Damage negligible in buildings of good design and construction; slight to moderate in well-built ordinary structures; considerable damage in poorly built or badly designed structures; some chimneys broken.
6.0 - 6.9 **Strong**	**VII - IX**	**VIII**. Damage slight in specially designed structures; considerable damage in ordinary substantial buildings with partial collapse. Damage great in poorly built structures. Fall of chimneys, factory stacks, columns, monuments, walls. Heavy furniture overturned. **IX.** Damage considerable in specially designed structures; well-designed frame structures thrown out of plumb. Damage great in substantial buildings, with partial collapse. Buildings shifted off foundations.
7.0 and higher **Major great**	**VIII or higher**	**X.** Some well-built wooden structures destroyed; most masonry and frame structures destroyed with foundations. Rails bent. **XI.** Few, if any (masonry) structures remain standing. Bridges destroyed. Rails bent greatly. **XII.** Damage total. Lines of sight and level are distorted. Objects thrown into the air.

Intensity scales

MM	RF	JMA	MCS	MSK
I	I		II	I
II		I	III	II
	II			III
III	III		IV	
IV	IV	II	V	IV
V	V	III	VI	V
	VI			
VI	VII	IV	VII	VI
VII	VIII	V	VIII	VII
VIII			IX	VIII
	IX		X	
IX		VI	XI	IX
X	X		XII	X
XI		VII		XI
XII				XII

MM – Modified Mercalli; RF – Rossi-Forel; JMA – Japanese Meteorological Agency;
MCS – Mercalli-Cancani-Sieberg; MSK – Medvedev-Sponheuer-Karnik

Intensity scales

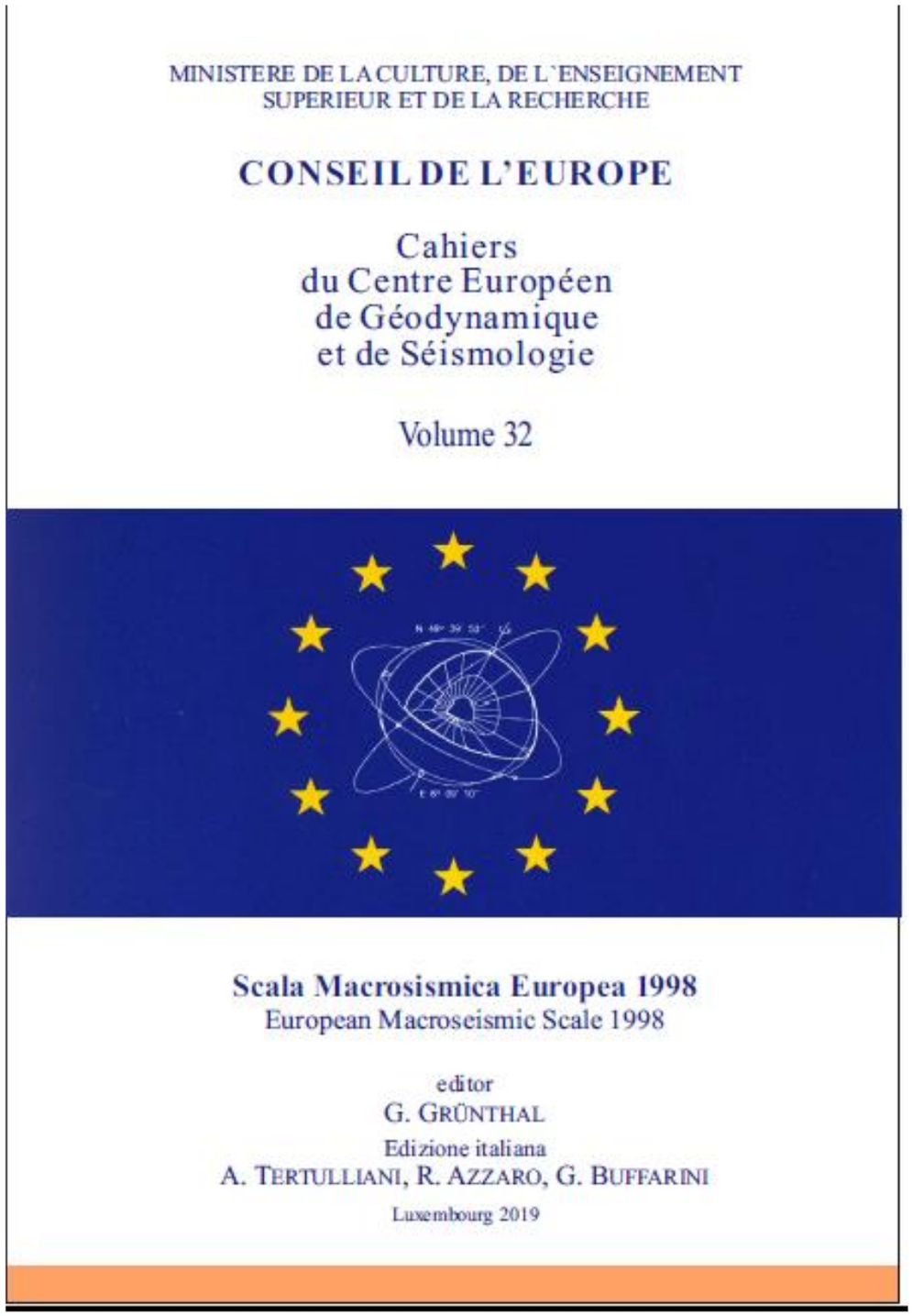

8 Tabella sintetica della EMS-98

La forma sintetica della Scala Macrosismica Europea, estratta dalla parte centrale, è fornita per dare una panoramica molto semplificata e generalizzata della Scala EM. Essa può, per esempio, essere usata per scopi divulgativi. *Questa forma sintetica ma non è adatta per le assegnazioni d'intensità.*

Intensità EMS	Definizione	Descrizione degli effetti tipici osservati (riassunto)
I	**Non avvertito**	Non avvertito.
II	**Appena avvertito**	Avvertito solo da poche persone in stato di riposo al chiuso.
III	**Debole**	Avvertito da alcune persone in casa. Persone a riposo avvertono una oscillazione o un leggero tremore.
IV	**Ampiamente osservato**	Avvertito all'interno da molta gente, da pochissimi all'esterno. Alcune persone si svegliano. Finestre, porte e piatti sbattono.
V	**Forte**	Avvertito all'interno dalla maggior parte delle persone, all'esterno da pochi. Molte persone che dormivano si svegliano. Alcuni si spaventano. Gli edifici tremano nel loro complesso. Oggetti appesi oscillano notevolmente. Piccoli oggetti vengono spostati. Porte e finestre si spalancano o si chiudono.
VI	**Danni lievi**	Molte persone si spaventano e corrono all'aperto. Alcuni oggetti cadono. Molti edifici subiscono leggeri danni non strutturali come sottilissime fessure capillari e caduta di piccoli pezzi di intonaco.
VII	**Danni diffusi**	La maggior parte delle persone si spaventano e corrono fuori. I mobili si spostano e gli oggetti cadono dalle mensole in grande numero. Molti edifici ben costruiti subiscono danni moderati: piccole crepe nei muri, caduta di intonaco, caduta di parti di camini; gli edifici più vecchi possono mostrare grandi crepe nei muri e cedimento dei tramezzi.
VIII	**Danni gravi**	Molte persone hanno difficoltà a stare in piedi. Molti edifici presentano grandi fenditure nei muri. Alcuni edifici ben costruiti mostrano cedimenti gravi dei muri, mentre strutture deboli e più vecchie possono crollare.
IX	**Distruttivo**	Panico generale. Molte costruzioni deboli crollano. Anche edifici ben costruiti mostrano danni molto gravi: gravi lesioni dei muri e parziali cedimenti strutturale.
X	**Molto distruttivo**	Molti edifici ben costruiti crollano.
XI	**Devastante**	La maggior parte degli edifici ben costruiti crollano; anche alcuni con un buon livello di progettazione antisismica vengono distrutti.
XII	**Completamente devastante**	Quasi tutti gli edifici vengono distrutti.

Offline application to Kyrgyzstan: Lead time for Repetition of the M 7.8 1911 Kemin Earthquake

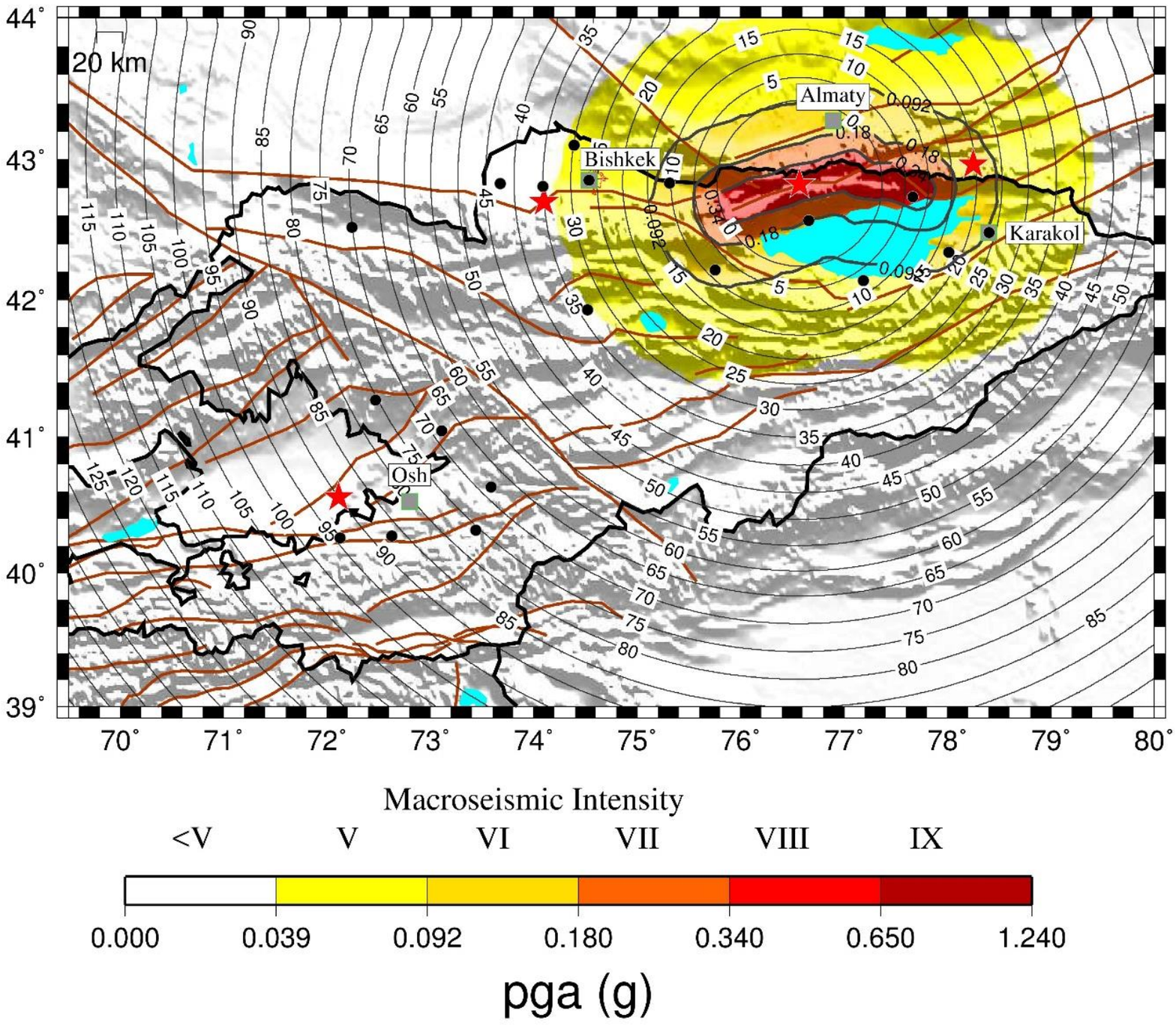

from
Parolai et al.,2017, Frontiers

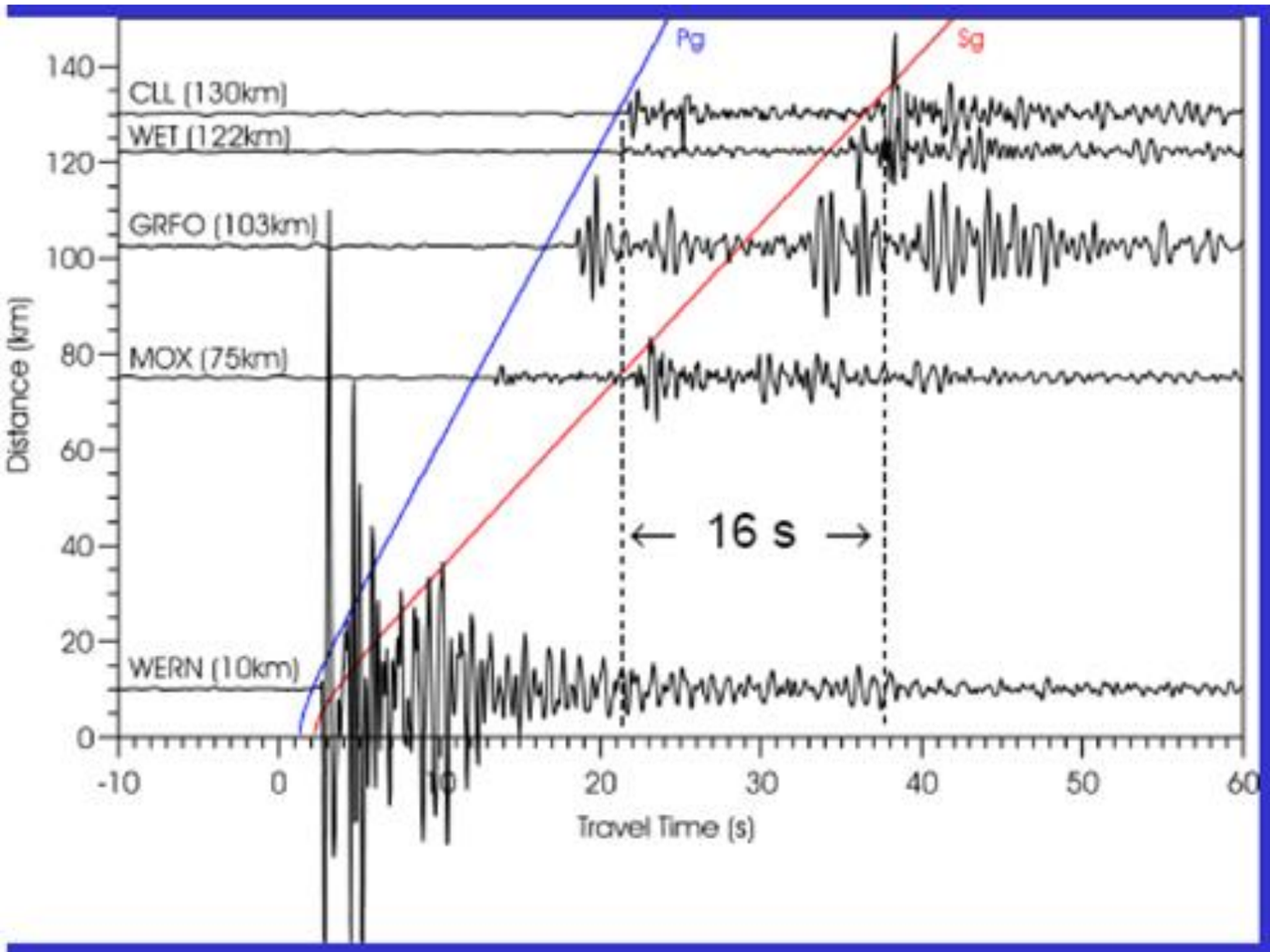
Pg
Sg
CLL (130km)
WET (122km)
GRFO (103km)
MOX (75km)
WERN (10km)
← 16 s →
Distance (km)
Travel Time (s)
140
120
100
80
60
40
20
0
-10
0
10
20
30
40
50
60

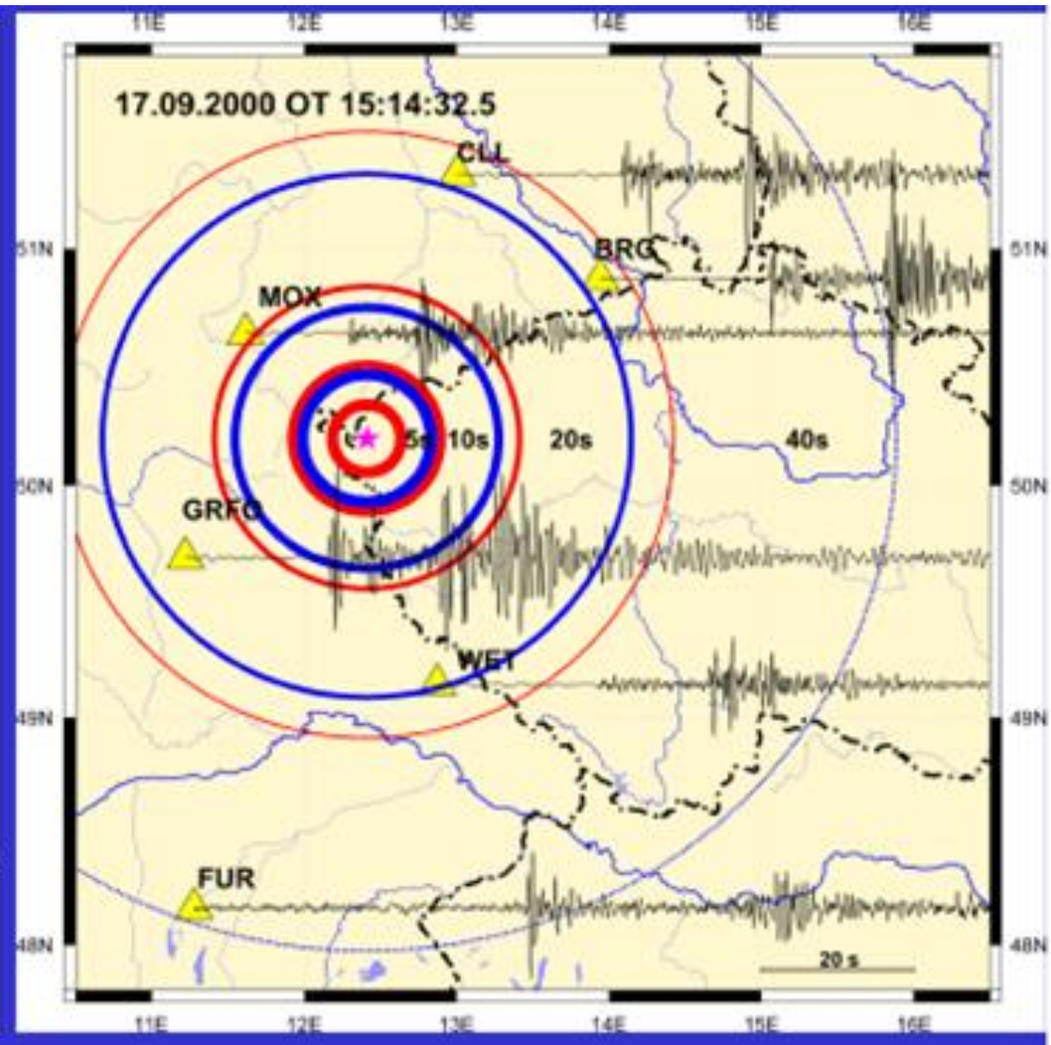
17.09.2000 OT 15:14:32.5
CLL
BRG
MOX
GRFO
WET
FUR
5s
10s
20s
40s
20 s
11E
12E
13E
14E
15E
16E
51N
50N
49N
48N

Tp=D/Vp

Ts=D/Vs

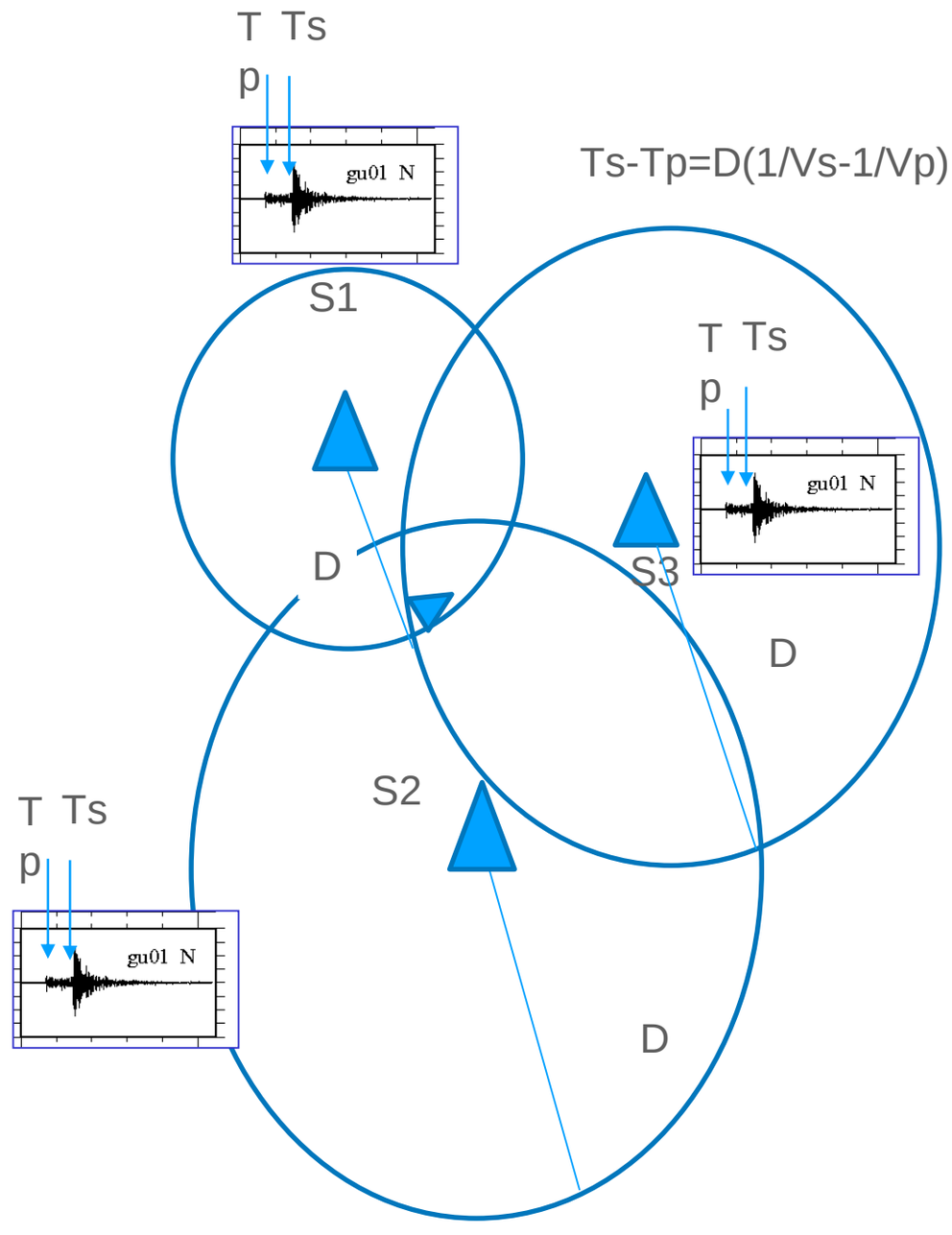

Confronto tra diversi metodi per la localizzazione dei terremoti

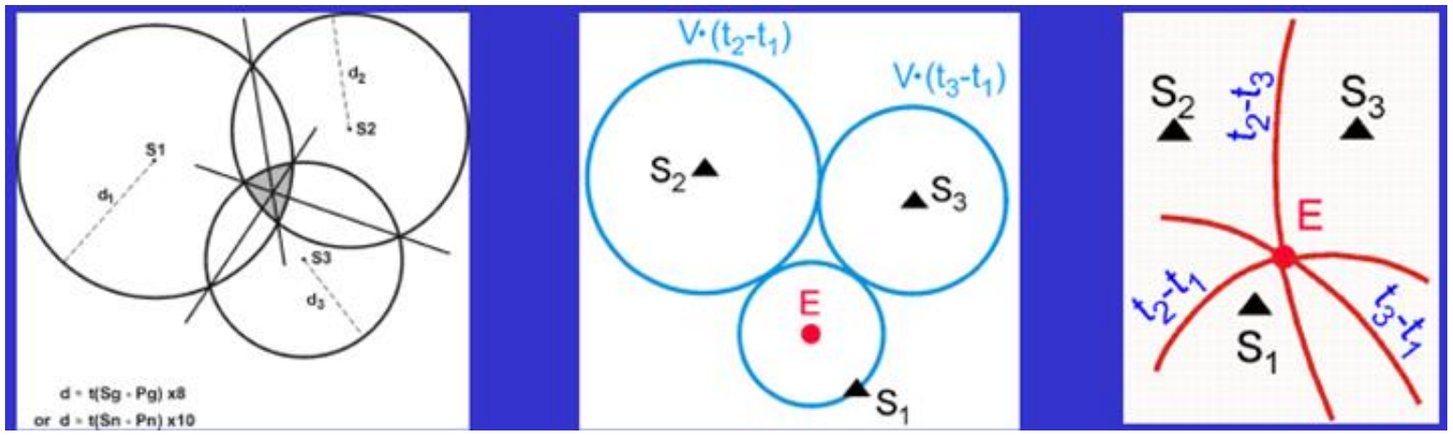

Tutti i metodi illustrati non considerano la forma della terra, e si basano su distanze planari cioè possono essere applicati solo su piccola scala, a livello locale.
Allo stesso modo, tutti i metodi si basano sul modello calcolo dei tempi di percorso mostrato nella diapositiva precedente

PlanetPhysics/Geigers Method

< PlanetPhysics

Geiger's method [1] is an iterative procedure using Gauss-Newton optimization to determine the location of an earthquake, or seismic event. Originally his method was developed to obtain the origin time and Epicentre but it is easily extended to include the Focal Depth for Hypocentre determination.

Given a set of M arrival times t_i find the origin time t_0 and the hypocentre in cartesian coordinatios (x_0, y_0, z_0) which minimize

the objective function

$$F(\mathbf{X}) = \sum_{i=1}^{M} r_i^2.$$

Here, r_i is the difference between observed and calculated arrival times

$$r_i = t_i - t_0 - T_i,$$

and the unknown parameter vector is

$$\mathbf{X} = (t_0, x_0, y_0, z_0)^{\mathrm{T}}$$

In matrix form (1) becomes

$$F(\mathbf{X}) = \mathbf{r}^{\mathrm{T}}\mathbf{r}$$

The Gauss--Newton procedure requires an initial guess of the sought parameters, denoted here as

$$\mathbf{X}^* = (t_0^*, x_0^*, y_0^*, z_0^*)^{\mathbf{T}},$$

which are then used to calculate the adjustment vector

$$\delta\mathbf{X} = (\delta t_0, \delta x_0, \delta y_0, \delta z_0)^{\mathrm{T}}$$

in

$$(1)\mathbf{A}^{\mathrm{T}}\mathbf{A}\delta\mathbf{X} = -\mathbf{A}^{\mathrm{T}}\mathbf{r}.$$

The Jacobian matrix $\mathbf{A}$ is defined as

$$\mathbf{A} = \begin{pmatrix} \partial r_1/\partial t_0 & \partial r_1/\partial x_0 & \partial r_1/\partial y_0 & \partial r_1/\partial z_0 \\ \partial r_2/\partial t_0 & \partial r_2/\partial x_0 & \partial r_2/\partial y_0 & \partial r_2/\partial z_0 \\ \vdots & \vdots & \vdots & \vdots \\ \partial r_M/\partial t_0 & \partial r_M/\partial x_0 & \partial r_M/\partial y_0 & \partial r_M/\partial z_0 \end{pmatrix}.$$

The partial derivatives are evaluated at the initial guess, or trial vector, $\mathbf{X}^*$. Equation (45) can be rewritten as

$$(2)\mathbf{G}\delta\mathbf{X} = \mathbf{g}.$$

Using (46) and an initial guess $\mathbf{X}^*$ an adjustment vector can be calculated. The initial guess can then be updated $\mathbf{X}^* + \delta\mathbf{X}$ and used as the inital guess in the next run of the algorithm. In this manner the sought parameters $\mathbf{X}$ can be determined to some tolerance.

De aggregazione

$$\lambda(IM > x) = \sum_{i=1}^{n_{sources}} \lambda(M_i > m_{\min}) \sum_{j=1}^{n_M} \sum_{k=1}^{n_R} P(IM > x | m_j, r_k) P(M_i = m_j) P(R_i = r_k) \tag{2.25}$$

where the range of possible M_i and R_i have been discretized into n_M and n_R intervals, respectively, using the discretization technique discussed earlier.

> One of the primary advantages of PSHA—that it accounts for all possible earthquake sources in an area when computing seismic hazard—is also a disadvantage. Once the PSHA computations are complete, a natural question to ask is "which earthquake scenario is most likely to cause *PGA*>x?" Because we have aggregated all scenarios together in the PSHA calculations, the answer is not immediately obvious. We saw in the example calculations above, however, that some of the intermediate calculation results indicated the relative contribution of different earthquake sources and magnitudes to the rate of exceedance of a given ground motion intensity. Here we will formalize those calculations, through a process known as deaggregation[1] (Bazzurro & Cornell, 1999; McGuire, 1995).
>
> Let us start with magnitude deaggregation. In this case, we are interested in the probability that an earthquake's magnitude is equal to m, given that a ground motion of $IM > x$ has occurred. Intuitively, this is equal to the rate of earthquakes with $IM > x$ and $M = m$, divided by the rate of all earthquakes with $IM > x$

$$P(M = m | IM > x) = \frac{\lambda(IM > x, M = m)}{\lambda(IM > x)} \tag{3.1}$$

$$\lambda(IM > x, M = m) = \sum_{i=1}^{n_{sources}} \lambda(M_i > m_{\min}) \sum_{k=1}^{n_{R_i}} P(IM > x|m, r_k) P(M_i = m) P(R_i = r_k) \tag{3.2}$$

Per Magnitudo e Distanza

$$P(M = m, R = r|IM > x) = \frac{\lambda(IM > x, M = m, R = r)}{\lambda(IM > x)} \tag{3.8}$$

where the numerator of equation 3.8 is computed using the basic PSHA equation but not summing over either M or R

$$\lambda(IM > x, M = m, R = r) = \sum_{i=1}^{n_{sources}} \lambda(M_i > m_{\min}) P(IM > x|m_j, r_k) P(M_i = m) P(R_i = r)$$